2014

Host Proteins Interact with the Hiv-1 Core to Facilitate and Restrict

Zana Lukic
Loyola University Chicago

LOYOLA UNIVERSITY CHICAGO

HOST PROTEINS INTERACT WITH THE HIV-1 CORE TO FACILITATE AND RESTRICT HIV-1 INFECTION

A DISSERTATION SUBMITTED TO

THE FACULTY OF THE GRADUATE SCHOOL

IN CANDIDACY FOR THE DEGREE OF

DOCTOR OF PHILOSOPHY

PROGRAM IN INTEGRATIVE CELL BIOLOGY

BY

ZANA LUKIC

CHICAGO, IL

AUGUST 2014

ACKNOWLEDGEMENTS

I would like to thank all of the people who made this dissertation possible, starting with my mentor Dr. Edward M. Campbell, Ph.D., who is an associate professor in the Department of Microbiology and Immunology at Loyola University Chicago. Dr. Campbell has been an amazing mentor that constantly supported me and encouraged me to push my limits. He provided me with amazing opportunities at every step of the way so that I can be a well-rounded scientist. I would also like to thank my dissertation committee for their words of encouragement, scientific insight, and support throughout the entire process. Additionally, I want to thank Dr. Phong Le, Ph.D., and the program of Integrative Cell Biology for giving me the opportunity to join the program. I would also like to thank Loyola University Chicago and the Arthur J. Schmitt fellowship foundation for providing me with the funds to complete my dissertation. The Arthur J. Schmitt fellowship and the fellowship committee provided me with additional tools and insights into the way that a scientist can serve their community and the world.

I wanted to thank my friends in the Campbell lab for their support throughout the years. It was a joy to work with a team that is passionate about their work. Finally, I would like to thank my family and friends for their love, understanding, encouragement, and never-ending support. Last but not least, I

would like to thank my parents Svjetlana and Miodrag Lukic. They are my heroes because they are the perfect examples of what it means to work hard, to be passionate, and strong. Without their sacrifices and support, I would not be where I am today.

I am not afraid, for I was born to do this.

Joan of Arc

TABLE OF CONTENTS

LIST OF FIGURES

ABSTRACT

Host cell proteins, termed restriction factors, which inhibit viral replication at various stages of the viral life cycle, determine the species-specific tropism of numerous retroviruses. Many members of the TRIM family of proteins act as viral restriction factors. One well-characterized example is the ability of TRIM5α from rhesus macaques (rhTRIM5α) to inhibit human immunodeficiency virus type-1 (HIV-1) soon after viral entry but prior to reverse transcription (RT). It is well established that the restriction requires an interaction between the viral capsid lattice and the B30.2/SPRY domain of TRIM5α. Following the binding of the viral core, TRIM5α mediates an event or series of events that result in the abortive disassembly of the viral core in a manner that prevents the accumulation of reverse transcription (RT) products. When the proteasome was inhibited using pharmacological drugs, TRIM5α-mediated inhibition of RT products and abortive disassembly of the viral core were relieved without affecting the ability of TRIM5α to inhibit retroviral infection. Even though parts of the mechanism of TRIM5α-mediated restriction of HIV-1 were identified, the specific roles of individual molecules have yet to be examined. In **AIM 1** I identify a direct interaction between TRIM5α and the proteasome complex. Furthermore, this interaction occurs during restriction of HIV-1. Additionally, in **AIM 2** I demonstrate that SUMO-1 and SUMO

interacting motifs (SIMs) are important for TRIM5α restriction of HIV-1 and TRIM5α stability.

As mentioned before, the viral capsid is the determinant of TRIM5-mediated restriction. The capsid houses the viral RNA and other necessary proteins for a productive infection. However, the precise process of HIV-1 uncoating is still unknown. Studies suggest that the process of uncoating is modulated by viral and cellular factors. Previously, HIV-1 was shown to traffic on microtubules, in a dynein and kinesin dependent mechanism. However, key host proteins that mediate uncoating of the core are unknown. **In AIM 3** I show that HIV-1 utilizes microtubules, and in particular dynein to facilitate uncoating of the core.

This dissertation further establishes that HIV-1 core interacts with various proteins in the host during early events of the viral life cycle.

CHAPTER I

INTRODUCTION

HIV-1 Epidemic/Statistics

Human Immunodeficiency Virus type 1 (HIV-1) is a lentivirus that primarily infects CD4+ T cells and the gradual loss of these cells ultimately leads to Acquired Immunodeficiency Syndrome (AIDS) in the absence of antiretroviral therapy. Currently, 1.2 million people in the United States and 30 million people worldwide are living with HIV-1. Nearly 30 million people with AIDS have died since the epidemic began. While huge strides were made in the development of drug therapies to help patients living with HIV-1/AIDS, new therapies are needed due to drug resistance. Since HIV-1 mutates at a relatively fast rate the emergence of drug resistant viruses prompted the treatment regimen to consist of three antiretrovirals that target various steps in the viral life cycle. Therefore, there is a requirement for the development of additional therapeutic intervention strategies. Understanding the molecular interactions between HIV-1 and host proteins will be critical in the development of future therapies.

Stages of HIV-1 Infection

Acute Infection

In most cases HIV-1 is transmitted through the genital tract or rectal mucosa. While barriers exist in the genital tract and rectum, such as columnar and stratified squamous epithelium, the virus penetrates these barriers to gain access to target cells. The target cells are predominately CD4+ T cells, monocytes and macrophages. While the translocation across the epithelial and mucosal barriers is inefficient, a productive infection in the body arises from a single infecting virus (founder virus). During this phase the person experiences influenza-like symptoms that include fever, swelling of the lymph nodes, and inflammation, which is common to many diseases. Therefore, in most cases initial HIV-1 infection goes unrecognized. Following transmission of the virus, there is a period of about 10 days that is known as the eclipse phase (Figure 1). During this phase the viral RNA cannot be detected in plasma. Following this phase, the virus reaches the draining lymph nodes where it infects activated T cells, and further disseminates throughout the body to other lymphoid tissues. Within 21-28 days after initial infection, the plasma viremia reaches a peak that is usually more than a million RNA copies per ml of blood (Figure 1). During the peak of viremia, CD4+ T cells are reduced but return to near normal levels in the blood (remain low in the gut associated lymphoid tissue (GALT) (1).

Chronic Infection

Following the acute infection, a person can be asymptomatic for 8 to 10 years without any clinical signs of an infection. However, this period can vary between individuals. During this time, there is a standoff between the immune system and HIV-1. CD4+ T cells continue to die because of cytotoxic T lymphocyte (CTL) responses, active viral replication, virus induced cytotoxic effects, and immune activation (Figure 1).

AIDS Progression

In the absence of antiretroviral therapy, CD4+ T cell levels become insufficient to control opportunistic infections and tumors, which leads to progression of AIDS (2, 3) (Figure 1). Therefore, AIDS patients succumb to complications associated with opportunistic infections and cancers.

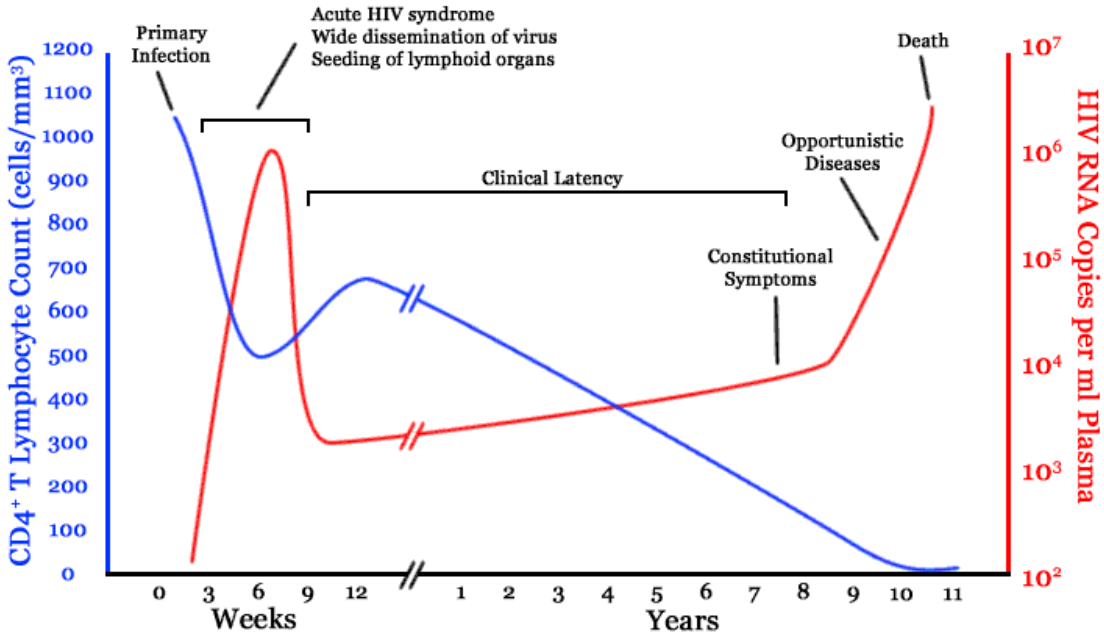

Figure 1. Stages of HIV-1 infection. Following initial infection, at 6 weeks the viral RNA levels are high and the CD4+ T cell levels decline. After this primary infection, the patient will enter clinical latency (or chronic infection), during which they remain asymptomatic for up to 10 years. During this phase, the viral RNA levels are relatively constant and CD4+ T cell levels continue to decline. In absence of antiretroviral intervention, this phase eventually leads to the progression of AIDS which occurs when opportunistic infections and cancer arise, ultimately leading to death. Open access-image dedicated to public use.

HIV-1 Structure and Genome

HIV-1 9.7 kb genome like all retroviruses encodes Group specific antigen (Gag), Polymerase (Pol), and Envelope (Env) genes. Env is translated and cleaved to generate gp120 (SU), a surface protein and gp41 (TM), a transmembrane protein that are within the viral membrane to mediate fusion events. Pol is cleaved into reverse transcriptase (RT), integrase (IN), and protease (PR). Shortly after virus budding, Gag is further processed by the HIV-1 PR into mature Gag proteins p17 matrix (MA), p24 capsid (CA), p7 nucleocapsid (NC), and p6. This maturation causes a morphological shift in virion structure from a spherical core to a conical one due to the condensation of CA to form a shell around the viral RNA/NC complex. The virus has two strands of RNA coding for the viral genome that are encased in a capsid core, which is surrounded by a membrane derived from the host plasma membrane (Figure 2A). Within the RNA primary transcript there are sequences that are important for replication such as Primer binding site (PBS), encapsidation signal (ψ), Rev response element (RRE), and a polypurine tract (PPT). The RNA is reverse transcribed into DNA by RT, which is subsequently be integrated into the host genome. The long terminal repeats (LTRs) are composed of U3, R, and U5 elements that flank the genome on the 5' and 3' that contain sequences that are important for transcription. Additionally, the genome encodes for two regulatory proteins known as Tat and Rev, and accessory proteins Vpu, Vpr, Vif, and Nef (Figure 2B). These

proteins participate in various points of the viral life cycle to facilitate successful infection.

A

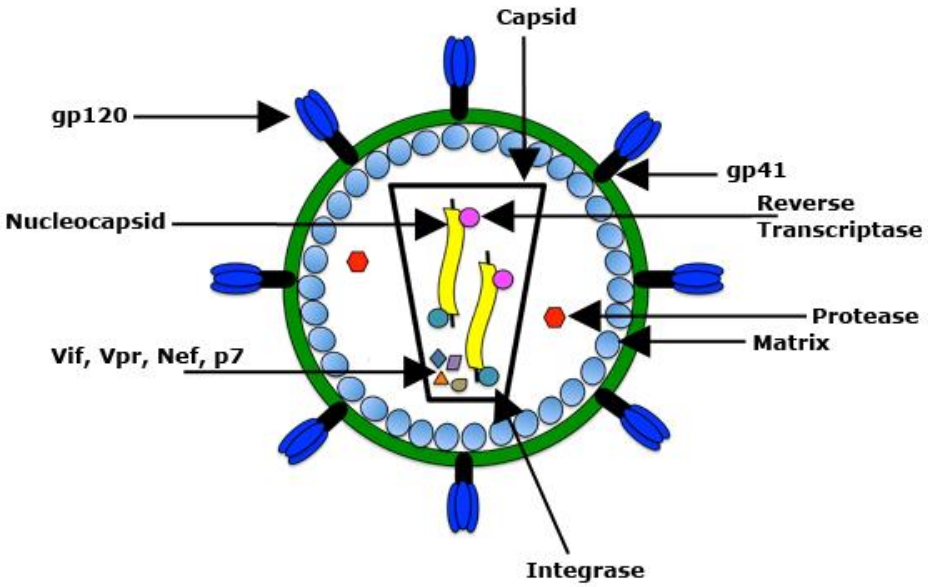
Capsid
gp120
gp41
Reverse
Transcriptase
Nucleocapsid
Protease
Matrix
Vif, Vpr, Nef, p7
Integrase

B

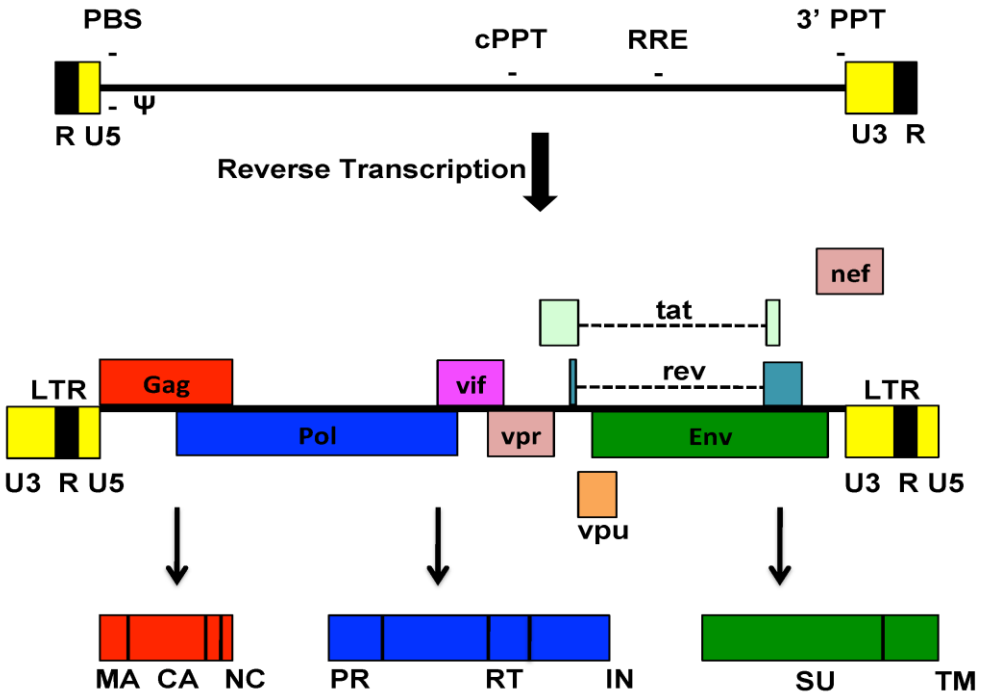
PBS
cPPT
RRE
3' PPT
Ψ
R U5
U3 R
Reverse Transcription
nef
tat
rev
LTR
Gag
vif
LTR
Pol
vpr
Env
U3 R U5
U3 R U5
vpu
MA CA NC
PR RT IN
SU TM

Figure 2. Structure and organization of the HIV-1 genome. **A.** Following budding from the cell or concomitantly during budding, the viral PR cleaves gag to generate a mature infectious particle as depicted here. A lipid membrane that is derived from the host during the budding process surrounds the virus. Within the membrane is the fullerene cone that is composed of p24 protein (black cone). It houses the viral RNA (two strands covered in nucleocapsid (yellow)) along with viral and host proteins. Various viral proteins are identified in the diagram. Adapted and Modified from http://web.archive.org/web/20050531012945/http://www.niaid.nih.gov/factsheets/howhiv.htm). **B.** HIV-1 RNA contains sequences that are important for replication such as the Primer binding site (PBS), encapsidation signal (ψ), Rev response element (RRE), and the polypurine tract (PPT). The RNA is reverse transcribed into DNA by reverse transcriptase enzyme. The long terminal repeats (LTRs) are composed of U3, R, and U5 elements that flank the genome that are important for transcription. The gag, pol, and env are further processed to create individual structural and non-structural proteins. Additionally, there are accessory proteins that are generated from alternative splice sites, such as Tat and Rev. Adapted and Modified from (4).

HIV-1 Life Cycle

The viral life cycle in the target cell is divided into early and late events. Early events characterized from the fusion of the virus to integration into the genome and late events occur from transcription to budding (Figure 3).

Fusion and Infection of Target Cells

Primary targets of HIV-1 infection are cells of the immune system. It infects cells expressing high levels of CD4 on their surface such as T cells because it is the receptor for entry. In addition to infecting T cells, it also infects macrophages since they express CD4 as well. While dendritic cells are not directly infected, they can capture virus with their surface receptors and subsequently migrate to CD4+ T-cell-enriched lymphoid tissue, where HIV-1 *trans*-infection of CD4+ T cells occurs. In order for the viral core to enter the cytoplasm of a target cell, the viral and cellular membranes have to fuse. The viral env proteins mediate the fusion process between the two membranes. The envelope proteins are expressed as a 160kDa (gp160) polyprotein that is cleaved by a cellular protease into the gp41 transmembrane subunit and gp120 surface subunit, which are associated with one another. The fusogenic activity of gp41 is activated once gp120 surface subunit binds to CD4 receptor and CXCR4 or CCR5 co-receptor on the target cell (5, 6).

C-X-C chemokine receptor type 4 (CXCR4) and C-C chemokine receptor type 5 (CCR5) are chemokine receptors that belong to the superfamily of the seven-transmembrane G-protein coupled receptors (GPCRs) (6-8). HIV-1 strains are characterized as R5 or X4 strains depeneding on which co-receptor they utilize

during entry. Initially, CXCR4 was shown to mediate entry of T cell line-tropic (T-tropic) HIV-1 strains (9), while CCR5 mediates entry of macrophage-tropic (M-tropic) viral strains (10-13). However, it was subsequently determined that all primary isolates replicate in activated, primary CD4+ T-cells (14). Therefore, a new nomenclature was developed. Isolates that use CCR5 but not CXCR4 are R5 viruses, isolates that use CXCR4 but not CCR5 are designated X4, and isolates that utilize both are called R5X4 (15). R5 viruses are strains that are most commonly transmitted, whereas X4 strains appear late in the infection. Whether HIV-1 fusion happens at the cell surface or in endosomes is still a point of debate. HIV has long been thought to fuse directly with the cell plasma membrane. However, other data suggests that endocytic entry of HIV can lead to infection as well. Following successful fusion, the viral core is released into the cytoplasm.

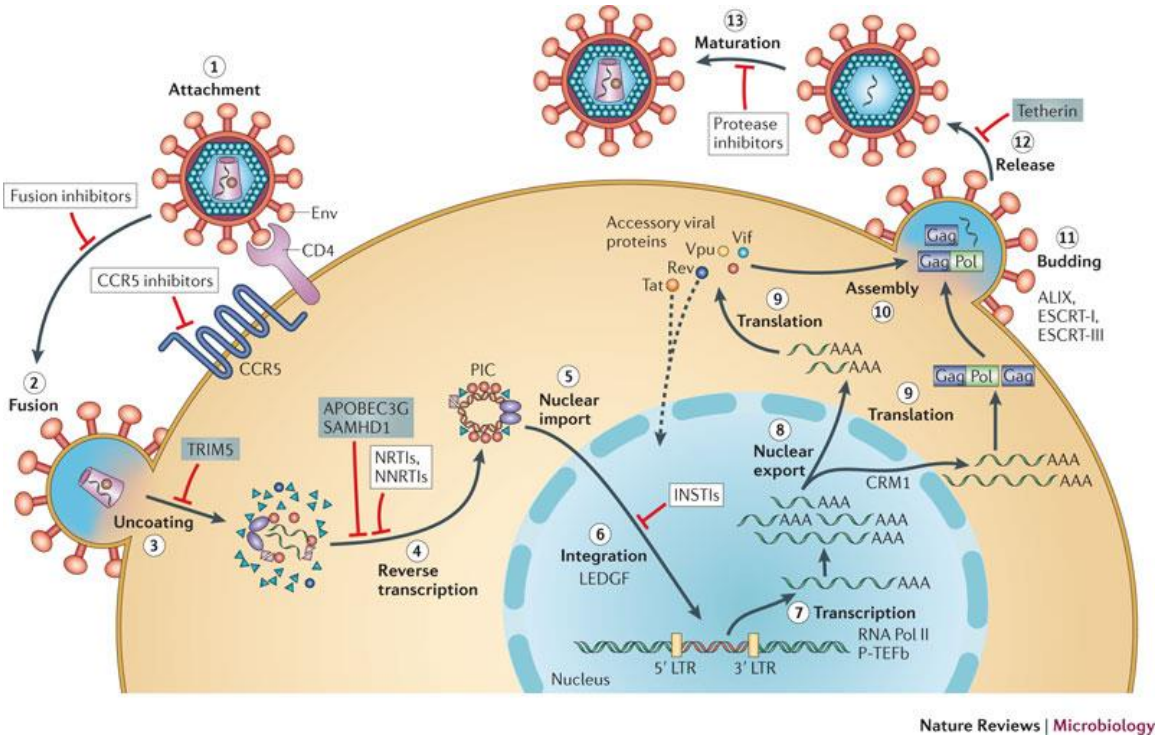

Figure 3. HIV-1 Life Cycle. Following attachment to the target cell, utilizing CD4 as the receptor and CCR5 or CXCR4 as co-receptors, HIV-1 goes through envelope-mediated fusion to release the viral core into the cytoplasm. The core traffics towards the nucleus during which it uncoats and reverse transcribes the genome to generate a pre-integration complex (PIC). The PIC translocates into the nucleus by interacting with the nuclear pore proteins (NUPs) where it integrates into the host genome. The viral genome is transcribed and exported out of the nucleus where it is translated into structural and non-structural proteins. These proteins will traffic to the plasma membrane and assemble. Following assembly the virus buds from the cell by utilizing the endosomal-sorting complex required for transport (ESCRT) proteins. During budding or right after the budding process, the protease cleaves gag to convert the immature virus into a mature and infectious particle. Rights and Permission granted from (16).

Capsid and Uncoating

The viral core is generated from approximately 1,500 CA molecules. CA consists of two independently folded domains, the N-terminal and the C-terminal, separated by a flexible linker. The N-terminal domain (NTD) is composed of seven α-helices, an amino-terminal β-hairpin and a partially ordered cyclophilin A (CypA) binding loop. The C-terminal domain (CTD) is globular with a single turn 3_{10}-helix and four short α-helices. CA is expressed as part of a 55-kDA Gag polyprotein or 160-kDA Gag-Pol polyprotein. During proteolytic cleavage and maturation, the viral core adopts a conical shape, which consists of 216 CA hexons (Figure 4A) and 12 CA pentons (Figure 4A) (seven at the top and five at the bottom) to generate a fullerene cone (also known as a core) (Figure 4C). While an immature HIV-1 particle contains approximately 5000 Gag molecules, only 1000-1500 CA molecules assemble into the mature capsid (17). CA hexamers are stabilized by an inner ring of six NTDs, and an outer "girdle" of CTDs that also form intersubunit contacts with adjacent NTDs (18). The core houses the viral RNA genome and both viral and cellular proteins (17). A core with an optimal stability is crucial for viral fitness. This was demonstrated by introducing various mutations in the viral capsid. CA mutations that rendered the core hyperstable as compared to wild type generated viruses that were severely attenuated. On the other hand, viruses that were less stable than wild type exhibited decreased infectivity as well (19).

Following fusion, the core is released into the cytoplasm. At this point the viral core goes through a poorly understood process of disassembly, termed uncoating, to release the viral RNP (vRNP). Analysis of isolated reverse transcription complexes (RTCs) at various time-points post infection demonstrated that most of CA, MA, and RT dissociated soon after infection, as compared to Vpr, that remained associated with the RTC for at least seven hours. This suggests that CA is lost relatively quickly following entry into the cells. However, not detecting CA in isolated RTCs may be attributed to the poor behavior of HIV-1 cores in biochemical assays (20). On the other hand, when Moloney murine leukemia virus (MoMLV) cores were isolated and characterized, differences were observed when compared to HIV-1 RTCs. The viral CA remained associated with the RTC for at least 7 hours following infection (21). Having an extremely stable core in the cytoplasm of cells is one defining feature of retroviruses that separates them from lentiviruses.

Since lentiviruses actively translocate into the nucleus, a nuclear factor for translocation was demonstrated to be the HIV-1 CA (more details below) (22). While some CA may be lost after entry, some has to remain associated with the RTC as it traffics towards the nucleus in order to import the PIC. This would suggest that uncoating is a controlled process that begins after the core enters the cell and continues through reverse transcription and trafficking towards the nucleus. However, other data suggests that the intact core traffics to the nuclear pore where it docs and uncoats (23-25). Recently, the timing of uncoating and the connection with reverse transcription were demonstrated. The half-life of uncoating was

calculated to be around 39.12 minutes +/- 4.14 minutes. Additionally, when reverse transcription was inhibited uncoating was significantly delayed, suggesting a relationship between uncoating and reverse transcription (26). There are multiple host factors that interact with CA, but whether host factors participate in core uncoating remains to be determined. For other viruses such as HSV-1, Adenovirus and Hepatitis C, the mechanism of uncoating and host protein involvement in the process is well defined (27, 28). Since CA is crucial for virus integrity and infectivity, it is a good candidate for new antiretroviral therapy. Currently, antiretrovirals target many different aspects of the viral life cycle (described further below) but antiretrovirals that target the core do not exist.

A.

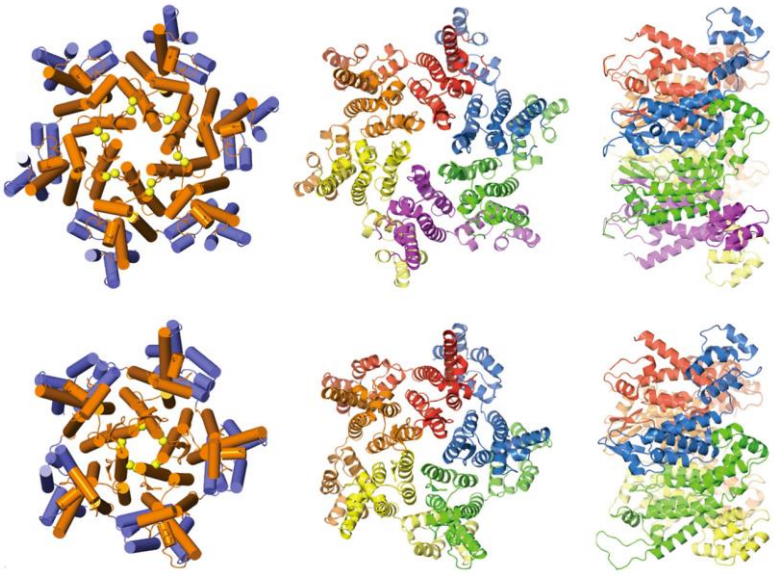

B.

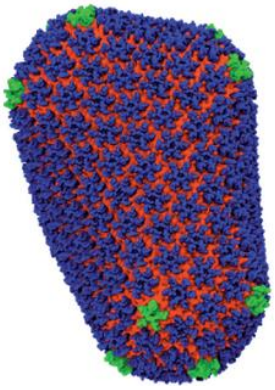

Figure 4. Capsid Structure. A. Top panel: First image is the CA hexamer, with the NTD in orange and CTD in blue. Second image and third image are the top view and side view of the hexamer with helices as ribbons. Each subunit is a different color. An inner ring of six NTDs, and an outer "girdle" of CTDs that also form intersubunit contacts with adjacent NTDs stabilize CA hexamers. **Bottom panel:** Same representation of the CA pentamer. **B.** CA can assemble into hexamers and pentamers to generate the fullerene cone that was simulated here by utilizing Cryo-electron tomography analysis of isolated native cores. Rights and Permission granted from (29).

Trafficking

Following entry into the cell, the virus has to traverse the vast cytoplasm to reach the nucleus. McDonald et al. demonstrated that GFP-Vpr labeled HIV-1 traffics on microtubules and incorporates labeled dNTPs in the RTC (30) suggesting that the virus reverse transcribes as it traffics on microtubules. Some of these RTCs contained detectable levels of CA while others did not demonstrating that they probably uncoated. Depending on the cell type, the journey to the nucleus can be extremely long or in some cases shorter. However, it was demonstrated that the cytoplasm is viscous and crowded due to cellular organelles and cytoskeleton imposing barriers and limiting free diffusion. Studies using fluorescence recovery after photobleaching (FRAP) with fluorescently labeled dextran particles demonstrated that particles larger than 20nm have an extremely difficult time moving through the cytoplasm (31, 32). Therefore, an HIV-1 PIC that is predicted to be at least 50 nm in diameter (33) is not efficient at trafficking to the nuclear pore by freely diffusing through the cytoplasm.

One efficient way to navigate through the cytoplasm is to utilize microtubules and motor proteins (34, 35). Microtubules are a component of the cellular cytoskeleton that are hollow rods that are approximately 25nm in diameter. They are dynamic structures that undergo continuous disassembly and assembly. They are generated from tubulin, which is a dimer consisting of α and β-tubulin (Figure 5A). They serve as scaffolds for microtubule associated proteins (MAPs) and motor proteins such as dyneins and kinesins. Dyneins transports cargo to the minus end of

microtubules (retrograde), while kinesins transports cargo to the plus end of microtubules (anterograde), which are often located at the cell periphery (36, 37). Cytoplasmic dynein 1 is a large protein complex that contains six different subunits. There are two heavy chains (DYNC1H1), each containing a globular motor domain and an N-terminal stalk. The N-terminal stalk interacts with dimers of intermediate chains and light intermediate chains (DYNC1LI and DYNC1I). Three light chain families (LC7, LC8, and Tctex) bind the intermediate chains, and collectively act as the cargo-binding domain (32) (Figure 5B). Kinesins are a large family of proteins that are either expressed ubiquitously or in specific tissues. Kinesin-1 is the most conventional in the family and it is composed of three structural domains: a large globular N-terminal domain that is responsible for the motor activity of kinesin, a central alpha-helical coiled coil domain that mediates the heavy chain dimerization; and a small globular C-terminal domain which interacts with other proteins (such as the kinesin light chains) (38) (Figure 5B). To mediate trafficking and uncoating of their cores, viruses sometimes exploit these motor proteins.

For example, herpes simplex virus type 1 (HSV-1) and adenovirus use dynein and kinesin motors to traffic on microtubules and disassemble the cores to deliver the genome to the nucleus. For HIV-1 the mechanism of microtubule trafficking was not defined well. However, it was demonstrated that GFP-Vpr labeled HIV-1 associates with and traffics on microtubules in a dynein and kinesin dependent manner. Additionally, RTCs were shown to associate with microtubules and these RTCs contained matrix and capsid protein. This suggests that HIV-1

utilizes microtubules to traffic the RTC/PIC to the nucleus and possibly mediate uncoating.

A.

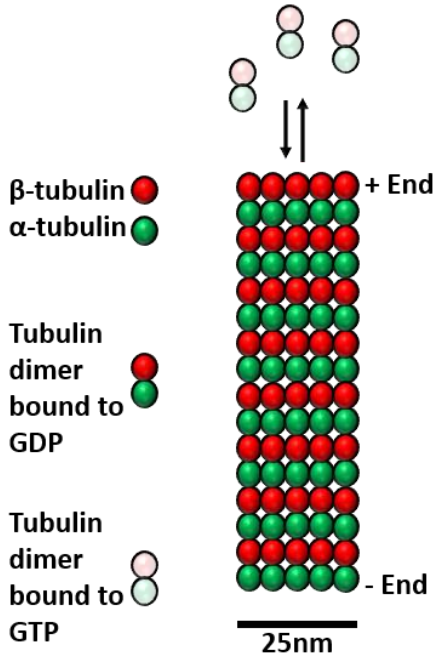
β-tubulin
α-tubulin
Tubulin dimer bound to GDP
Tubulin dimer bound to GTP
+ End
- End
25nm

B.

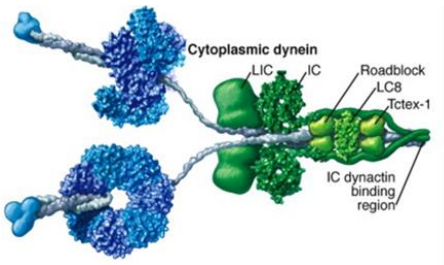
Cytoplasmic dynein
LIC
IC
Roadblock
LC8
Tctex-1
IC dynactin binding region

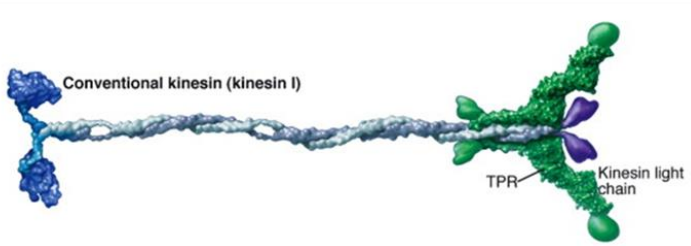
Conventional kinesin (kinesin I)
TPR
Kinesin light chain

Figure 5. Microtubules and Motor Proteins. A. Microtubules are dynamic tubes that are composed of α and β tubulin. During polymerization, both the α- and β-subunits of the tubulin dimer are bound to a molecule of GTP. The GTP bound to α-tubulin is stable and it plays a structural function in this bound state. However, the GTP bound to β-tubulin can be hydrolyzed to GDP. A GDP-bound tubulin subunit at the tip of a microtubule is prone to depolymerization. Motor proteins and MAPs associate with microtubules to transport cargo throughout the cell. Adapted and Modified from (39). **B.** Dynein is composed of two heavy chains (DYNC1H1), each containing a globular motor domain and an N-terminal stalk. The N-terminal stalk interacts with dimers of intermediate chains and light intermediate chains (DYNC1LI and DYNC1I). Three light chain families bind the intermediate chains, and collectively act as the cargo-binding domain. Kinesin-1 consists of two heavy chains that have a large motor domain at the N-terminus, an alpha-helical coiled coil domain and a small C-terminal domain that interacts with light chains. Rights and Permissions granted from (40).

Reverse Transcription

Following uncoating or concomitantly during uncoating, the viral RNA is converted into DNA by the RT enzyme. The ability to reverse transcribe the genome from RNA to DNA is one of the hallmarks of retroviruses (Figure 6). RT contains two enzymatic activities that are sufficient and necessary to carry out reverse transcription. These are a RNA-dependent DNA polymerase that copies the RNA into DNA, and an RNase H that degrades RNA when it is part of an RNA-DNA duplex. Reverse transcription is initiated soon after virus entry and viral DNA can be detected within hours of infection. The rate of DNA synthesis varies depending on the target cell. For example, the rate of synthesis is slow in quiescent cells where the dNTP levels are low. While reverse transcription can successfully happen in vitro, in vivo it is connected to other early events and viral proteins in the life cycle. Previous data demonstrated that mutations in CA have extreme effects on reverse transcription (19). Additionally, NC has nucleic acid chaperone activity that helps RT through regions of secondary structure and it facilitates strand transfer during reverse transcription process. While the structure of the RTC is not known, changes in the conical core were observed in the early events of the viral life cycle (30). One hypothesis is that RTC changes as DNA synthesis proceeds and aids the uncoating process, which eventually transforms the RTC into a pre-integration complex (PIC). Another hypothesis is that the RTCs form a structure that is similar to the intact viral core, allowing the DNA synthesis to occur within the cone. This structure is

trafficked to the nuclear pore where it interacts with the nuclear pore components to translocate into the nucleus.

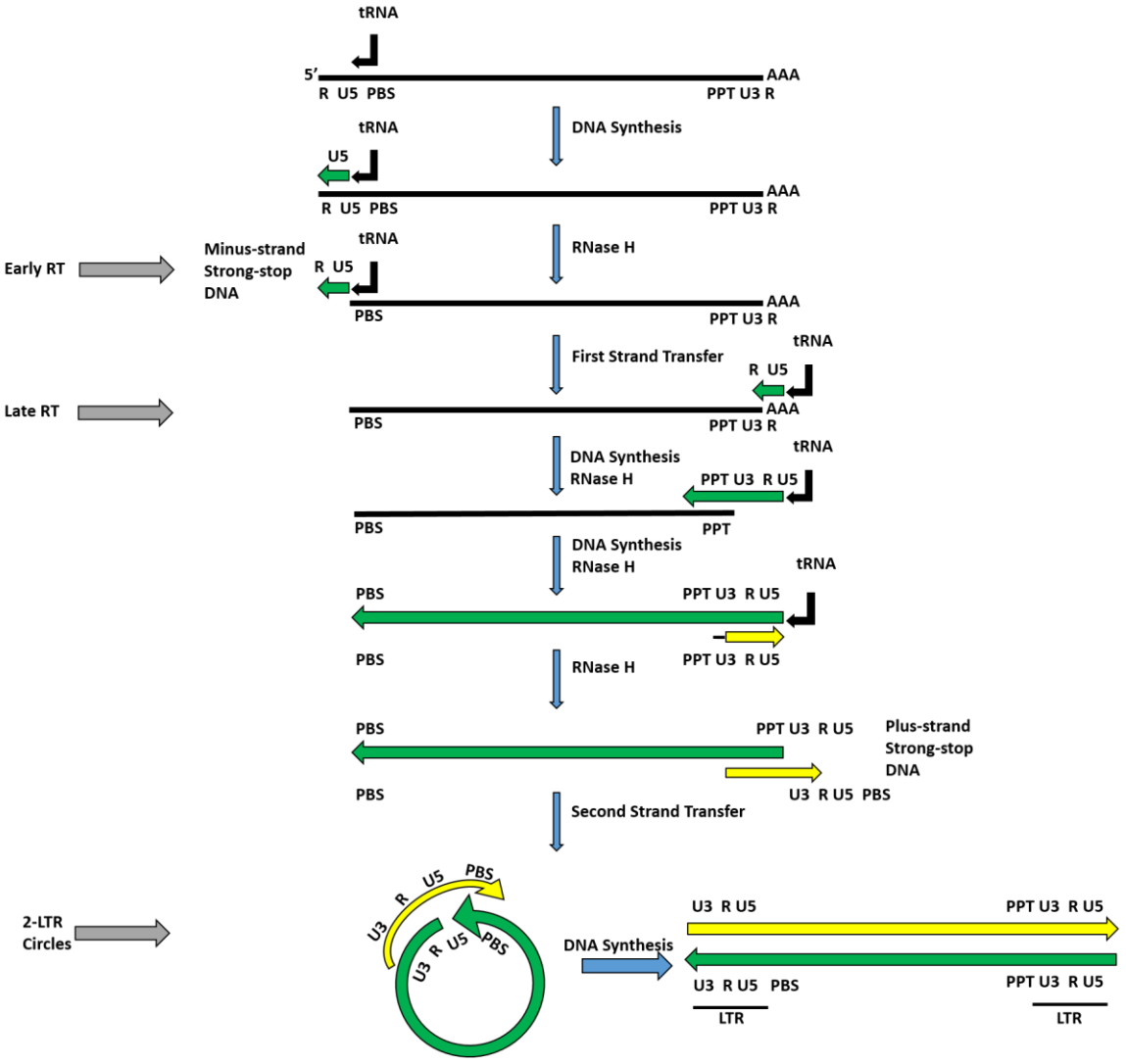

Figure 6. Reverse Transcription Process. HIV-1 genome is a positive strand RNA that is reverse transcribed into DNA by the viral RT enzyme. This process can be quantified by utilizing primers that target early reverse transcription, and late reverse transcription. Also, following reverse transcription, the viral DNA is translocated into the nucleus where it integrates into the host genome. However, some of the proviruses ligate back on themselves and create aberrant products known as 2-LTR circles. Primers are also designed to measure the quantity of these 2-LTR circles, which is used a measure of nuclear import of the viral genome. Adapted and Modified from (41).

Nuclear Import

Once the PIC traffics towards the nucleus, it is actively translocated into the nucleus through the nuclear pore because it is too large for passive diffusion. Unlike MLV, which is a retrovirus, HIV-1 can gain access into the nucleus whether the cell is actively diving or not, due to its ability to utilize host proteins for the translocation process. On the other hand, MLV waits for the nuclear membrane to break down, as it lacks the capability to infect non-dividing cells. While many HIV-1 proteins such as MA, Vpr, IN, and the DNA flap were implicated to be the determinants for nuclear import, CA was identified as the primary determinant for nuclear import (22).

In order for the HIV-1 PIC to actively translocate itself into the nucleus and subsequently integrate, the CA has to interact with various proteins of the nuclear pore complex and soluble transport receptors. Once again, this suggests that a substantial amount of CA remains associated with the PIC following reverse transcription (23, 42). For example, one CA mutant Q63A/Q67A is impaired for nuclear entry as measured by the formation of 2-LTR circles (aberrant products of the viral DNA ligating to itself instead of the host genome, which is thought to only occur in the nucleus) but retains higher than normal levels of CA in the PIC, suggesting there is an optimal amount of PIC-associated CA that is necessary for nuclear import (22). Recently, many nuclear pore residing proteins were demonstrated to participate in HIV-1 translocation into the nucleus. Nucleoporin 358 (Nup358) depletion, which is also known as RanBP2, was shown to inhibit nuclear import of HIV-1 PIC and not nuclear export of viral mRNA species (43).

Further, the requirement for Nup358 is CA dependent, and CA mutations that render the virus less sensitive to Nup358 depletion results in the virus integrating in regions that are devoid of transcriptional units (24). Other factors were shown to participate in this part of the viral life cycle as well. mCPSF6-358, a truncated version of cleavage and polyadenylation factor 6 (CPSF6) inhibits nuclear entry of HIV-1 and a single amino acid substitution within CA bypasses the restriction (44). Additionally, transportin-3 (TNPO3), a karyopherin is known to promote HIV-1 infectivity by opposing cytoplasmic CPSF6 from stabilizing CA too much (Figure 7) (45, 46). This suggests that interaction at the nuclear pore with host proteins dictates whether the PIC successfully translocates into the nucleus and subsequently integrate into an area of high or low transcriptional density.

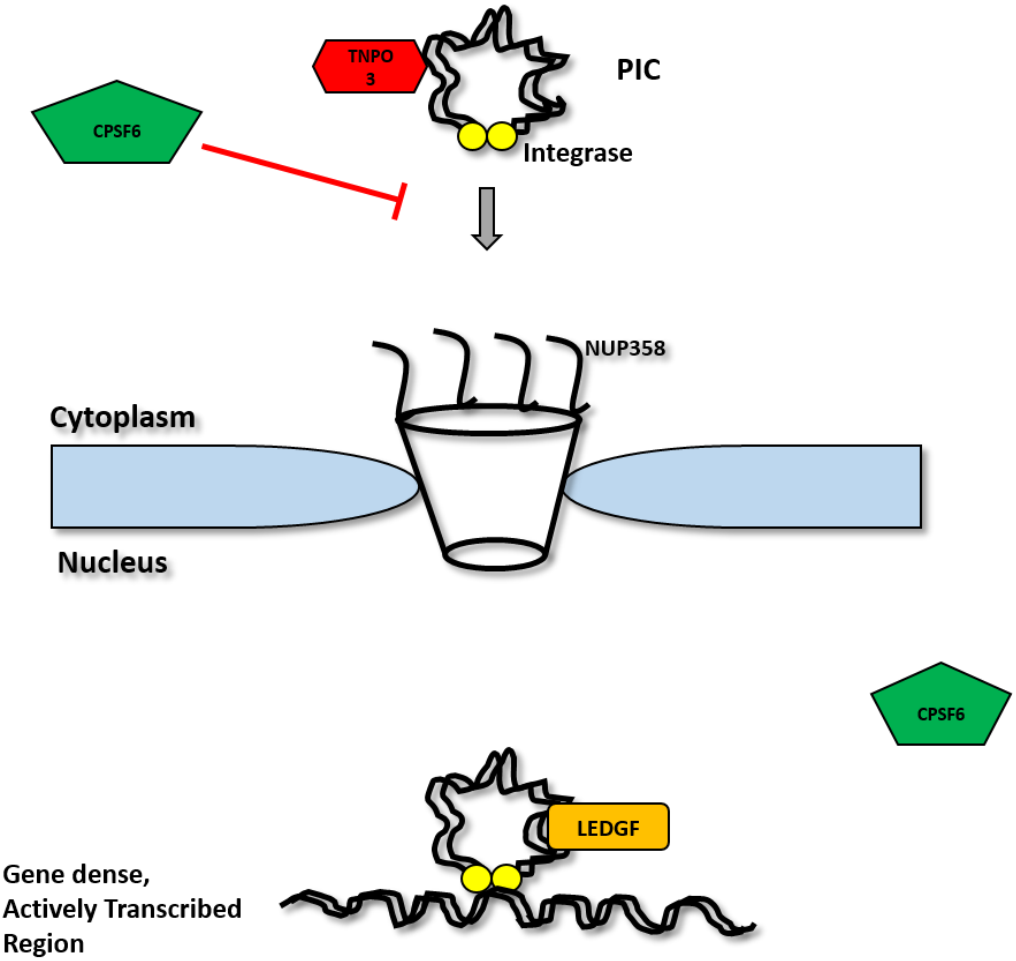

Figure 7. Pre-integration complex (PIC) Nuclear Import. Following reverse transcription, the PIC is actively translocated into the nucleus and integrates into gene dense regions of the chromatin. This process is known to be assisted by lens epithelium-derived growth factor (LEDGF). CA was identified as the determinant that is necessary for successful nuclear import. The PIC and the CA interact with NUP358 (a nuclear pore complex protein) in order to successfully translocate into the nucleus. Additionally, a host protein known as Transportin-3 (TNPO3), which a karyopherin was demonstrated, to be important for the translocation process as well. It has the ability to interact with the HIV-1 CA and knockdown of TNPO3 decreases HIV-1 infectivity at the nuclear import level. Also, cleavage and polyadenylation specific factor 6 (CPSF6) is known to inhibit HIV-1 nuclear import when TNPO3 is knocked down or when CPSF6 is manipulated to reside in the cytoplasm as opposed to its predominant location in the nucleus. Adapted and modified from (47)

Integration and Transcription/Translation

Following successful nuclear import of the PIC, the viral genome integrates into the host genome, which is one of the reasons why it is difficult to eradicate the virus. The integration process is carried out by the viral IN enzyme and the host protein lens epithelium-derived growth factor (LEDGF)/p75, which promotes infection and tethers IN to preferred integration target sites. For HIV-1, it favors integration within transcription units while gammaretroviruses favor integration at transcription start sites (48). As mentioned above, the PIC's interaction at the nuclear pore with host proteins somehow dictates whether the HIV-1 DNA is integrated into rich areas of rich transcription on the outer surface of DNA wrapped on nucleosomes (49). The mechanism by which these sites are selected is not well known but it seems to be IN dependent, as a swap between HIV-1 IN and MLV IN causes HIV-1 PICs to integrate at transcriptional start sites as an MLV PIC does (50). After integration, the viral DNA is transcribed with the help of the viral transactivator protein Tat that recruits host transcription factors to facilitate successful transcriptional elongation. These mRNAs undergo splicing, leading to the production of early genes, including Tat, Rev and Nef. The smaller processed mRNAs are exported in a CRM1-dependent mechanism while large mRNAs are exported via the viral protein Rev. Viral mRNAS are then translated to produce the structural and non-structural proteins. The genomic RNA serves as the mRNA for Gag and Gag-Pro-Pol, but singly and multiply spliced RNAs are translated to produce Env and accessory proteins. Gag-Pro-Pol is generated when translating ribosomes

shift into the -1 reading frame at a site near the 3' end of the *gag* open reading frame, and then continue to translate the *pol* gene. Gag, Gag-Pro-Pol and most accessory proteins are translated on cytosolic polysomes. However, Env and Vpu are translated on the rough ER because they are encoded on the same mRNA (51).

Assembly, Budding, and Maturation

Following translation of viral proteins in the cytosol, these proteins and the RNA traffic to the plasma membrane in order to assemble and subsequently bud. Gag and Gag-Pro-Pol have a myristate at their amino termini that is required for their plasma membrane localization (52). Binding of the Gag domain MA to PI (4,5) P2 exposes the amino-terminal myristoyl group and provides a mechanism for anchoring Gag in the inner leaflet of the plasma membrane (53, 54). The viral Env glycoproteins reach the plasma membrane independently of Gag (55). In addition to Gag and Env, the virus packages two copies of the capped and polyadenylated full-length RNA (56-58). The two RNA strands are noncovalently dimerized in their 5' UTR (58). Removal of the RNA packaging sigma (ψ) causes the virus particles to assemble but contain high levels of nonspecific cellular mRNAs (59). Additionally, it the RNA packaging requires recognition of the noncovalently bound and unspliced RNA (60). Gag assembly leads to the formation of the immature particles (61). The Gag molecules in the immature virion are extended and are oriented radially, with the amino-terminal MA domain bound to the plasma membrane (62). The cellular Endosomal Sorting Complex Required for Transport (ESCRT) pathway mediates

budding from the plasma membrane. The viral protein p6 contains two "late domain" motifs that bind and recruit ESCRT proteins to mediate scission of the virus from the plasma membrane (63-66). The virus maturation is thought to occur during or right after the scission process. Maturation is mediated by the viral PR cleavage of Gag and Gag-Pro-Pol to produce the individual MA, CA, NC, p6, PR, RT, and IN proteins (67-69). Significant remodeling occurs when the virus transitions from an immature to a mature virion such as the formation of the conical core that contains approximately 1200 copies of CA (70, 71). Following maturation, the virus is considered fully infectious and ready to infect a new target cell (Figure 8).

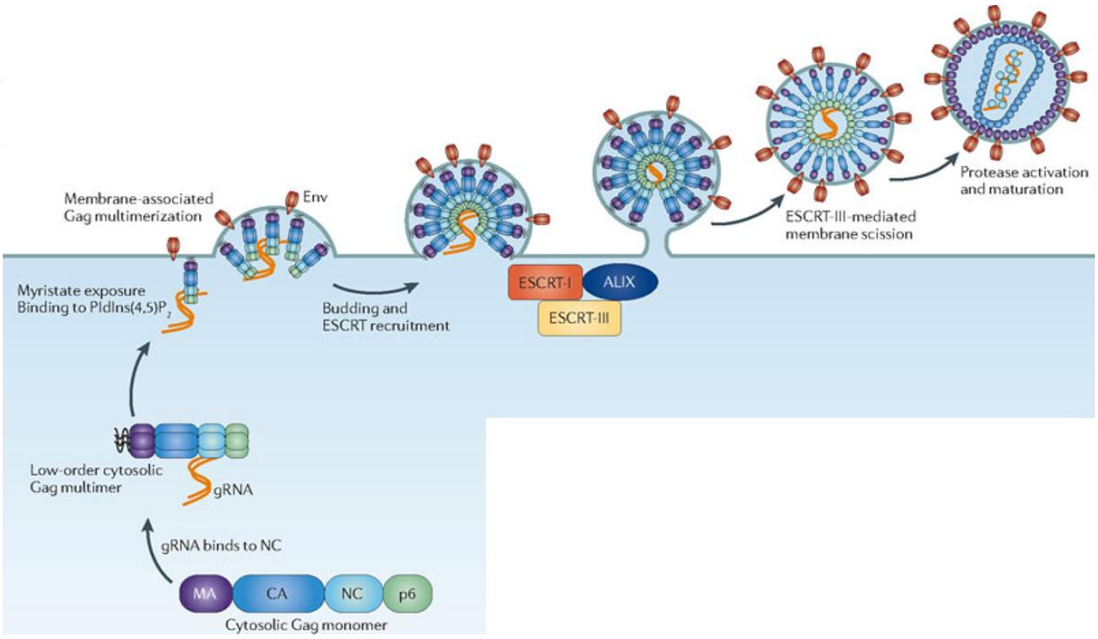

Figure 8. Assembly and Egress of HIV-1. Binding of the MA Gag domain to PI (4,5) P2 exposes the amino-terminal myristoyl group and provides a mechanism for Gag to anchor in the inner leaflet of the plasma membrane. The viral Env glycoproteins reach the plasma membrane independently of Gag. The cellular Endosomal Sorting Complex Required for Transport (ESCRT) pathway mediates budding from the plasma membrane. PR cleaves Gag to generate a mature infectious particle. Rights and Permissions granted from (72).

Antiretroviral Therapy

Following the discovery of HIV-1 as a causative agent of AIDS, there was a dire need for a mode of treatment. While the hope for a cure proved to be more difficult than anticipated, the Food and Drug Administration approved the first antiretroviral drug for HIV-1 in 1987. The drug, 3'-azido-3'deoxythymidine (AZT) is a chain terminating nucleoside analog reverse-transcriptase inhibitor (NRTI) that binds to the RT and prevents the RNA from converting into DNA. It has a greater affinity for reverse transcriptase than thymidine triphosphate. Therefore, RT incorporates AZT into the growing strands of HIV-1 DNA, and DNA synthesis and replication are terminated. Subsequently, antiretrovirals were designed to target various pathways/enzymes of the virus such as fusion/entry, reverse transcription, integration and protease cleavage (Figure 9) (Reviewed in (73)). Originally antiretrovirals were given as a monotherapy until it was demonstrated to be inefficient due to the high mutation rate and resistance of HIV-1. Therefore, a new concept was devised where patients receive a combination of a non-nucleoside reverse transcriptase inhibitor (NNRTI), an NRTI, and protease inhibitor (PI). This regimen is known as Highly Active Antiretroviral Therapy (HAART). Targeting the virus at multiple points in the viral life cycle at once significantly reduces the chance that resistant HIV-1 strains will arise (Reviewed in (73)). HAART does not cure the infection but rather keeps it under control. If a patient ceases HAART, the viremia rebounds due to latent reservoirs (74). The requirement for lifelong drug treatment, failure of therapeutics, and the cost of these therapeutics, especially in

third world countries that are most affected by HIV-1 is driving scientists to look for new avenues of treatment such as stem cell therapies.

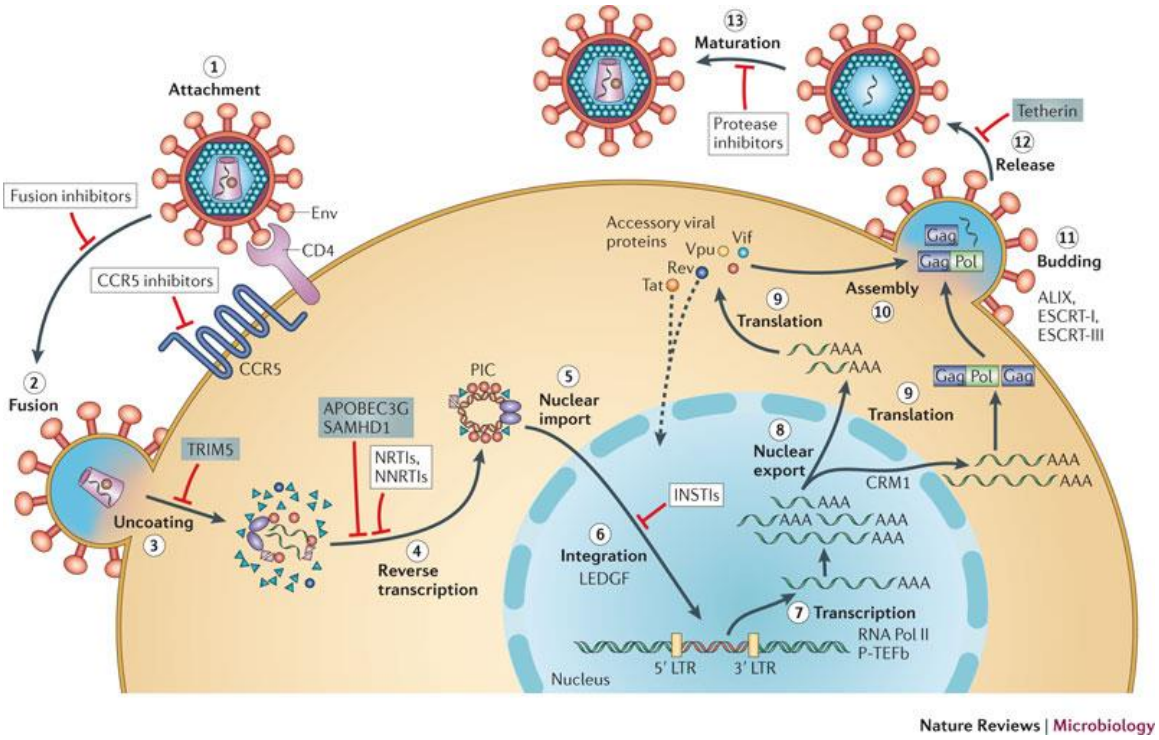

Figure 9. Antiretroviral drugs and their targets. Therapeutic drugs were developed to target HIV-1 at various steps in the life cycle. Currently, there are antiretrovirals that target fusion (CCR5 and gp41 agonists), reverse transcription inhibitors (non-nucleoside reverse transcriptase inhibitors (NNRTI), nucleoside reverse transcriptase inhibitors (NRTIs)), integrase inhibitors (INSTIs), and protease inhibitors (PRIs). Rights and Permissions granted from (16).

Autologous and Allogeneic Stem Cell Transplants

In the hope of finding a cure for HIV-1, an interesting observation was made in an HIV-1 positive patient suffering from acute myeloid lymphoma. To treat his lymphoma he received an allogeneic hematopoietic stem cell transplantation from a donor. This donor was homozygous for a specific CCR5 mutation which prevents the expression of the full-length protein (CCR5 Δ32). Subsequently, it was demonstrated that this patient Timothy Brown, also known as the Berlin Patient was functionally cured of HIV-1. Analysis demonstrated that there wasn't detectable viral replication in any lymphoid tissue four years following transplantation and disruption of HAART (75). These findings opened a whole new door to HIV-1 research that was aimed at recapitulating this effect (76). This is currently being explored by utilizing HSC-derived cells resistant to HIV-1 infection (allogeneic) or patient's own stem cells (autologous). While in theory the idea is simple, in practice it has proven to be much more complex. In addition to HSC transplants, other avenues are currently being explored to develop novel treatment strategies.

Cellular Restriction Factors of HIV-1

During an infection, HIV-1 antagonizes the host by impairing the immune system, and hijacking cellular proteins to successfully replicate in the host. However, the host has defenses against incoming viruses as well. One example of

the host defense is the expression of host proteins, known as restriction factors that inhibit viral infection. In the case of HIV-1, there are restriction factors that target various steps of the viral life cycle. The first restriction factor Fv1 was identified in mice and it prompted the search for other restriction factors. This protein dictates whether a mouse is resistant to a strain of murine leukemia virus MLV. Similarly to mice, in humans a restriction factor of N-tropic MLV (N-MLV) but not B-tropic MLV (B-MLV) was identified (more below) (77, 78). Afterwards, additional restriction factors were identified in humans and other mammalian species, demonstrating that these restriction factors are not unique to mice but are rather expressed in a variety of species. Following these initial discoveries, many studies identified restriction factors that restrict HIV-1 throughout its life cycle. These restriction factors are APOBEC3G, SAMHD1, TRIM5, and Tetherin/BST2. They target early and late events of the retroviral life cycle (Figure 10). For example, Tetherin/BST2 inhibits HIV-1 budding from the infected cell, while TRIM5 restricts the virus soon after entry into the target cell (16, 79).

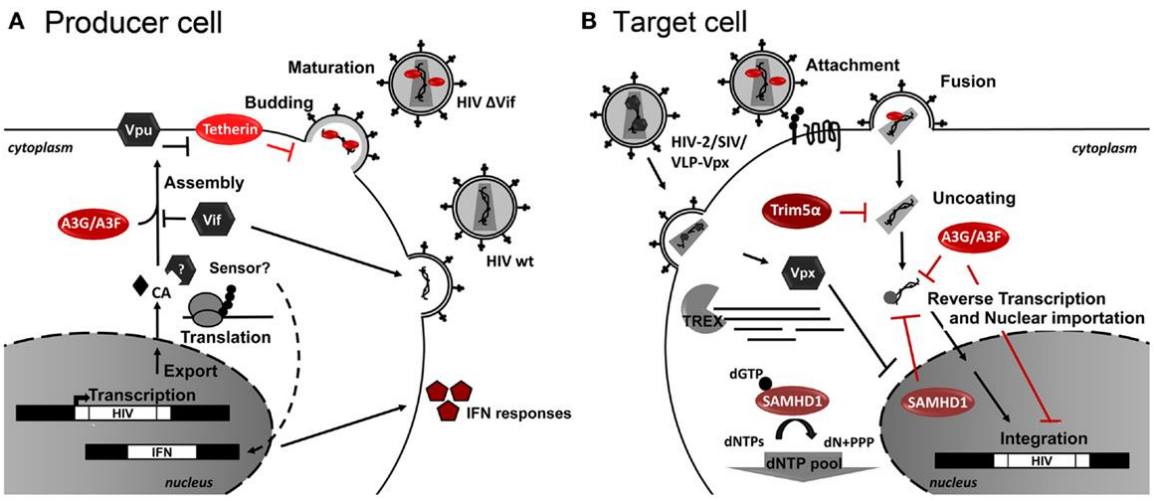

Figure 10. Restriction Factors. Many restriction factors exist in producer cells and target cells of HIV-1. In producer cells APOBEC3G and 3F are packaged into the virus. When the virus infects the target cell and begins to reverse transcribe, APOBEC3G and 3F induce numerous deoxycytidine to deoxyuridine mutations in the negative strand of the HIV DNA. If APOBEC3G and 3F are not present in those cells, other restriction factors such as TRIM5 and SAMHD1 act on early events on the viral life cycle by binding to the incoming viral core and depleting the pool of nucleotides, respectively. Another restriction factor, Tetherin prevents HIV-1 budding from the producer cell. Rights and Permissions granted from (80).

The TRIpartite Motif (TRIM) Family of Proteins

TRIpartite Motif (TRIM) family of proteins is a large family consisting of over 70 currently identified TRIMs. These proteins are expressed in a wide variety of species and participate in many cellular functions such as cell proliferation, differentiation, development, oncogenesis, innate immune signaling and viral restriction (81). Due to the large number of TRIM genes and their sequence homology, it suggests a rapid evolution of these genes by gene duplication (82, 83). In recent years extensive research has been done to further understand the mechanism by which these proteins perform their functions.

Domain Structure of TRIM Proteins

TRIM proteins are characterized by the presence of the RBCC motif that is composed of a really interesting new gene (RING) domain, one or two B-Boxes (B-Box1 and B-Box2), and a Coiled-Coil domain. These domains are conserved amongst the family of proteins. The RING domain is present at the N-terminus, which is usually found within 10-20 amino acids from the first methionine (84). Within the RING domain are conserved cysteine and histidine residues that are buried within the core. They help maintain the domain structure by binding two zinc atoms (85, 86). Most RING domains function as ubiquitin-protein isopeptide (E3) ligases (87), however some do not possess E3 activity themselves. Therefore, the RING domains that do not have intrinsic E3 activity interact with a second RING domain partner (88, 89). The B-box domains have a similarity in tertiary structure to the RING domain, suggesting that they arose from gene duplication from a

common ancestor (90). Like the RING domain, B-Box domains bind and coordinate zinc atoms and they are present in one or two copies (84, 91). B-Box domains were demonstrated to contain hydrophobic surfaces that are important for protein turnover, self-association and retroviral restriction (92-95). The coiled-coil domain is required for homo-interactions and hetero-interactions (96, 97). The ability of TRIM proteins to form higher molecular weight species and exist in discrete subcellular compartments within cells is mediated by self-association of the coiled-coil domain (84). One or more C-terminal domains that generally account for the unique function of each TRIM protein follow the RBCC motif. Roughly, two-thirds of TRIM proteins contain a B30.2/SPRY domain at the C-terminus (84). Within this domain there are four regions that contain extensive amino acid differences among TRIM proteins. These regions within B30.2/SPRY domain have been termed variable regions v1, v2, v3 and v4 (98). In the case of many TRIMs, the B30.2/SPRY domain mediates the recognition of many retroviruses as an antiviral response (99, 100) (Figure 11A).

TRIM5 Proteins

In 2004, Stremlau et al. identified TRIM5α as the protein responsible for restriction of HIV-1 infection in rhesus macaques (101). Owl monkeys (New World monkey species) express a restriction factor that is similar to rhesusTRIM5α that also restricts HIV-1. CyclophilinA (CypA) retrotransposition into the TRIM5 locus

occurred as a result of two independent events in the primate lineage to generate TRIMCypA (102-104) (Figure 11B). Additionally, TRIM5 proteins were shown to restrict other retroviruses in a wide-variety of species, including humans. In other species such as mice, a homolog of TRIM5 exists that restricts MLV. TRIM5 proteins (huTRIM5α, rhTRIM5α, and TRIMCyp) are interferon inducible and have been under strong positive selection as restriction factors against many retroviruses (84, 105).

TRIM5 is characterized by the presence of the RING domain, B-Box2, and Coiled-Coil domains that are conserved amongst the TRIM family of proteins (84). Each domain was demonstrated to participate in HIV-1 restriction. The RING domain is required for TRIM5 auto-ubiquitination, and it classifies TRIM5α as an E3-ubiquitin ligase (94, 106). Mutations in the RING domain reduce TRIM5α restriction of HIV-1 (94), suggesting a role for the ubiquitin-proteasome system (UPS) during restriction. The B-Box2 and Coiled-Coil mediate higher order self-association and dimerization of TRIM5, respectively those are necessary for restriction (93-95, 107, 108). At the C-terminus, TRIM5α has a B30.2/SPRY domain, which recognizes and directly binds to the retroviral core (Figure 11A). This domain determines the species-specificity of retroviral restriction that is mediated by TRIM5.

Like TRIM5α, TRIMCyp restricts retroviral infection by recognizing and binding to CA with CypA and disrupting the retroviral capsid after it enters into the target cell before reverse transcription (102, 104, 109, 110). In the case of human

TRIM5α, it restricts N-MLV and Equine Infectious Anemia Virus (EIAV) but it does not restrict B-MLV and HIV-1 (Figure 12). However, rhTRIM5α and TRIMCyp restrict HIV-1 and also N-MLV (Figure 12) (77, 111).

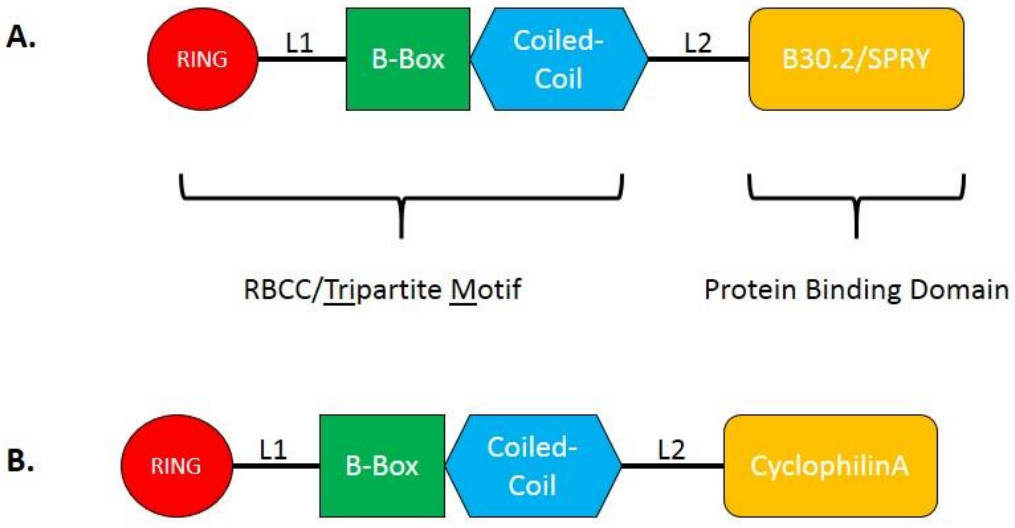

Figure 11. Domain Organization of TRIM5 Proteins. Tripartite motif containing family of proteins consist of an RBCC motif (RING, B-Box and Coiled-Coil) followed by a variable C-terminal domain. A. TRIM5α contains a B30.2/SPRY domain at the C-terminus that recognizes the incoming viral capsid to mediate species-specific restriction. B. TRIMCyp contains a CyclophilinA domain at the C-terminus that recognizes the incoming viral capsid as well. Adapted and Modified from (112).

A.

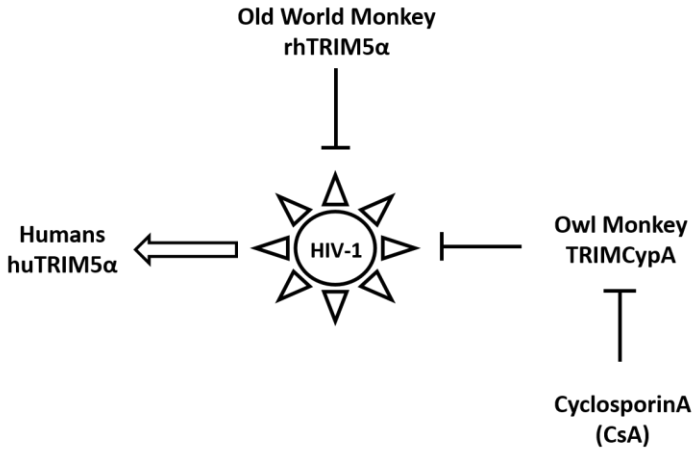

B.

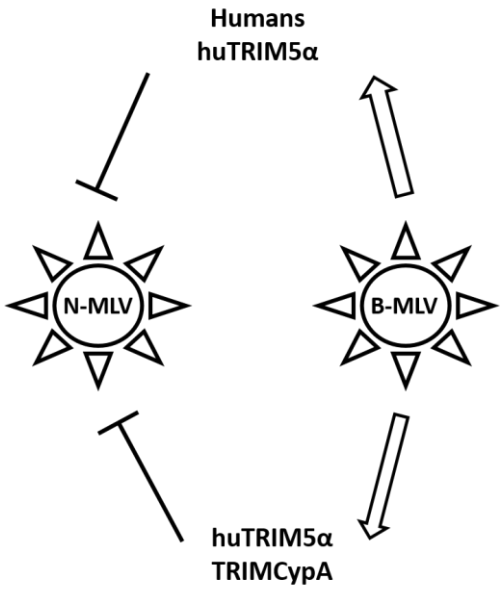

Figure 12. Restriction of retroviruses by TRIM5. A. rhTRIM5α and TRIMCypA potently restrict HIV-1 by binding to the intact viral core, while huTRIM5α does not bind well to the HIV-1 capsid and it does not restrict infection. CyclosporinA (CsA), a drug, can be used to block TRIMCyp from functioning in experiments. **B.** huTRIM5, rhTRIM5 and TRIMCypA block N-MLV but they do not block B-MLV. Once again, this restriction is carried out by binding to the incoming intact core. Adapted and modified from (112).

Cytoplasmic Body (Cytoplasmic Assembly) Formation of TRIM5 during Restriction

To elucidate the mechanism by which TRIM5 proteins restrict retroviruses, many mutagenesis and biochemical studies were performed on the proteins. It was quickly determined that TRIM5 proteins were difficult to purify and work with in biochemical studies due to their propensity to self-associate. In the TRIM5α literature, self-association is used to describe the higher order association of TRIM5α dimers. To remain clear and consistent with literature, I will use self-association this way and explicitly state dimerization where appropriate. TRIM5 proteins and most members of the TRIM family of proteins have conserved domains and regions that are responsible for this self-association capability. The coiled coil domain is required for hetero and homodimerization (107, 113), B-Box2, and Linker 2 are responsible for higher-order multimerization (93-95, 114, 115), that will eventually assemble into what we refer to as cytoplasmic bodies (cytoplasmic assemblies), primarily facilitated by Linker 2 (115).

The biological significance of cytoplasmic bodies in TRIM5-mediated retroviral restriction was controversial due to two studies demonstrating that pre-existing cytoplasmic bodies are not required for HIV-1 restriction (116, 117). Song et al. demonstrated that treatment with geldanamycin, a heat shock protein 90 (Hsp90) inhibitor prevented the formation of TRIM5α cytoplasmic bodies without having an effect on the ability of these cells to restrict HIV-1 infection (117). In the second study, treatment of cells with sodium butyrate resulted in a 10-fold increase

in TRIM-Cyp levels and an increase in TRIM-Cyp localization to cytoplasmic bodies. However, the localization of TRIM-Cyp to cytoplasmic bodies in these cells did not dramatically increase HIV-1 restriction (116). Critically, these experiments examined cytoplasmic body formation prior to infection, they did not determine if cytoplasmic bodies formed during restriction. Therefore, these studies demonstrated that pre-existing cytoplasmic bodies are not relevant for HIV-1 restriction. However, it was demonstrated that TRIM5α cytoplasmic bodies are dynamic structures that turn over rapidly and traffic on microtubules (118). When cells that express TRIM5α were treated with the proteasome inhibitor MG132, it resulted in accumulation of virions within large rhTRIM5α cytoplasmic bodies. Additionally, live cell imaging demonstrated *de novo* formation of rhTRIM5α cytoplasmic bodies around individual virions, which was followed by the loss of the fluorescent signal within 3-5 minutes (119). This data suggests that TRIM5α cytoplasmic bodies that are formed in the presence of restriction sensitive virus are important and relevant for restriction. It was further demonstrated that certain residues within the Linker 2 region mediate the formation of cytoplasmic bodies. RhTRIM5α Linker 2 mutants that were unable to form cytoplasmic bodies also lost the ability to restrict HIV-1 (115). This suggests that the ability of TRIM5α to form these bodies during infection is required for the restriction process.

Capsid Recognition and Retroviral Restriction

It is well known that TRIM5α binds to the intact retroviral core soon after it enters the cytoplasm by recognizing specific determinants in the capsid. Pornillos et al. proposed a model of this binding in which TRIM5 assembles into a large hexameric lattice over the smaller HIV-1 hexameric capsid lattice (Figure 13). As mentioned above, the B30.2/SPRY domain of rhTRIM5α/huTRIM5α and the Cyclophilin A domain of TRIMCypA mediate the recognition of the retroviral capsid. Within B30.2/SPRY domain there are variable regions/loops that evolved to recognize the capsid in a species-specific manner (120). It was demonstrated that the major determinant of restriction in TRIM5α is the amino terminal segment of B30.2 V1 region. Specifically, huTRIM5α H (R328-332) and H (R323-332) mutants inhibit HIV-1 to levels comparable to rhTRIM5α. In addition, huTRIM5α R332P potently restricts HIV-1 as well, unlike the wt huTRIM5α. These data demonstrate that the B30.2 domain is the major determinant for the ability to restrict HIV-1 between human and rhesus macaque TRIM5α and that specific amino acids within the B30.2 domain mediate this specificity (99).

Following recognition of the CA, a poorly understood mechanism occurs to mediate restriction of infection. One reason for the difficulty in defining the precise mechanism of action is that TRIM5alpha binds the capsid in a context of an assembled core and not free capsid monomers. While TRIM5alpha can interact with capsid monomers, the interaction is extremely weak (121). The ability to purify

recombinant/modified HIV-1 CA and assemble it into tubes CA tubes (to serve as a model system for the HIV-1 core) is providing some insight into TRIM5 mechanism of restriction. To further elucidate the mechanism of TRIM5-mediated restriction a few models have been proposed.

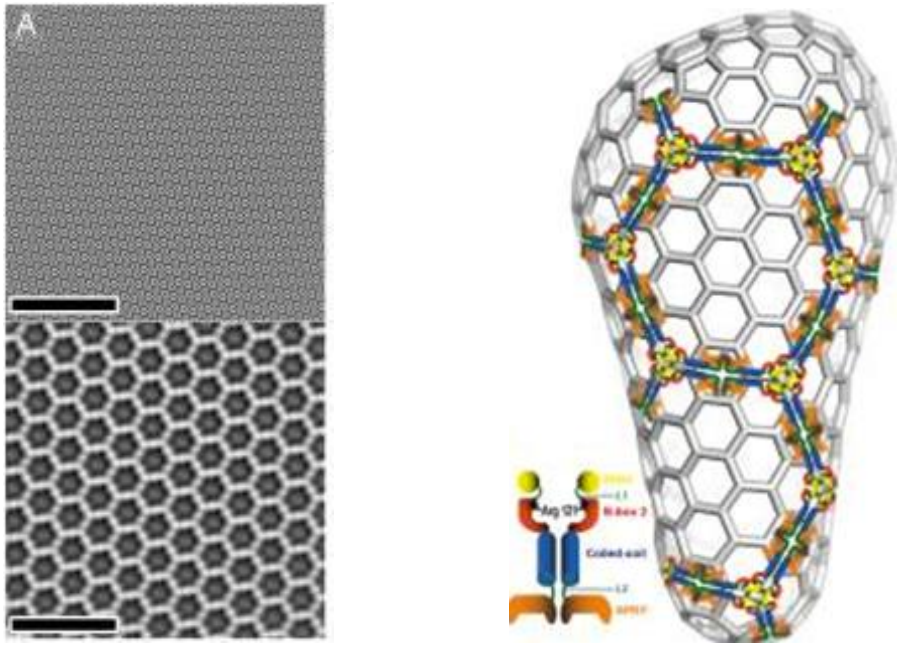

Figure 13. Model of TRIM5α Assembly around HIV-1 Core. In **A** the top image are the capsid-nucleocapsid (CA-NC) hexameric lattice crystals alone and the bottom image is TRIM5-21R (RING domain of TRIM5 was replaced by RING domain of TRIM21 for purification) hexameric lattice crystals alone. The TRIM5-21R hexameric lattice forms in absence of virus but it forms more efficiently when the capsid hexameric lattice is present. On the left is the proposed model of TRIM5α hexagonal assembly around the HIV-1 assembled core. Rights and Permissions granted from PNAS (122).

Two-Step Model of Restriction

The Hope lab proposed this particular model where TRIM5-medated restriction occurs in two steps. Following proteasome inhibition, in cells expressing rhTRIMα, reverse transcription products were alleviated but infection was still restricted. Further, proteasome inhibition did not prevent the formation of a functional PIC (as measured by the ability to integrate into DNA in *in vitro* experiments), but it was defective for nuclear import (123). This suggests that the pre-integration complexes generated in presence of TRIM5 and proteasome inhibition are functional but are inhibited from translocating into the nucleus due to TRIM5. Additionally, it was demonstrated by the Aiken lab that TRIM5 is degraded in a proteasome-dependent mechanism in presence of restriction sensitive virus (124). Finally, when TRIM5 expressing cells were treated with a proteasome inhibitor and infected with fluorescently labeled viruses, it was demonstrated that these viruses were sequestered in large TRIM5 cytoplasmic bodies (119). These data generated the two-step model of restriction. Following entry into the target cell, TRIM5 will bind to the assembled core via the CypA or SPRY domain and prevent reverse transcript products from being synthesized. This recognition and binding is sufficient to restrict the virus. However, if proteasome function is inhibited (utilizing MG132 drug) in presence of TRIM5, the virus reverse transcribes the genome but remains restricted (123, 125) (Figure 14). All these data suggest that there is a proteasome component to TRIM5 restriction of retroviruses, but the precise mechanism and the interaction with the proteasome components and other

host proteins are not known.

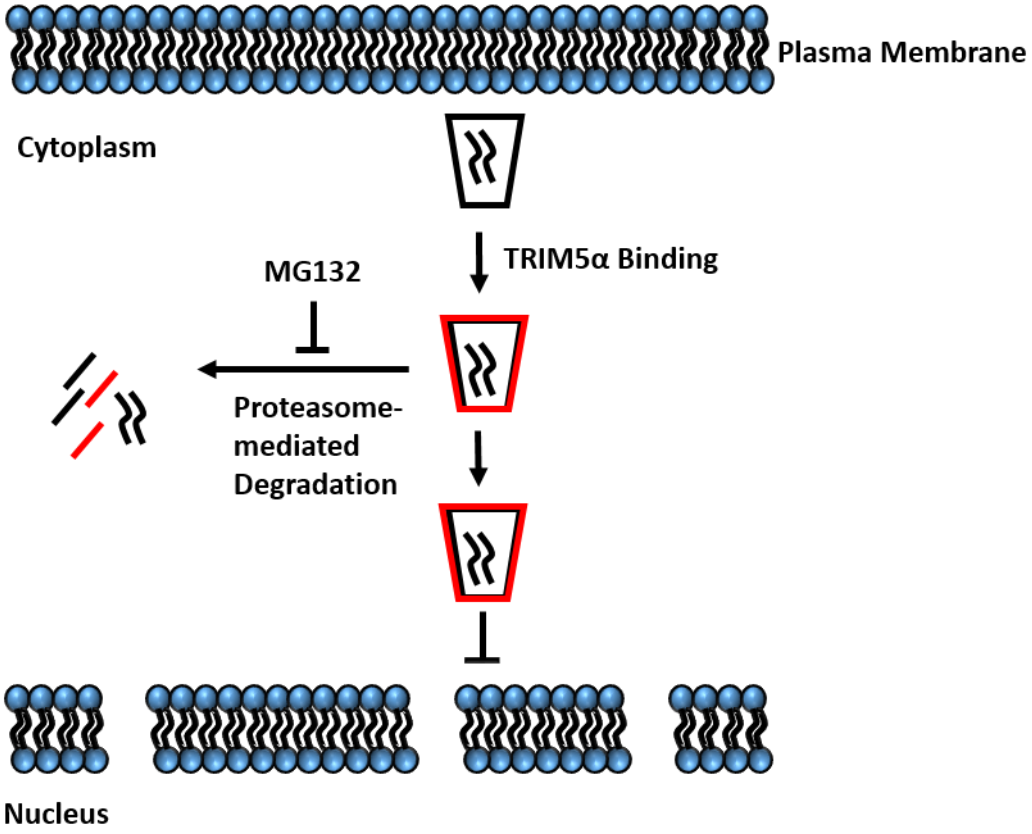

Figure 14. Two-Step Model of TRIM5-mediated Restriction. Following entry into the target cell, rhTRIM5α binds to the HIV-1 core, which prevents accumulation of late RT products and further infection of the cell. However, in the presence of a proteasome inhibitor in rhTRIM5α expressing cells, late RT products are relieved and a functional PIC is generated but the infection is still restricted. This suggests that there is a proteasome-dependent step in rhTRIM5α restriction of HIV-1. Adapted and Modified from (125).

Accelerated Uncoating

Another mechanism by which TRIM5alpha is hypothesized to restrict HIV-1 is by binding to the assembled core and prematurely uncoating it (accelerating uncoating). The Sodroski lab utilized the fate of capsid assay to measure the disassembly of the assembled viral capsid. In this assay they measured the amount of pelletable capsid (intact cores) at the bottom of the sucrose cushion following an infection in presence of TRIM5 and compared it to capsid in the top fractions (uncoated or free capsid) of the sucrose cushion. These studies showed that TRIM5α lead to a decrease in the amount of pelletable capsid and an increase in free capsid, without affecting the total amount of capsid present in the cells. This data suggests that TRIM5α mediates an accelerated uncoating of the incoming assembled capsid (126). Recently, the Bieniasz lab used a biochemical assay to determine the fate of various components of the retroviral core when the infection was carried out in the presence and absence of TRIM5 proteins (127). Following synchronized infection of cells lacking glycosaminoglycans (for efficient and specific virus fusion) with VSV-g-pseudotyped retroviruses (MLV and HIV-1), the cytosolic proteins were fractionated on linear gradients. The state of viral core components including capsid, integrase, viral RNA and RT were monitored. They demonstrated that in absence of TRIM5 proteins the retroviral core components formed large subviral complexes because they sediment to the lower fractions of the sucrose gradient. However, in the presence of huTRIM5α, N-MLV infection was restricted

and the IN and RT products could not be detected while the capsid and the viral genomic RNA were both in soluble fractions (top fractions), suggesting disassembly. Similarly, loss of IN, RT and the viral RNA was observed upon restriction of HIV-1 by rhTRIM5α and TRIM-Cyp. However, even though CA was lost from the bottom fractions, additional soluble CA was not observed due to the already large amount of soluble CA present in non-restricting (without TRIM5) and restricting conditions, possibly due to the instability of HIV-1 cores in sucrose gradients. As previously demonstrated, the inhibition of the proteasome blocked these consequences of TRIM5-mediated restriction without affecting viral restriction. These data do not support the model proposed by the Gallay laboratory suggesting that capsid degradation occurs rapidly in a proteasome-independent manner (128) but it does support the Two-Step model of restriction proposed by the Hope laboratory (125) and the accelerated uncoating model (126).

Role of TRIM Proteins in Innate Immune Signaling and Viral Restriction

In evolutionary studies, the time frame of TRIM gene expansion coincided with the emergence of traits specific to the adaptive immune system, suggesting a role for TRIM proteins in the function of the immune system. Many organisms that have a complex immune system also have a large number of TRIM genes (129). The short arm of chromosome 11 contains many TRIMs that were demonstrated to restrict either a single virus or multiple viruses (TRIM3/5/6/21/22/34/66/68). Also, a screen for antiretroviral activity involving over 50 TRIMs revealed 20 of

them with the ability to inhibit entry or release of retroviruses (130). Additionally, it was shown that many of these TRIMs are under great positive selective pressure, demonstrating their importance in the organisms. Many of these TRIM proteins were shown to restrict a wide-variety of viruses, either by directly inhibiting them at a particular step in the viral life cycle or indirectly by regulating the antiviral cell signaling (82, 83, 130-134). They can stimulate cytokine-signaling pathways that result in induction of many interferon-stimulated genes (ISGs) or target proteins for proteasome-mediated degradation. One well-known TRIM that promotes immune signaling is TRIM25. It was shown that it interacts with RIG-I and acts as an ubiquitin E3 ligase, which promotes RIG-I K63 linked polyubiquitination. In cells deficient of TRIM25, they fail to induce cytokines in response to viruses that are normally sensed by RIG-I. On the other hand, a virus like influenza A has a non-structural protein 1 (NS1) that interacts with TRIM25 to prevent it from ubiquitinating RIG-I and initiating an antiviral response (135). Like TRIM25, many TRIMs positively and negatively regulate many signaling pathways.

Additionally, TRIM5 was shown to act as a pattern recognition receptor (PRR) during a viral infection. TRIM5α activates signaling pathways that lead to the activation of NF-κB and AP-1. In order to activate signaling pathways, TRIM5α associates with the TAK1 complex, which includes TAK1, TAB1 and TAB2. Additionally, it interacts with E2 ubiquitin conjugation enzymes UBC13 and UEV1a to promote the synthesis of unanchored K63 linked ubiquitin chains. This results in the activation of TAK1 and subsequent expression of NF-κB and AP-1-dependent

genes (Figure 15). TRIM5α-mediated signaling occurs in the absence of virus, but the binding of TRIM5α to HIV-1 capsid lattice enhances the signaling cascade. Therefore, not only does TRIM5α mediate quick destruction of the retroviral capsid soon after it enters the cytoplasm, but it also functions as a PRR to recognize the capsid and activate inflammatory signaling pathways (136).

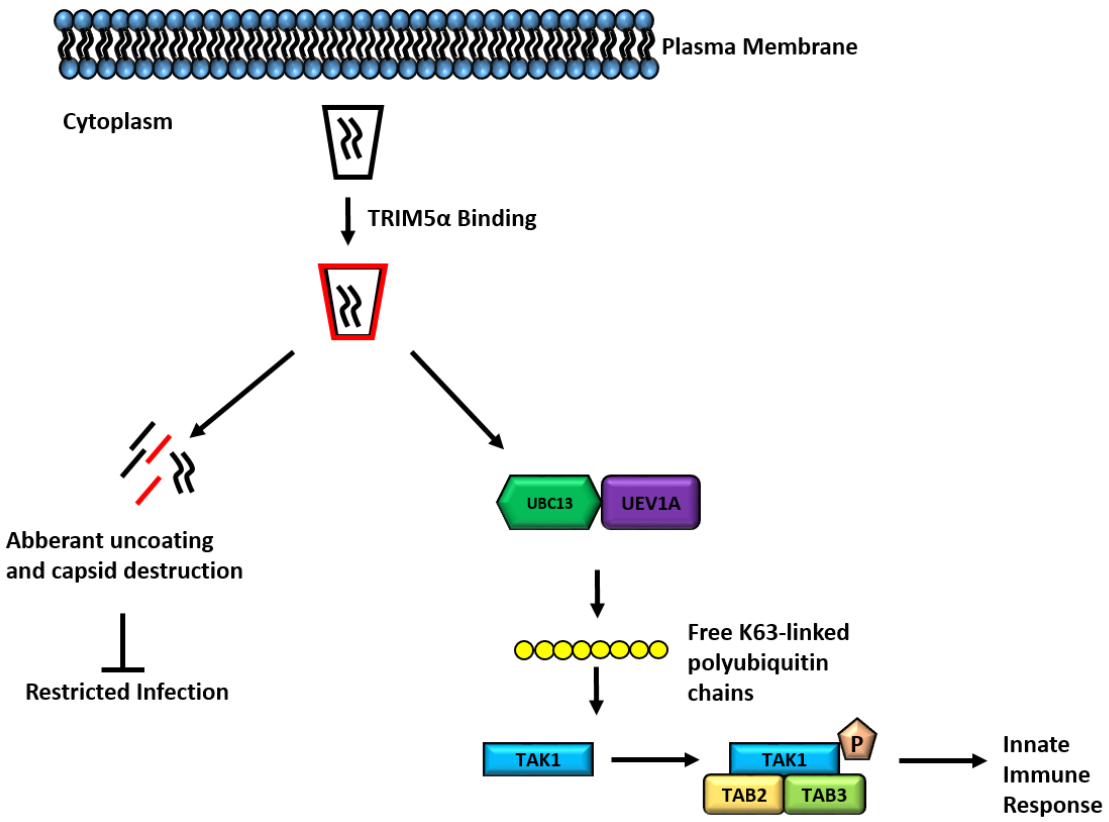

Figure 15. TRIM5 Innate Immune Signaling. Following entry into the cytoplasm, the viral core is recognized by TRIM5, which will restrict further infection from occurring. Additionally, TRIM5 along with UBC13/UEV1A generate unanchored K63-linked poly-Ub chains that activate TAK1 (that associates with TAB2 and TAB3) and initiate NF-κB and AP-1 dependent innate immune responses. While signaling occurs in absence of virus, these activities are enhanced in presence of restriction sensitive virus. Adapted and modified from (136).

Host Protein Involvement during TRIM5 Retroviral Restriction

While the basic mechanism of TRIM5-mediated restriction of retroviruses was determined, the precise players involved in the process have yet to be identified. A few different properties of the viruses and TRIM5 have provided some clues as to the possible interacting proteins. As mentioned above, the RING domain in TRIM5 proteins hinted at the possibility of the proteasome-ubiquitin system (UPS)-dependent mechanism of restriction that was demonstrated in the two-step model of restriction. Additionally, other proteins have been implicated in TRIM5-mediated restriction of retroviruses that will be discussed below.

Proteasome-Ubiquitin System (UPS)

26S Proteasome Complex

The 26S proteasome is an ATP-dependent protease that functions with the ubiquitin system in many different processes. The ubiquitin system, amongst other things, tags proteins with polyubiquitin chains as a marker for protein degradation by the proteasome. The proteasome is involved in many different processes, including DNA repair, cell-cycle progression, apoptosis, immune response, signal transduction, metabolism, developmental programs, and of course protein quality control. It is a large complex that consists of two parts: the catalytic 20S core particle (CP) and the 19S regulatory particle (RP) that are further divided into multiple subunits. The 20S CP is a cylindrical structure that is formed by stacking of two α-rings (outer) and two β-rings (inner) that are each composed of seven subunits (Figure 16). The β-rings form a proteolytic chamber of which, β1, β2

and β5 subunits have hydrolytic activity as Threonine proteases. They cleave peptide bonds at the carboxyl-terminal side after acidic, basic, and hydrophobic residues, respectively. These activities are often referred to as caspase-like activity, trypsin-like activity and chymotrypsin-like activity, respectively.

The 19S RP is further subdivided into a lid and a base that recognize and unfold the substrate. The base is composed of six different homologous AAA+ ATPase subunits, regulatory particle triple-A protein 1 (RPT1/PSMC2)-RPT6, and three non-ATPase subunits, regulatory particle non-ATPase 1 (RPN1), RPN2 and RPN13. The ATPase subunits are required for substrate unfolding and α-ring channel opening. Specifically, RPN1, RPN13, RPT5, and RPN10 capture ubiquitinated proteins. RPN10 sits at the interphase between the base and the lid. The lid is composed of nine non-ATPase subunits: RPN3, RPN5-RPN9, RPN11, RPN12 an RPN15 (Figure 16). The function of most of these subunits is not known, but RPN11, a metalloisopeptidase is important for de-ubiquitination of captured substrates. The 19S RP can attach at one or both ends of the 20S proteasome to generate a 26S proteasome complex (137).

Since TRIM5 proteins contain a RING domain at the N-terminus, it was thought that the intrinsic E3-ubiquitin ligase activity might be important for restriction. As mentioned above, when cells were treated with a pharmacological inhibitor of the proteasome (MG132), reverse transcription products were observed in presence of TRIM5, which are usually undetected during restriction (123, 125).

This would suggest that there is a proteasome dependent step during the restriction process. However, an inhibitor such as MG132 not only inhibits the proteasome but also depletes the free ubiquitin pool in the cells, which is important since we know from the Pertel et al. study that TRIM5 generates unanchored polyubiquitin chains during innate immune signaling and restriction (136). Ubiquitin is required for proteasome degradation because substrates that are degraded via proteasomes are polyubiquitinated by the ubiquitin conjugation pathway (137).

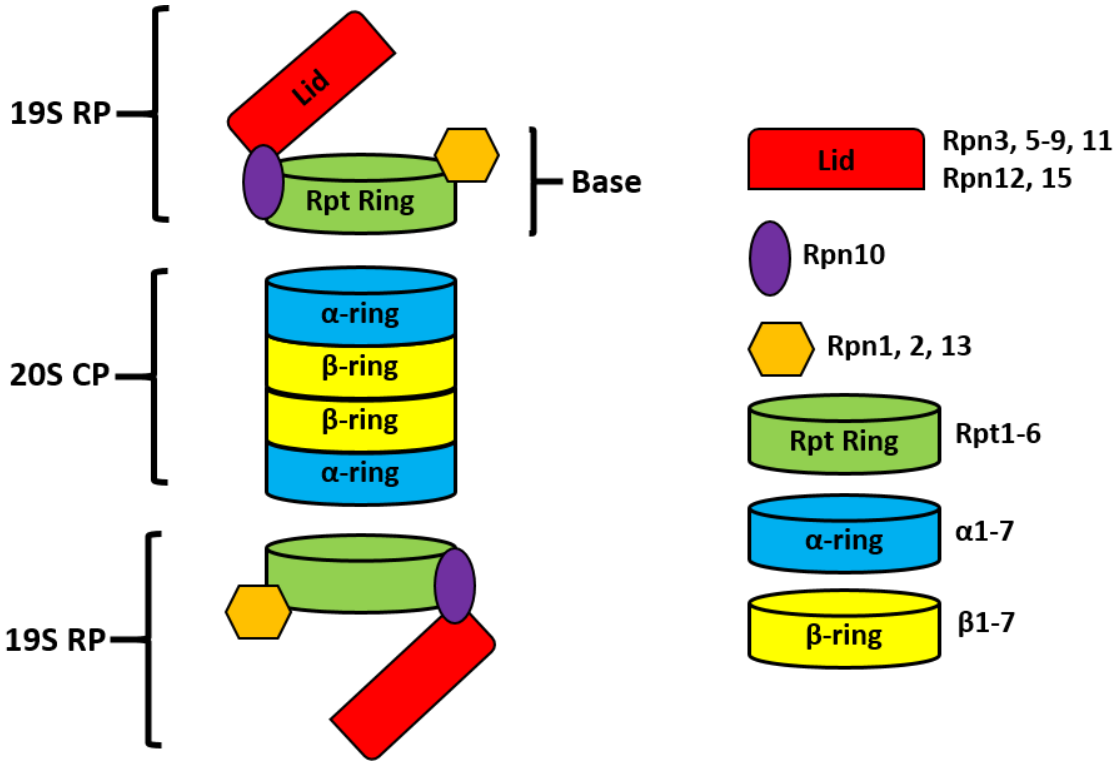

Figure 16. 26S Proteasome Complex. The 26S proteasome is a large complex that is divided into the 19S regulatory particle (19S RP) and the 20S core particle (20S CP). The 19S RP is further divided into a lid and a base. The base contains RPT1-6 subunits (green), while the lid contains subunits RPN3, 5-9, 11, 12, and 15 (red). RPN10 (purple) sits at the interphase between the base and the lid. The lid is thought to capture ubiquitinated cargo while the base facilitates the threading of the substrate to the core particle. The 20S CP is a barrel that consists of two α-rings (blue) and two β-rings (yellow). The α-ring is composed of α1-6 subunits and the β-ring is composed of β1-6 subunits of which β1, β2, and β5 are catalytically active. Modified and Adapted from (138).

Ubiquitin Conjugation Pathway

Ubiquitin (Ub) is a protein that is involved in post-translational modification of other proteins to lead to a variety of downstream events such as signaling, and degradation. It is a 76 residue long protein with seven lysines in positions 6, 11, 27, 29, 33, 48 and 63. The most common ubiquitin polymer that targets substrates for degradation via the proteasome is a chain where the Ub molecules are linked to one another via an isopeptide bond between the C-terminal Gly76 of the distal molecule and Lys48 of the previously conjugated one. The K48-based polyubiquitin chains on proteins are the canonical modification and signal for proteasomal degradation. However, some proteins that are monoubiquitinated or polyubiquitinated with chains linked in Lys48-independent manner are also degraded via the proteasome (Figure 17B). The conjugation of Ub on substrates is ATP dependent and it involves activating enzymes (E1), conjugating enzymes (E2) and ligases (E3) (Figure 17A). To achieve high specificity for a variety of proteins and processes, cells express many different E2 enzymes and an even greater number of E3s of which the RING and HECT families are the most common (139).

TRIM5α is an E3-ubiquitin ligase and this activity lies in the RING domain of the protein. With the E2 conjugating enzyme UbcH5b, it can autoubiqitinate its' self. Basally, TRIM5 itself is not degraded in a proteasome-dependent manner (106); however, in presence of virus it becomes sensitive to proteasome degradation by an unknown mechanism. This suggests that the virus is also degraded by the

proteasome during restriction; however, the data cannot discern the fate of the viral core degradation (124). Mutagenesis studies of the RING domain demonstrated that mutants that lost the ability to self-ubiquitinate also lost the ability to restrict HIV-1. The mutations were located in the E2-binding region of the RING domain (140). This suggests that the ability to self-ubiquitinate is important for retroviral restriction. Also, another study also looked at mutations in the RING domain. In their experiments, mutations in the RING domain of TRIM5 E3 ubiquitin ligase activity correlated with the potency of restriction of HIV-1 infection by TRIM5α_{rh} RING mutants, consistent with previously reported results. However, all the mutants tested were able to restrict HIV-1 infection with at least moderate potency. Therefore, RING-mediated E3 ubiquitin ligase activity may not be absolutely essential for the early restriction of HIV-1 infection (141). However, the results are difficult to interpret due to the nature of the experiments being performed *in vitro* in absence of any other host proteins. Moreover, as mentioned above, Pertel et al. demonstrated that TRIM5 with the help of the ubiquitin-conjugating enzyme UBC13-UEV1A catalyzes the formation of unanchored K63-linked polyubiquitin chains that activate the TAK1 kinase complex and consequently stimulate AP-1 and NF-κB (136).

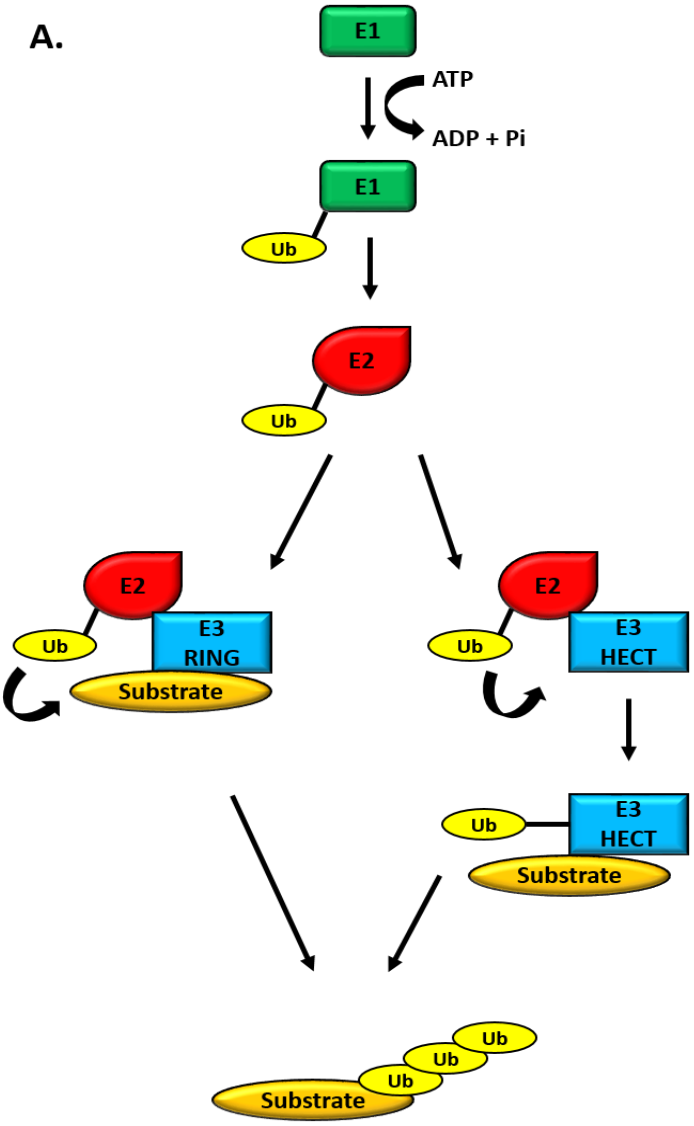
A.
E1
ATP
ADP + Pi
E1
Ub
E2
Ub
E2
Ub
E3
RING
Substrate
E2
Ub
E3
HECT
Ub
E3
HECT
Substrate
Ub
Ub
Ub
Substrate

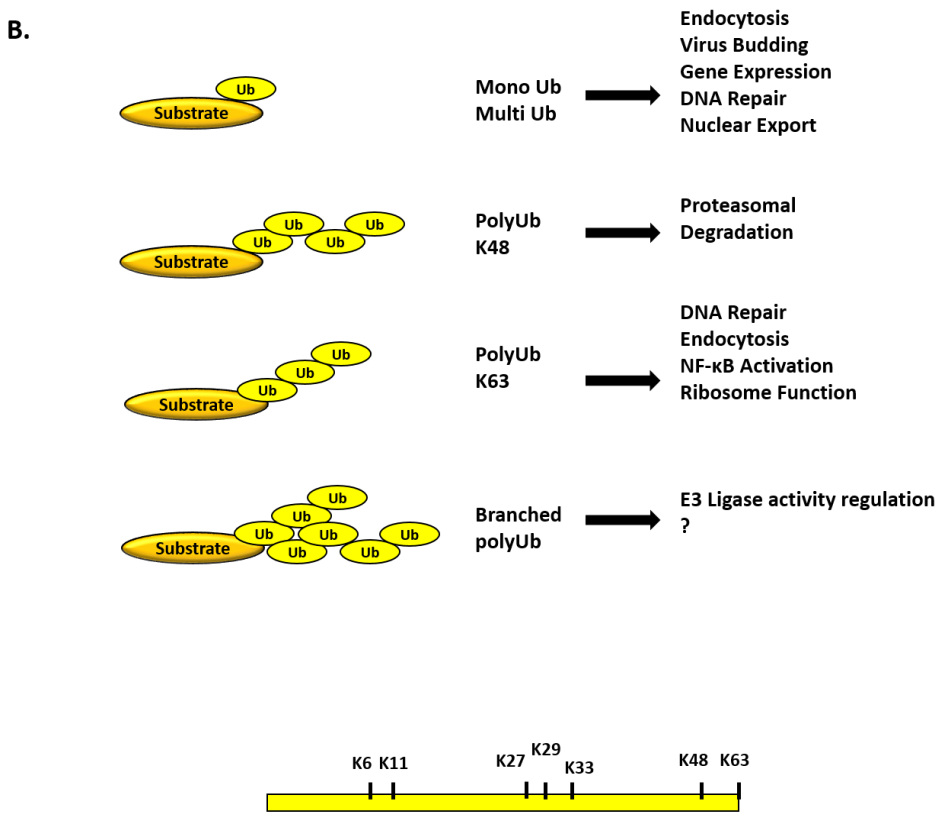

Figure 17. The ubiquitin conjugation pathway and modifications. A. Conjugation of substrates requires three groups of enzymes: an activating enzyme (E1), a conjugating enzyme (E2), and a ligase (E3). This ATP-dependent mechanism conjugates mono and poly ubiquitins onto substrates. **B.** Diagram demonstrating different forms of ubiquitin modifications and the functional roles of these modifications. Modified and Adapted from (142).

SUMO Conjugation Pathway

Similar to ubiquitin, another post-translational modification that was shown to function in TRIM5-mediated restriction of viruses is a small ubiquitin-like modifier 1 (SUMO-1). SUMOylation, like ubiquitination acts on a large variety of substrates as a post-translational modification to regulate processes such as intracellular trafficking, cell cycle progression, transcription, and DNA repair. It has a much simpler conjugation pathway that involves an E1 (AOS1-UBA2), a single E2 (Ubc9) and a few E3 ligases (Figure 18A). SUMOylation machinery usually targets a lysine residue within a consensus sequence (ΨKxE, where Ψ is a hydrophobic residue and x is any amino acid), but other lysines outside of this sequence can be modified too. Vertebrates have three SUMO variants (SUMO-1, 2 and 3). SUMO is produced as a precursor protein that is processed to the mature form by SUMO-specific proteases. During this process, some amino acids are removed from the C terminus of SUMO to reveal a di-glycine motif that is required for the attachment to target proteins. Predominantly, SUMO is present in the nucleus and most SUMOylation events occur within the nucleus as well (143). Additionally, there are specific motifs that mediate non-covalent interactions with SUMO modified proteins. These SUMO-interacting motifs (SIMs) have the consensus sequence V/I/L-x-V/I/L-V/I/L or V/I/L-V/I/L-x-V/I/L (where x is any amino acid) (Song et al. J Biol Cem 2005, Hecker et al. J Bio Chem 2006). Therefore, a protein does not need to be directly SUMOylated, but rather it can non-covalently interact with a SUMO

molecule that is attached to another protein (Figure 18B). SUMO is known to be involved in virus replication by modifying either viral or host proteins to impair infection. Conversely, viruses have mechanisms to counteract the pathway as well (144, 145). In the case of Mazon-Pfizer monkey virus, Moloney murine leukemia virus (MoMLV) and HIV-1, Gag proteins are known to interact with the SUMO-conjugation pathway (106, 146, 147). The E2 and E3 SUMO-conjugating enzymes, UBC9 and PIAS4/y interact with the capsid (CA) protein of MLV to conjugate SUMO on it. Mutagenesis of lysine residues eliminated CA SUMO conjugation and impaired virus replication after reverse transcription before nuclear entry (148), suggesting SUMO involvement in successful MLV infection.

Furthermore, huTRIM5α restriction of N-MLV is enhanced when SUMO levels are increased. This restriction is dependent on SUMOylation of CA. Additionally, three SIMs were identified in the B30.2 domain of huTRIM5α of which two SIMs are required for the enhanced N-MLV restriction (149). This data suggests that binding to SUMO-modified CA via the two SIMs enhances huTRIM5α restriction of CA.

Overall there is significant evidence that host proteins interact with TRIM5α and the viral core to restrict and facilitate infection. While the mechanism of TRIM5α restriction of HIV-1 has been determined, the precise proteins that aid in the process have yet to be identified. Additionally, if other proteins interact with the HIV-1 core to facilitate uncoating is not known. This dissertation provides evidence that the proteins in the ubiquitin-proteasome system and SUMO-conjugation

pathway play a role in TRIM5α-mediated restriction of HIV-1. Furthermore, it demonstrates that not only does HIV-1 traffic on microtubules, but also utilizes the microtubule network to facilitate uncoating of the viral core.

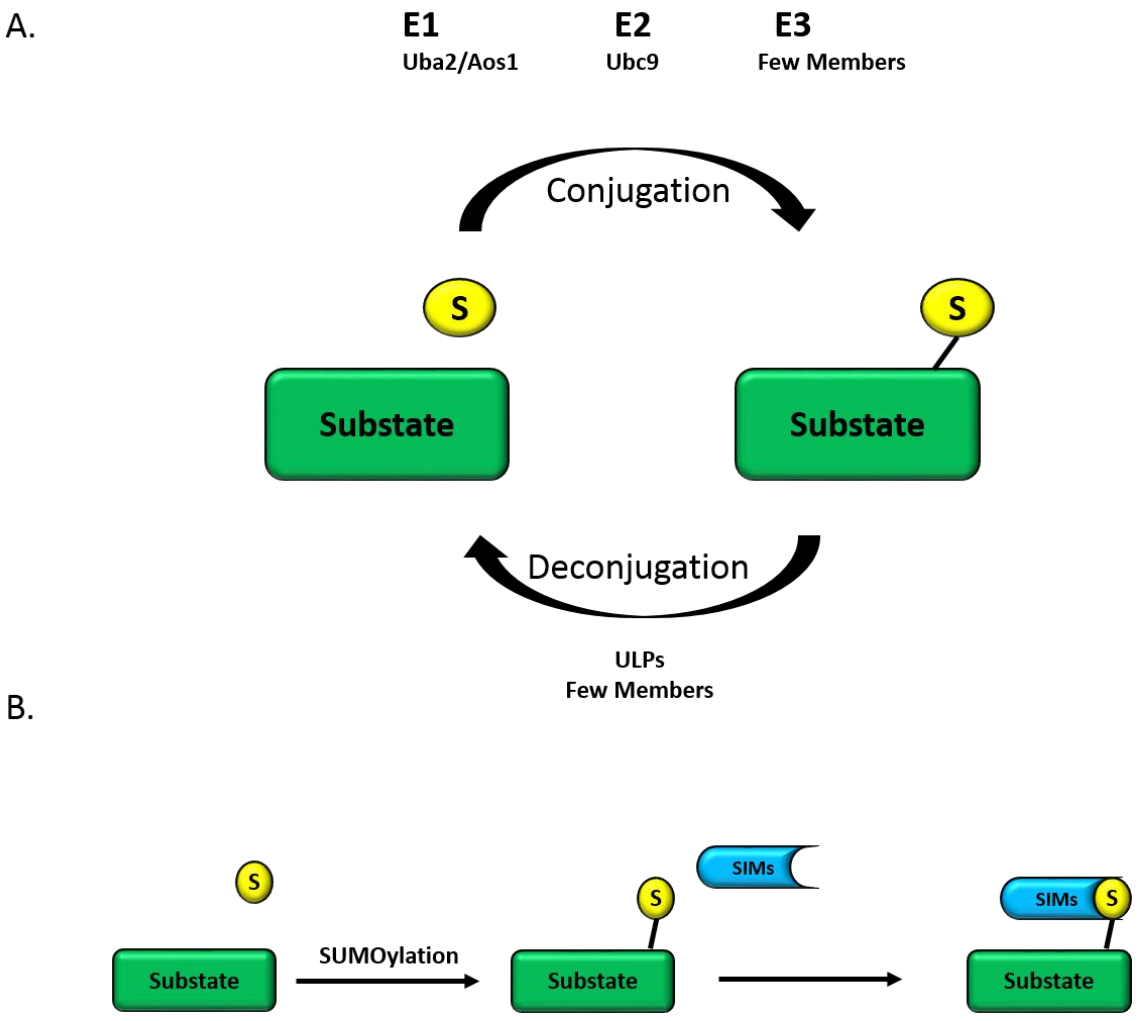

Figure 18. SUMO Conjugation Pathway and SUMO Interacting Motifs (SIMs). A. The conjugation pathway that involves an E1 (AOS1-UBA2), a single E2 (Ubc9) and a few E3 ligases. Just like ubiquitin conjugation, the SUMO conjugation is an ATP-dependent process. **B.** It was demonstrated that SUMO-interacting motifs mediate non-covalent interactions with SUMO modified proteins. A protein does not need to be directly SUMOylated, but rather it can non-covalently interact with a SUMO molecule that is attached to another protein. Adapted and Modified from (150).

CHAPTER II

MATERIALS AND EXPERIMENTAL METHODS

Cell Lines and Viruses

Tissue culture reagents were obtained from Hyclone and Fisher Scientific. HeLa, TE671, CRFK and 293T cells were kindly provided by Dr. Tom Hope, Ph.D. (Northwestern University). OMK cells were a kind gift from Dr. Theodora Hatziioannou, Ph.D. (ADARC). All cells were maintained in Dulbecco modified Eagle medium (DMEM, Hyclone) supplemented with 10% Fetile Bovine Serum (FBS, Fisher Scientific), 100 IU/ml penicillin, 1 mg/ml streptomycin, and 0.01 mg/ml ciprofloxacin hydrochloride.

HeLa cells stably expressing HA-rhTRIM5α were previously described (Wu, PNAS 2008, Stremlau Nature 2004) or YFP-rhTRIM5α (119). To generate HeLa cells to measure cytoplasmic body formation during viral infection, cells were transduced with YFP-rhTRIM5α retroviral vector and then selected in G418 (400 μg/mL) containing media. Single colony clones were screened by immunofluorescence to identify a cell line that expressed YFP-rhTRIM5α containing reduced pre-existing cytoplasmic bodies in the absence of restriction sensitive virus (diffuse phenotype).

In order to study aspects of a viral infection in laboratory settings, HIV-1 reporter viruses were generated to harbor GFP or Luciferase cassettes usually in

place of the viral accessory protein Nef. They are single cycle replication defective viruses. In most proviruses, envelope was deleted to allow for pseudotyping with envelopes from other viruses (ex: VSVg, AMLV) (Figure 19A). Pseudotyping is useful for safety measures and for infection of variety of cell types since the tropism of the virus depends on the envelope's interaction with a receptor on the cell surface.

VSVg and AMLV pseudotyped viruses were produced by transfecting 293T cells in a 15cm plate using 45ul of Polyethylenimine (PEI, Polysciences), 7.85 ug of pCMV-VSVg and 14.60 ug of the proviral construct R7ΔEnvGFP in which the Nef open reading frame was replaced by a GFP cassette. Virus was harvested 48 hours post transfection by filtering the culture medium from the transfected cells through a 0.45um filter (Millipore). Virus infectivity was titrated by spinoculating virus on cells at 1200 x g for 2 hours at 13° Celsius. Following spinoculation, the supernatant was aspirated and replaced with 37° Celsius fresh and warm medium. 48 hours later, cells were harvested and analyzed by FACS Canto II flow cytometer (Becton Dickinson) for GFP expression.

Vector expressing HA-TRIMCyp or YFP-rhTRIM5 WT or mutant proteins was made in a similar way by transfecting 293T cells in a 60 mm dish using PEI along with 1 μg of the plasmid of interest, 1 μg of VSV-g and 1 μg of pCig-B or ΔNRF. Vector was harvested 48 hours post transfection, filtered through the 0.45 μm filter and either frozen at -80° C or used to transduce HeLa cells. To make stable cell lines,

HeLa cells were plated at 50% confluency and transduced with the respective vectors for 14 hours, after which the vector was replaced with regular DMEM. 48 hours post transduction media containing G418 drug at a concentration of 400 µg/mL or Puromycin at 5ug/mL of DMEM was added to the cells. The expression of polyclonal or single colony clones was screened by immunofluorescence to ensure all cells expressed the transduced protein. Furthermore, cell lines were then analyzed by western blot analysis, immunofluorescence staining and infectivity assays.

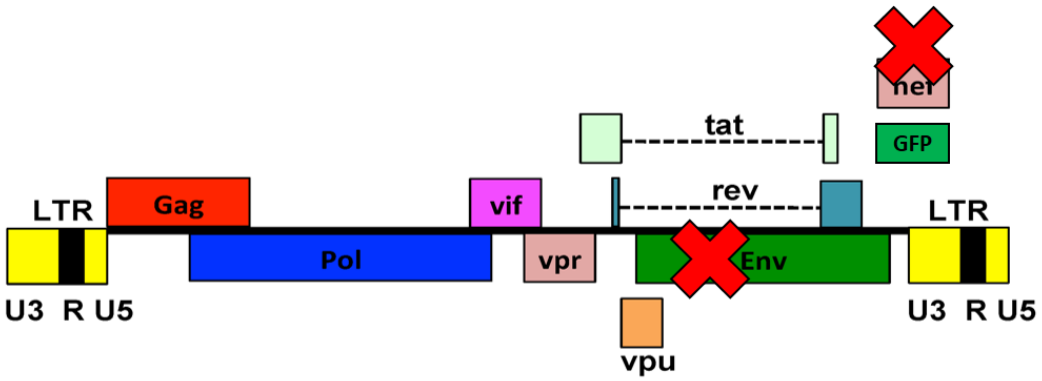

Figure 19. HIV-1 Reporter Virus. HIV-1 proviruses like R7ΔEnv GFP are generated to express a reporter cassette such as GFP in the place of the Nef gene. The env is deleted to allow for pseudotyping with other glycoproteins like VSVg and amphotropic MLV (AMLV) to generate single-cycle replication defective pseudoviruses with wide tropisms. Adapted and modified from (151).

Recombinant DNA Constructs

The pcDNA3.1 Flag-tagged proteasome subunits were a kind gift from Dr. Shigeo Murata, Ph.D. (University of Tokyo). To generate the retroviral HA-tagged wt rhTRIM5α construct, SmaI and EcoRI restriction sites were inserted flanking rhTRIM5α using the primers GCCTGGCATTATGCCCAG and AGCTTGCCAAACCTAC. Polymerase chain reaction (PCR) was performed and the PCR product was digested with SmaI (New England BioLabs) and EcoRI (New England BioLabs) and inserted into the EXN retroviral vector (also digested with SmaI and EcoRI). The EXN plasmid was generously provided by Dr. Greg Towers, Ph.D. (University College London). This EXN vector was used to derive the YXN retroviral vector, which was generated by PCR amplification of the Yellow fluorescent protein (YFP) coding region of the YFP-N1 (Clontech) plasmid, using the primers TGGATGAACTATACAAGTGGATCCGGCCG and CGGCCGGATCCACTTGTATAGTTCATCCA. The PCR amplified YFP fragment was then digested with AgeI (New England BioLabs) and BsrGI (New England BioLabs) and inserted into the similarly digested EXN plasmid. To facilitate easier subsequent cloning, the BamHI site of wt rhTRIM5α was disrupted by SOEing PCR using the interior primers CCCCAGTATCCAAGCACTTTT and AGTGCTTGGATACTGGGGGTATGT and exterior primers GCGGCGGGATCCATGGCTTCTGGAATCCT and GGCCGGCTCGAGTCAAGAGCTTGGTGAGC. These primers introduced a silent

mutation in the wt rhTRIM5α open reading frame that eliminated the BamHI. This PCR product was then digested with BamHI and XhoI and inserted into the similarly digested YXN plasmid. The same cloning strategy was used to clone rhTRIM5α SIM mutants into YXN. To clone the lentiviral pLVX-HA-TRIMCyp, EXN-TRIMCyp was digested with

NF-kB-responsive firefly luciferase construct was a kind gift from Dr. Susan Baker, Ph.D. (Loyola University Chicago) and pRL-CMV was purchased from Promega.

Infectivity assay

Equivalent numbers (0.75×10^5) of cells were plated in a 24-well plate, infected with VSVg or AMLV pseudotyped GFP reporter HIV-1 (R7ΔEnvGFP) by spinoculation (1200xg, 2 hours, 13°C) in a tabletop centrifuge (Beckman Coulter), after which the DMEM was removed and warm DMEM was added to the cells. For TRIM-Cyp expressing cells, the infection was performed in the presence or absence of the drug cyclosporine A for the first 16 hours. 48 hours following the infection, cells were harvested and percentage of GFP positive cells was determined using a FACS Canto II flow cytometer (Becton Dickinson).

Immunofluorescence and Imaging

Cells were plated on fibronectin-treated coverslips (Sigma-Aldrich). After they adhered to the glass, they were subjected to drug treatments and/or virus

infection. Following the treatment, cells were fixed for 5 minutes with 3.7% formaldehyde (Polysciences) in 0.1 M PIPES, pH 6.8 [piperazine-N, N'-bis (2-ethanesulfonic acid)] (Sigma-Aldrich). Cells were stained for proteins of interest utilizing primary anti-mouse, rabbit, and rat antibodies (Table 1) followed by secondary antibodies conjugated to FITC, TRITC, and CY5 (Jackson Immunoresearch) in 1X Phosphate Buffered Saline (Hyclone) containing 0.1% Saponin or TritonX-100 (Sigma-Aldrich), 0.01% NaN3 and 10% Normal Donkey Serum. Images were collected on a widefield deconvolution DeltaVision microscope (Applied Precision) equipped with EMCCD and CCD cameras (Photometrics), using a 1.4-numerical aperture 100X objective lens. Images were deconvolved with SoftWoRx software (Applied Precision).

Image Analysis

20 Z-stack images were acquired using identical acquisition parameters. Surfaces for cytoplasmic bodies in all samples analyzed were defined by using a fluorescence threshold (600 relative fluorescence units) for YFP-rhTRIM5α, and all YFP-rhTRIM5α bodies over a volume of 0.011 μm^3were used in the analysis. Deconvolved images were analyzed for SUMO-1, PSMC2, RPT5, Alpha 4, Alpha 6, and 20S mean fluorescence intensity (MFI) in cytoplasmic bodies using the Surface Finder function of the Imaris software package (Bitplane) and the data was plotted in Prism (Graphpad Software Inc) for statistical analysis.

Western Blotting

Whole cell lysates were prepared by lysing cells with NP-40 lysis buffer (100mM Tris pH 8.0, 1% NP-40, 150 mM NaCl) containing protease inhibitor cocktail (Roche) for 10 minutes on ice. Following the incubation on ice, 2x Laemmli sample buffer was added to the lysed cells and incubated at 100°C for 10 minutes. Samples were loaded into a 10% polyacrylamide gel for SDS-polyacrylamide gel electrophoresis (SDS-PAGE). After separation, the proteins were transferred to nitrocellulose membrane (Bio-Rad) and detected by incubation with anti-HA conjugated to Horseradish Peroxidase (HRP) (Roche), anti-FLAG (Sigma) and anti-Myc. Secondary antibodies conjugated to HRP (Thermo Scientific) were used where necessary and antibody complexes were detected using SuperSignal™ West Femto Chemilluminescent Substrate (Thermo Scientific). Chemiluminescence was detected using the UVP EC3™ Imaging System (UVP LLC).

Co-Immunoprecipitation

Rhesus TRIM5α Co-immunoprecipitation

Sub-confluent 293T cells grown in 10-cm dishes were transfected with 10 ug of total plasmid DNA using PEI. 48-hours post transfection cells were washed with 1 ml ice-cold phosphate buffered saline (PBS) and lysed with 1 ml ice-cold lysis buffer (50 mM Tris, pH 7.4, 125 mM NaCl, 1% NP-40) supplemented with phosphatase inhibitor cocktail (Roche). Crude cell lysates were collected, transferred to a pre-chilled 2 ml microcentrifuge tube, and agitated at 4° for one

hour. Following agitation, cells were sonicated for 10 seconds continuously, and centrifuged at 13,000 × *g* for 20 minutes at 4°C. 50 uL of supernatant were aliquoted for total cell lysate, and an equal volume of 2X Laemmli sample buffer was added; samples were then boiled for five minutes at 100°C. To pull down HA-rhTRIM5α, anti-HA antibody (Sigma) was added to the remaining supernatant at a 1:200 dilution and incubated at 4°C for two hours. 50 ul of protein A beads (Miltenyi Biotec) were added to the supernatant and incubated at 4°C for an additional hour. Samples were loaded on MACS separation columns (Miltenyi Biotec), followed by three washes with wash buffer (150 mM Tris, pH 7.4, 125 mM NaCl, and 1% NP-40). Protein complexes were eluted in 30 uL of pre-warmed 1X sample buffer.

Human TRIM5α co-immunoprecipitation

Sub-confluent HEK293 cells grown in 10-cm dishes were transfected with 24 µg total plasmid DNA using Lipofectamine 2000 (Invitrogen), following the manufacturer's protocol. Forty-two hours post-transfection, cells were washed with 5 ml ice-cold PBS and lysed with 800 µl ice-cold lysis buffer ((50 mM Tris, pH 7.5, 150 mM NaCl, 1% Triton X-100, 1 mM EDTA 10% glycerol), supplemented with protease inhibitor cocktail (Roche). Crude cell lysates were collected, transferred to pre-chilled 2 ml microcentrifuge tubes, and centrifuged at 10,000 × *g* for 10 minutes. The clarified lysate was transferred to pre-chilled microcentrifuge tubes. To prepare antibody conjugated beads, 2 µg of antibody (mouse anti-flag M2; Sigma F1804) was conjugated to 50 µL of Protein G Dynabeads® (Invitrogen) following the manufacturer's protocol. The beads were washed three times with 1 ml ice-cold

lysis buffer, resuspended in 50 µL lysis buffer, and added to the clarified cell lysates. After two hours rotating at 4°C, the bead-immune complexes were washed five times with 1 ml ice-cold lysis buffer, resuspended in 100 µL of 1 × Laemmli sample buffer, incubated at 100°C for five min.

Forster Resonance Energy Transfer (FRET)

Immunofluorescent Acceptor Photobleaching in Fixed Cells

Cells stably expressing HA-rhTRIM5α (152) were plated on coverslips at a sub confluent density. Coverslips were fixed with 3.7% formaldehyde (Polysciences) in 0.1 M PIPES [piperazine-*N*, *N*'-bis(2-ethanesulfonic acid)], pH 6.8. Cells were immunostained with a rabbit anti-HA primary antibody (Sigma) and mouse anti-PSMC2 or rabbit anti-20S primary antibodies (Enzo Life Sciences). Primary anti-HA antibody was labeled with a secondary Cy5-conjugated anti-rabbit antibody (Jackson ImmunoResearch), and proteasomal subunits were labeled with a secondary anti-mouse or anti-rabbit Alexa546 (Invitrogen). Cy5 fluorophore was bleached for total of two minutes every five seconds while fluorescence intensities were detected in the Alexa546 and Cy5 channels. Using SoftWoRx software, maximum intensities were analyzed over the course of the experiment for Alexa546 and Cy5 and graphed in Microsoft Excel.

Fluorescent Protein Acceptor Photobleaching in Live Cells

FRET by acceptor photobleaching was performed as previously described (153). Briefly, progressive acceptor photobleaching was performed as following: 50

images were obtained at 10-second intervals for both donor (CFP: excitation 427/10, emission 473/30, 100 ms exposure) and acceptor (YFP: excitation 504/12, emission 542/27, 40 ms exposure), with a period of acceptor photobleaching (excitation 504/12) between each acquisition. The CFP/YFP fluorescence intensity of each cell in the field was quantified in Meta-Morph, and FRET efficiency was calculated from the CFP initial and final fluorescence values, according to $E = 1-(F_{prebleach}/F_{postbleach})$.

Fluorescence imaging was performed with an inverted microscope equipped with a 1.49 numerical aperture objective, and a back-thinned CCD camera (iXon 887; Andor Technology, Belfast, Northern Ireland). Image acquisition and acceptor photobleaching was automated with custom software macros in Meta-Morph (Molecular Devices Corp., Downingtown, PA) that controlled motorized excitation/emission filter wheels (Sutter Instrument Co., Novato, CA) with filters for CFP/YFP/mCherry (Semrock, Rochester NY). The progressive photobleaching protocol was as following: 100-ms acquisition of CFP image and 40-ms acquisition of YFP image, followed by 10-s exposure to YFP-selective photobleaching (504/12-nm excitation).

E-FRET in Live Cells

E-FRET was performed as previously described (154).

E-FRET was calculated according to:

$$E=\mathrm{IDA}-a(\mathrm{IAA})-d(\mathrm{IDD})\mathrm{IDA}-a(\mathrm{IAA})+(G-d)(\mathrm{IDD})$$

where I_{DD} is the intensity of fluorescence emission detected in the donor channel (472/30 nm) with 427/10 nm excitation; I_{AA} is the intensity of fluorescence emission detected in the acceptor channel with 542/27 nm emission and 504/12 nm excitation; I_{DA} is the intensity of fluorescence emission detected in the "FRET" channel with 542/27 nm emission and 427/10 nm excitation; and *a* and *d* are cross-talk coefficients determined from acceptor-only or donor-only samples, respectively. We obtained a d value of 0.894 for CFP and a value of 0.108 for YFP. G is the ratio of the sensitized emission to the corresponding amount of donor recovery, which was 3.2.

Dual-luciferase Reporter Assay

SIMs

293T cells seeded in a 96-well plate were transfected with empty vector, ΔRING/SPRY rhTRIM5α (ΔRS, negative control), wild type rhTRIM5α, SIM1 mut, SIM2 mut, SIM3 mut or RIG-1 (positive control) in triplicate. Transfection was carried out using polyethylenimine (PEI) protocol in which the constructs were added at a 9 (EV/rhTRIM5α/RIG-I): 3 (NF-kB-responsive firefly luciferase construct, a kind gift from Dr. Susan Baker, Loyola University Chicago): 1 (Renilla luciferase construct for transfection efficiencies, pRL-CMV (Promega)) ratio. Cells were lysed 48-hours post transfection with Passive lysis buffer (Promega) and the luciferase activity was measured using a Dual-Glo luciferase assay system (Promega) in a Veritas Microplate luminometer. Firefly luciferase data were normalized to Renilla

luciferase readings in each well. Data were plotted by determining the fold increase over empty vector.

SUMO-1 overexpression

293T cells seeded in a 96-well plate were transfected with empty vector, and rhTRIM5α constructs in presence or absence of SUMO-1 in triplicate. Transfection was carried out using PEI protocol in which the constructs were added at a 5 (rhTRIM5α): 4 (SUMO-1 or EV): 3 (NF-κB-responsive firefly luciferase construct): 1 (Renilla luciferase construct for normalization of transfection efficiencies) ratio. Cells were lysed 48-hours post transfection with Passive lysis buffer (Promega) and the luciferase activity was measured using a Dual-Glo luciferase assay system (Promega) in a Veritas Microplate luminometer. Firefly luciferase data were normalized to Renilla luciferase readings in each well. Data were plotted by dividing SUMO-1 siRNA NF-κB activation by Control siRNA NF-κB activation x 100.

SUMO-1 knockdown

293T cells seeded in a 12-well plate were transfected with Control siRNA or SUMO-1 siRNA (Santa Cruz Biotechnology, Inc) following a Lipofectamine2000 (Invitrogen) protocol for two days. On the third day the cells were seeded in a 96-well plate in triplicate and transfected with empty vector or wild type rhTRIM5α using PEI in which constructs were added at a 9 (EV/rhTRIM5α): 3 (NF-kB-responsive firefly luciferase construct): 1 (Renilla luciferase construct for transfection efficiencies) ratio. Cells were lysed 48-hours post transfection with

Passive lysis buffer (Promega) and the luciferase activity was measured using a Dual-Glo luciferase assay system (Promega) in a Veritas Microplate luminometer. Firefly luciferase data were normalized to Renilla luciferase readings in each well. Data were plotted by dividing SUMO-1 siRNA NF-κB activation by Control siRNA NF-κB activation x 100.

In Situ Uncoating Assay

Fluorescently labeled viral proteins and host proteins are incorporated into the virus to generate fluorescently labeled HIV-1. For example, viral protein R (Vpr) is tagged to a green fluorescent protein (GFP), which is incorporated into the virus during production to track the virus in cells with microscopy (30). To generate fluorescently labeled HIV-1, 293T cells seeded in a 25cm dish at a 60% confluency were transfected with 8.45 ug S15-mCherry, 2.8 ug GFP-Vpr, 6.75 ug R7ΔEnvGFP, and 4.5 ug pCMV-VSVg using PEI. S15-mCherry is a fluorescent fusion protein that contains the 15 N-terminal amino acids of the cellular Src protein. This 15–amino acid sequence contains a myristoylation sequence that is sufficient to cause membrane association and incorporation of S15-mCherry into the virion. Following fusion, the S15-mCherry labeled viral membrane is lost which allows for effective discrimination between virions that have been non-productively endocytosed by the target cells (S15-mCherry+, GPF-Vpr+) from those that have productively entered the cell cytoplasm (S15-mCherry−, GFP-Vpr+) (Figure 20 and Figure 21). Two days following the transfections, virus was collected, centrifuged at 2000 rpmi for 5

minutes, and filtered through a 0.45 um filter (Milipore). Harvested viruses were spinoculated on coverslips, stained for p24 using anti-p24 mAb AG3.0 (NIH AIDS Research and Reference Reagent Program) in blocking solution (10% normal donkey serum [Jackson ImmunoResearch Laboratories], 0.1% Saponin, 0.01% NaN_3 in PBS) for 1 hour at room temperature, followed by a secondary antibody conjugated to Cy5 (Jackson ImmunoResearch Laboratories) for 30 minutes at room temperature in the same blocking solution. Determining the percent of virions in a field that were positive for S15-mCherry, GFP-Vpr and p24 assessed labeling efficiency. For infections, OMK, HeLa and THP-1 (PMA differentiated) cells were seeded on fibronectin treated coverslips and spinoculated in presence or absence of drugs of interest. Following spinoculation, media was aspirated and changed to warm media containing drugs and cells were incubated at 37°C. At various time points post infection, coverslips were fixed with 3.75% Formaldehyde in 0.159 M PIPES buffer (pH 6.8) for 5 minutes and washed with 1xPBS. Coverslips were stained with anti-p24 mAb AG3.0 as described above and mounted on glass slides with Gel Mount (Biomedia). Z-stack images were collected using identical acquisition parameters with a DeltaVision microscope (Applied Precision) equipped with a digital camera (CoolSNAP HQ; Photometrics), using a 1.4-numerical aperture 100× objective lens, and were deconvolved with SoftWoRx deconvolution software (Applied Precision). Following deconvolution, images were quantified by Imaris (Bitplane) software using the Surfaces feature and generating surfaces around GFP-

Vpr puncta. These surfaces were then quantified for their S15-mCherry and p24 maximum fluorescence intensity.

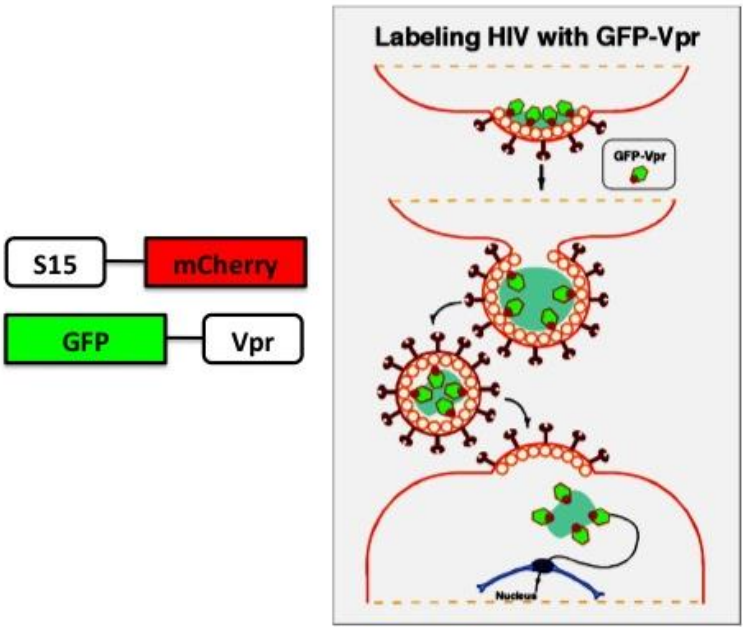

Figure 20. Double-labeled HIV-1. In addition to reporter viruses, during virus production, S15-mCherry and GFP-Vpr are transfected along with the proviruses and env to generate double-labeled HIV-1. These viruses are used in immunofluorescence assays to discern between viruses that have productively fused (S15-mCherry negative, GFP-Vpr positive) and those that haven't (S15-mCherry positive, GFP-Vpr positive). Image on the right was a courtesy of the Hope Lab-Northwestern University.

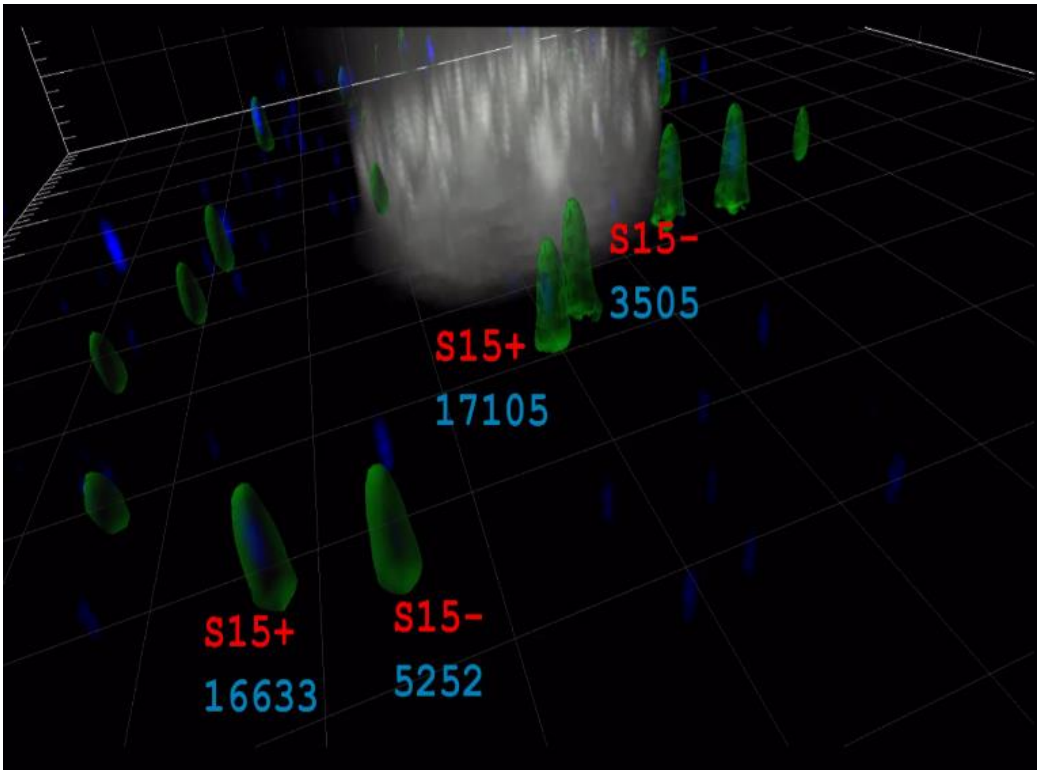

Figure 21. Imaris quantification of fluorescently labeled HIV-1. The cell nucleus is in grey and the particles are individual viruses. Based on the intensity of GFP-Vpr that is labeling the virus artificial surfaces are created (green) around the virus. Subsequently within that surface, S15-mCherry and p24 intensities are obtained. From these numbers, we determine which viruses are S15-mCherry negative (background levels of mCherry intensity →fused) and then plot the p24 intensity values (blue) within those viruses to determine their uncoating status since p24 intensity decreases as the virus uncoats.

Statistical Analysis

Statistical significance was assessed using the Student's t test or Multiple comparisons whenever two groups were compared. Data is represented as mean +/- SEM or SD depending on the graph. When more than two groups were compared, one-way ANOVA was used. Calculations were performed in GraphPad Prism software (GraphPad Software, Inc.).

CsA Washout Assays

OMK, HeLa HA-TRIMCyp and THP-1 HA-TRIMCyp cells were plated in 24-well plates. Cells were spinoculated with GFP reporter virus in the presence of CsA/DMSO or CsA/Nocodazole, CsA/Taxol and CsA/CiliobrevinD for 2 hours at 13°C 1200 x g (temperature arrested-fusion). Following spinoculation, media was aspirated and changed to warm media containing drugs and cells were incubated at 37°C. Washout of CsA continued for throughout the entire time-course. After 2 or 4 hours, Nocodazole, Taxol and Ciliobrevin D were removed by washing the cells generously with PBS and adding back warm media containing CsA to be washed out in subsequent time points. Controls included Nocodazole, Taxol and CiliobrevinD without CsA, and continuous DMSO treatment. Two days following the time course, cells were harvested and fixed in 2% Formaldehyde (Polysciences) (Diluted in 1xPBS (Cellgro)). The percentage of GFP positive cells was determined using BD FACSCanto II flow cytometer (BD Biosciences).

Real Time-PCR

In conjunction with CsA Washout assays, samples were collected for RT-PCR at various hours post infection with and without drugs. Genomic DNA from cells was extracted following the DNeasy Blood and Tissue Kit protocol (Qiagen). The concentration of genomic DNA was determined using a NanoDrop 1000 (Thermo Scientific) and digested with DpnI (New England BioLabs) for 5 hours. RT-PCR was performed as previously described with primers for late reverse transcription, 2-LTR circles and β-actin (125, 155).

CHAPTER III

HYPOTHESIS AND SPECIFIC AIMS

Host cell proteins, termed restriction factors, which inhibit viral replication at various stages of the viral life cycle, determine the species-specific tropism of numerous retroviruses. Many members of the TRIM family of proteins act as viral restriction factors. One well-characterized example is the ability of TRIM5α from rhesus macaques (rhTRIM5α) to inhibit human immunodeficiency virus type-1 (HIV-1) soon after viral entry but prior to reverse transcription (RT) (101, 140). It is well established that the restriction requires an interaction between the viral capsid lattice and the B30.2/SPRY domain of TRIM5α. Following the binding of the viral core, TRIM5α mediates an event or series of events that result in the abortive disassembly of the viral core in a manner that prevents the accumulation of reverse transcription RT products (102, 121, 156). The RING domain of TRIM5α has E3-ubiquitin ligase activity, which is important for restriction and autoubiquitination (140). Incubation of TRIM5 with ubiquitin, E1 enzyme, UBC13 and UEV1A in vitro led to the production of unanchored K63-linked ubiquitin chains (136). Additionally, proteasome inhibitors prevent TRIM5α mediated inhibition of RT products and abortive disassembly of the viral core without affecting the ability of TRIM5α to inhibit retroviral infection (125). Furthermore, other proteins such as

p62, and SUMO-1 have been identified as interacting partners with TRIM5 that act as co-factors during restriction (149, 152). Recently, Pertel et al. identified TRIM5 as a pattern recognition receptor (PRR) that stimulates NF-κB and AP1 leading to downstream gene expression creating an antiviral state in the host (136). Even though parts of the mechanism have been identified, the specific roles of individual proteins in TRIM5-mediated restriction have not been determined.

Additionally, as mentioned before, the viral capsid is the determinant of TRIM5-mediated restriction, and the precise process of HIV-1 uncoating is still unknown. Uncoating is defined as the disassembly of the capsid structure from the viral complex (157). Studies suggest that the process of uncoating is modulated by viral and cellular factors (157, 158). Cytoskeletal network has been implicated in the trafficking of virions to the nucleus following fusion. Particularly, retrograde trafficking through the cytoplasm of HIV is accomplished on microtubules by dynein (30). Recently, a study investigated the timing of uncoating after viral fusion and the relationship between uncoating and reverse transcription utilizing a newly developed assay (26). However, key host proteins that mediate uncoating of the core are unknown. Also, since TRIM5 acts on the viral capsid, it is possible that the relationship between the viral core and microtubules is exploited by TRIM5 during restriction.

Therefore, we hypothesize that host proteins interact with the HIV-1 core to facilitate and restrict HIV-1 infection after entry and before integration.

To study the interaction between host proteins and HIV-1, I propose the following three specific aims:

Aim 1: I will test the hypothesis that proteins of the ubiquitin-proteasome pathway associate with rhTRIM5α while in complex with HIV-1 virions.

a) Determine the association between proteasome subunits and TRIM5α

b) Determine if there is a direct interaction between PSMC2 and TRIM5α

c) Determine if the proteasome associates with TRIM5α cytoplasmic bodies during restriction of HIV-1.

d) Determine the effect of Ubc13 knockdown on rhTRIM5α-mediated restriction.

Aim 2: I will test the hypothesis that post-translational modification protein SUMO-1 is necessary for rhTRIM5α-mediated restriction.

a) Quantify the subcellular localization and protein levels of rhTRIM5α following SUMO-1 knockdown, and mutation of SUMO-1 interacting motifs in TRIM5α.

b) Determine the role of SUMO-1 and SIMs in TRIM5-mediated restriction of HIV-1.

c) Determine if SUMO-1 modulates the innate immune signaling mediated by rhTRIM5α

Aim 3: I will test the hypothesis that initiation of HIV-1 uncoating occurs via microtubules

a) Determine the effects of disrupting microtubules on HIV-1 uncoating.

b) Determine the effects of disrupting microtubules on replication of HIV-1.

c) Determine if dynein or other MAPs facilitate HIV-1 uncoating.

CHAPTER IV

RESULTS: 26S PROTEASOME INTERACTS WITH TRIM5α DURING HIV-1 RESTROCTION.

TRIM5α associates with the 26S proteasome subunits

To examine the association between TRIM5α proteins and proteasome subunits in human cells, 293T cells were transfected with HA-rhTRIM5α and FLAG-PSMC2. Following rhTRIM5α pull down with an anti-HA antibody, FLAG-PSMC2 was detected on a Western blot utilizing an anti-FLAG antibody. This interaction with TRIM5α was not detected when pcDNA3.1 vector control was pulled down (Figure 22A-D), demonstrating a specific association between PSMC2 and rhTRIM5α. To determine if this association was specific to PSMC2 or other subunits of the proteasome, HA-rhTRIM5α was transfected with FLAG-tagged versions of the 19S RP subunits RPT3, RPT6, and RPN8. All three subunits were specifically pulled down with HA-rhTRIM5α, indicating that rhTRIM5α associates with numerous subunits of the 19S RP. To ensure the specificity of this pull-down, the same experiment was performed with FLAG-tagged Mixed Lineage Kinase 3 (MLK3) (159) that is not known to associate with TRIM5α. FLAG-MLK3 did not co-immunoprecipitated with HA-rhTRIM5α (Figure 22E). This demonstrates that TRIM5α specifically associate with the proteasome subunits. Additionally,

huTRIM5α-Myc was co-immunoprecipitated with FLAG-PSMC2 following transfection in HEK293 cells (Figure 22F). This established that the association of proteasome subunits with TRIM5α is conserved across species (160).

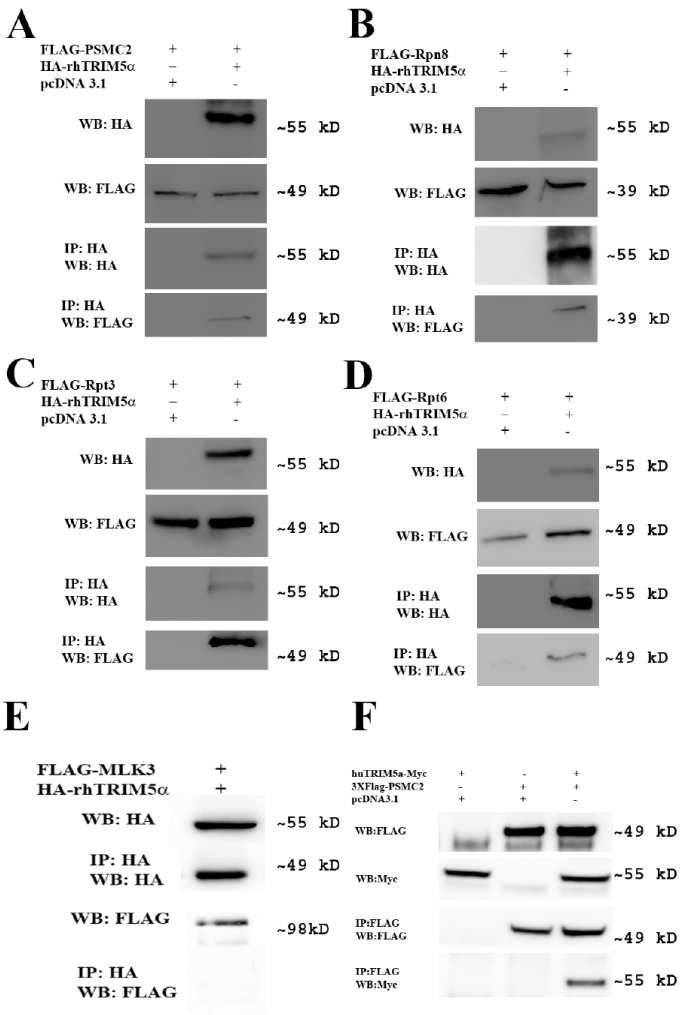

Figure 22. TRIM5α co-immunoprecipitates with 19S RP subunits. 293T or HEK293 cells were transfected with HA-rhTRIM5α or Myc-huTRIM5α with FLAG-tagged subunits of the 19S RP or control plasmid FLAG-MLK3 utilizing polyethylenimine (PEI). **A-D.** Following a pull down with an anti-HA antibody, FLAG-tagged PSMC2 (Rpt1), Rpn8, Rpt3, and Rpt6 were detected by Western blot when probed by an anti-FLAG antibody. **E.** Utilizing the same protocol, FLAG-MLK3 was not detected in a complex with rhTRIM5α when a Western blot was probed with an anti-FLAG antibody. **F.** FLAG-PSMC2 was pulled down using an anti-FLAG antibody and huTRIM5α was detected by Western blot using an anti-Myc antibody. (Data is representative of three independent experiments)

Subunits of the 26S proteasome localize to TRIM5α cytoplasmic bodies

The localization of proteasome subunits in HeLa cells stably expressing YFP-rhTRIM5α (118) was examined. Previously, we were unable to detect the localization of rhTRIM5α and the 20S CP of the proteasome using a polyclonal antibody (119). However, the results described above prompted us to speculate that this antibody did not accurately represent the localization of proteasomal subunits by immunofluorescence. Therefore, a more comprehensive study of proteasome localization was initiated using a large panel of antibodies to subunits of the proteasome. As shown in Table 1 and Figure 23 these antibodies typically fell into two categories when utilized for immunofluorescence: those in which a pronounced nuclear localization of the specified subunit was observed and those in which a pronounced nuclear localization was not observed. Numerous reports have shown that proteasome subunits, in addition to maintaining a noticeable and biologically relevant cytoplasmic fraction, exhibit a pronounced nuclear localization (161). Some antibodies in the panel examined (as well as the antibody used in the previous study) did not exhibit pronounced nuclear staining (Table 1), casting doubt on the utility of these antibodies for detecting proteasomal subunits by immunofluorescence. In contrast, the majority of antibodies did reveal a pronounced nuclear staining by immunofluorescence. Therefore, we used these antibodies to determine if proteasomal subunits localize to rhTRIM5α assemblies in HeLa stable cell lines expressing YFP-rhTRIM5α (118). Antibodies to numerous subunits demonstrated pronounced accumulation of proteasomal subunits in these

assemblies (Figure 24A). Specifically, PSMC2 could be detected in these assemblies (Figure 24A). Antibodies to the proteasomal subunits α2, α4, α6, and RPT5 also detected a pronounced accumulation of these proteins in YFP-rhTRIM5α assemblies. Also, we detected proteasome subunits associated with YFP-rhTRIM5α cytoplasmic assemblies using a rabbit polyclonal antibody to the 20S core particle of the proteasome (Figure 24A). To determine if proteasomal subunit localization was ubiquitous or if localization was specific to a subset of rhTRIM5α cytoplasmic assemblies, we quantified the proteasome specific immunofluorescent signal associated with individual cytoplasmic assemblies identified by automated image analysis. This analysis revealed that the vast majority of YFP-rhTRIM5α assemblies contained proteasomal subunits. Using an antibody to the 20S core, 99.6% of subunits had staining levels above background, which was defined as the staining observed using secondary antibodies in the absence of primary antibodies (Figure 24B). Similar results were also observed using mouse monoclonal antibodies to PSMC2 and another base subunit RPT5 as well as α4 and α6 subunits (Figure 24B) (160). Because of the strong degree of 20S core staining observed in YFP-rhTRIM5α assemblies using a rabbit polyclonal antibody, this suggests that virtually all TRIM5α assemblies associate with proteasomes. Therefore, we believe that alterations in the percentage of cytoplasmic bodies containing individual proteasomal subunits we observed using antibodies represent the ability of these antibodies to reliably detect subunits that are likely present in these assemblies. However, we cannot exclude the possibility that individual subunits are present in

more or less abundance, as proteasomal subunit populations may conditionally vary (162, 163).

Table 1 Characterization of proteasome antibodies for immunofluorescence

Proteasome Antibodies			
19S Base	**Catalog Number**	**Ab Nuclear Localization**	**Locialization with rhTRIM5a**
RPT1 mouse	BML-PW8825	INTERMEDIATE	YES
RPT1 rabbit	BML-PW8165	INTERMEDIATE	YES
RPT2 rabbit	BML-PW8305	NO	NO
RPT3 mouse	BML-PW8220	YES	NO
RPT3 rabbit	BML-PW8175	INTERMEDIATE	YES
RPT4 mouse	BML-PW8310	INTERMEDIATE	NO
RPT4 rabbit	BML-PW8830	NO	NO
RPT5 mouse	BML-PW8770	YES	YES
RPT5 rabbit	BML-PW8765	NO	NO
RPT6 rabbit	BML-PW8320	YES	NO
20S Alpha			
2 mouse	BML-PW8105	YES	YES
4 mouse	BML-PW8120	YES	YES
5 mouse	BML-PW8125	NO	NO
6 mouse	BML-PW8100	YES	YES
7 mouse	BML-PW8110	INTERMEDIATE	NO
Core rabbit	BML-PW8155	YES	YES
Alpha 1,2,3,5,6 & 7 mouse	BML-PW8195	NO	NO
20S Beta			
1i (LMP2-13) rabbit	BML-PW8345	NO	NO
1 mouse	BML-PW8140	NO	NO
2 mouse	BML-PW8145	NO	NO
2i (MECL-1) rabbit	BML-PW8350	YES	NO
3 mouse	BML-PW8130	INTERMEDIATE	NO
4 rabbit	BML-PW8890	NO	NO
5i (LMP7) mouse	BML-PW8845	NO	NO
5i (LMP7) rabbit	BML-PW8355	YES	NO
5 rabbit	BML-PW8895	NO	NO
6 rabbit	BML-PW9000	NO	NO
7 mouse	BML-PW8135	NO	NO

Antibodies were characterized based on their localization in the nucleus. Previous reports have shown that a large pool of proteasomes are located in the nucleus while a fraction remains in the cytoplasm thus the nuclear staining represents antibodies deemed successful for immunofluorescence.

Table 1. Antibodies to proteasome subunits that were analyzed for immunofluorescence staining. Antibodies to various subunits of the 19S RP and 20S RP (Enzo Life Sciences).

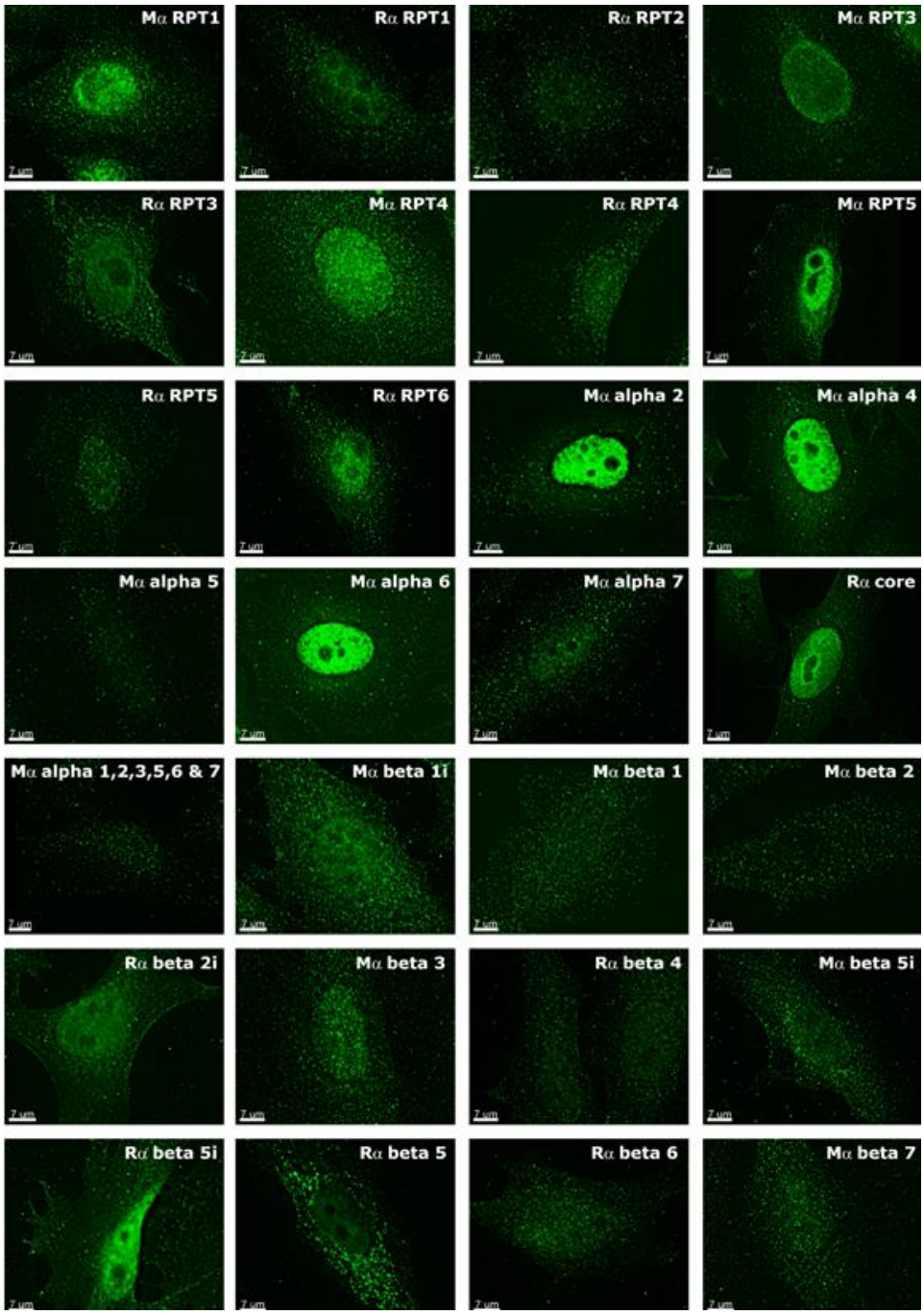

Figure 23. Endogenous subcellular localization of proteasome subunits in cells. HeLa cells were fixed with 3.7% formaldehyde in PIPES buffer and subsequently stained with the antibodies. Images were acquired on a DeltaVision widefield deconvolution microscope using a 100X objective. (Representative Images)

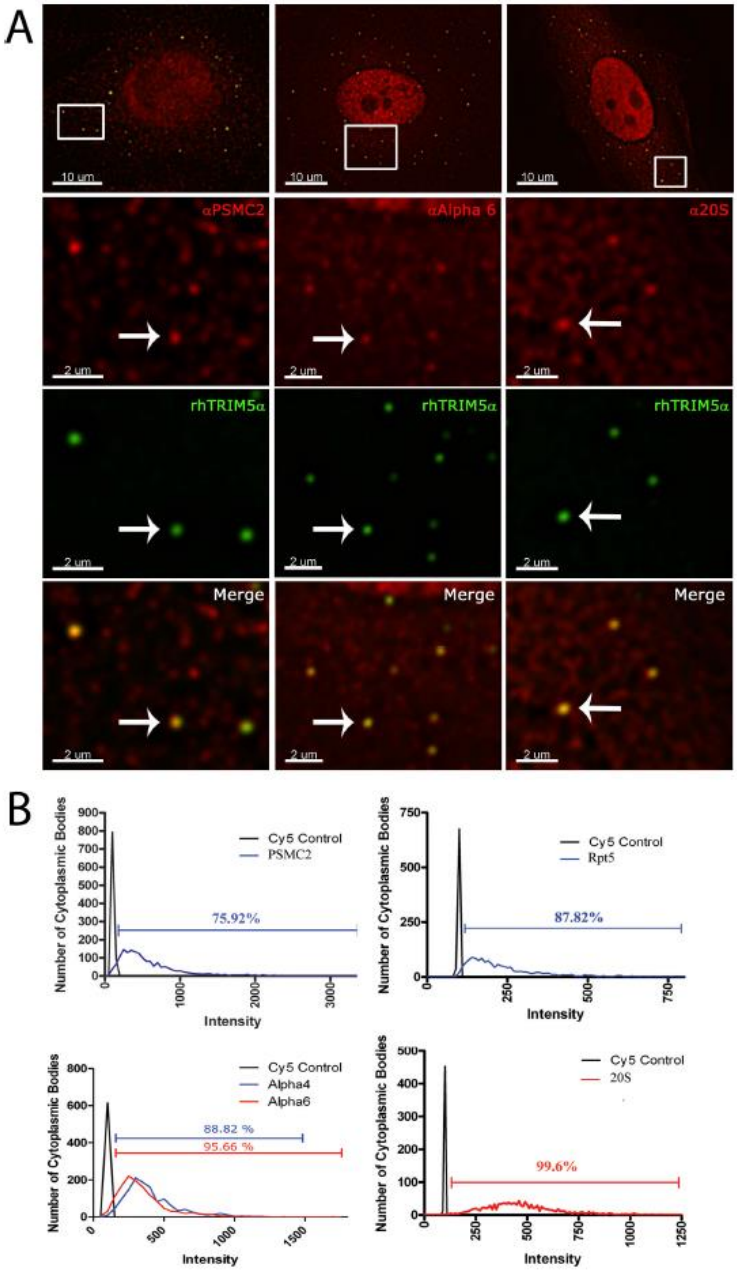
A
10 um
αPSMC2
αAlpha 6
α20S
2 um
rhTRIM5α
Merge
B
Number of Cytoplasmic Bodies
Intensity
Cy5 Control
PSMC2
75.92%
Rpt5
87.82%
Alpha4
Alpha6
88.82 %
95.66 %
20S
99.6%

Figure 24. Proteasome subunits localize to YFP-rhTRIM5α assemblies. A. HeLa cells expressing YFP-rhTRIM5α were stained for various subunits of the proteasome (Cy5) with the antibodies mentioned in Table 1. Individual channel images were superimposed to create the merged image. Arrows point to examples of co-localization between rhTRIM5α and proteasome subunits. **B.** Deconvolved images were analyzed for subunit mean fluorescence intensity (MFI) in YFP-rhTRIM5α by the use of the Surface Finder function in the Imaris software (Bitplane). For each YFP-rhTRIM5α cytoplasmic body, the MFI of the subunit or secondary antibody alone (Cy5 control) were determined and the data was plotted in GraphPad Prism 5 software. (Representative Images and Quantification)

TRIM5α directly associates with subunits of the 26S Proteasome

To better understand the association between rhTRIM5α and proteasome subunits, we performed immunofluorescence based Forster Resonance Energy Transfer (FRET) analysis on immunofluorescently labeled rhTRIM5α assemblies and proteasome subunits. For these studies, we utilized a well-characterized HeLa cell line stably expressing HA-rhTRIM5α (101). As previously observed with our YFP-rhTRIM5α cell line, proteasomal subunits localize to rhTRIM5α assemblies in these cells (Figure 25C). We labeled HA-rhTRIM5α and proteasomal subunits using secondary antibody combinations that have been previously used to measure FRET interactions in cells (164). To measure FRET, we utilized the acceptor photobleaching approach, in which the acceptor of a FRET pair is serially photobleached, and the fluorescence of the donor fluorophore is measured over time (152, 153, 165). In this system, if FRET occurs between two fluorophores, then bleaching of the acceptor will result in an increase in the fluorescence of the donor fluorophore as the acceptor fluorophore becomes unable to absorb the energy released from the donor. When PSMC2 was labeled using Alexa546 (donor) and HA-rhTRIM5α was labeled using Cy5 (acceptor), serial photobleaching of Cy5 resulted in an increase in the fluorescence detected for PSMC2 (Alexa546). Control bleaching of Cy5 in cells stained with Cy5 secondary antibody alone, in the absence of αHA primary antibody, did not exhibit this pattern (Figure 25A) (160). Similar results were obtained when a rabbit polyclonal antibody to the 20s proteasome was used (Figure 25B). FRET measurement is generally accepted to indicate a direct (< 5 nm)

association between two proteins. In this case, because both primary and secondary antibodies were used in this assay, we cannot definitively state this to be true because the addition of a secondary antibody, which has a hydrodynamic radius of 5.5 nm (166) results in a two-fold decrease in the resolution of this assay (> 10 nm). However, these experiments provide evidence that TRIM5α and proteasomal subunits exist in very close proximity in rhTRIM5α assemblies, well below what can be observed using colocalization analysis (Figure 24), which is limited by the resolution limit of light microscopy (~200 nm).

To determine if these proteins were within proximity (typically less than 5 nm) and therefore directly interacting, we performed FRET analysis using fusion proteins in which rhTRIM5α and PSMC2 were fused to the commonly used FRET pair of CFP and YFP, respectively. In live cells transfected with both CFP-rhTRIM5α and YFP-PSMC2, colocalization of rhTRIM5α and PSMC2 could be readily observed (Figure 26A and B left panels). We then utilized acceptor photobleaching to determine if FRET occurred between these two proteins in areas of notable colocalization. In this method, the acceptor (YFP-PSMC2) is serially photobleached. FRET is subsequently measured as an increase in donor fluorescence (CFP-rhTRIM5α) which occurs as the acceptor is bleached and therefore no longer absorbs the resonant energy from the donor (167). In these experiments, notable increases in the CFP-rhTRIM5α fluorescence were observed following YFP-PSMC2 photobleaching but an increase was not detected when YFP empty vector was photobleached (Figure 26 A and B right panels, Figure 27A) (160). While the FRET

difference between YFP-PSMC2 and YFP empty vector samples was statistically significant ($p < 0.0001$), there were also numerous CFP-rhTRIM5α assemblies in which photobleaching of YFP-PSMC2 did not induce an apparent increase in CFP-rhTRIM5α fluorescence. This suggests that these two proteins do not directly interact in some assemblies. Although we attempted to focus our analysis only on assemblies that did not enter or leave the plane of focus during the course of the experiment, we were concerned that the disparate results obtained were a result of the movement of some assemblies relative to the focal plane during the analysis period. To address this concern, we also performed E-FRET analysis on these assemblies by measuring the amount of YFP fluorescence induced following CFP excitation. Because this method allows a calculation of FRET efficiency derived from three individual images taken in rapid succession, movement of TRIM5α assemblies during the acquisition period was not a concern. When this method of analysis was utilized, we again observed that the FRET efficiencies of individual assemblies varied considerably (Figure 27B).

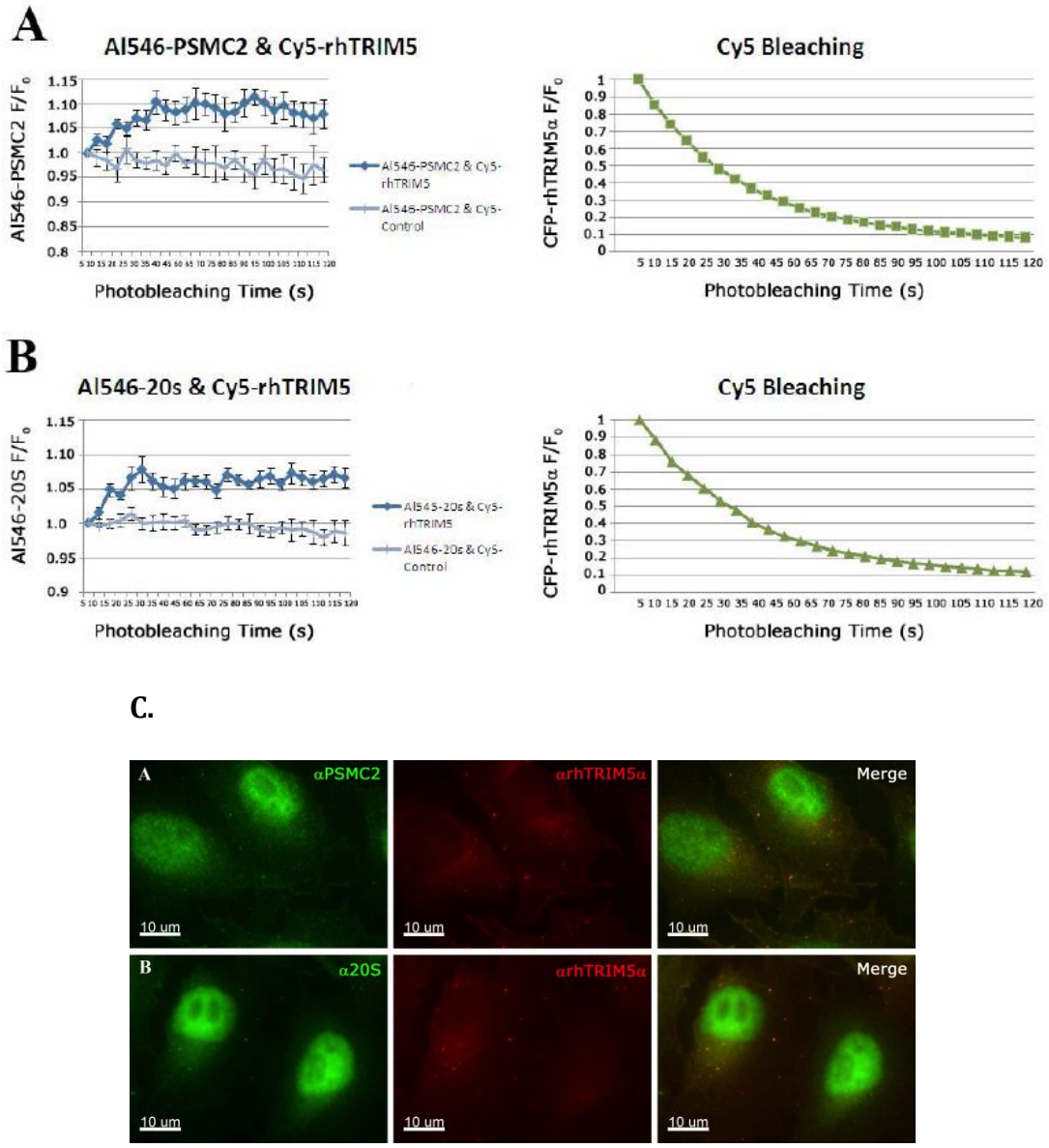

Figure 25. rhTRIM5α interacts with PSMC2 and 20S CP via an immunofluorescence based FRET assay. A. Cells stably expressing HA-rhTRIM5α were immunostained for HA using a primary anti-HA antibody and a secondary antibody conjugated to Cy5. Endogenous PSMC2 and 20S CP were stained with primary antibodies followed by secondary antibodies conjugated to Alexa546 (Al546). Cy5 fluorescence was progressively bleached and Cy5 and Al546 fluorescence intensity was detected over time. **B.** Same experiment was performed except an antibody was used to stain endogenous 20S CP. Representative images of co-localization between HA-rhTRIM5α and endogenous PSMC2 and 20S CP are shown. (Data is representative of three independent experiments)

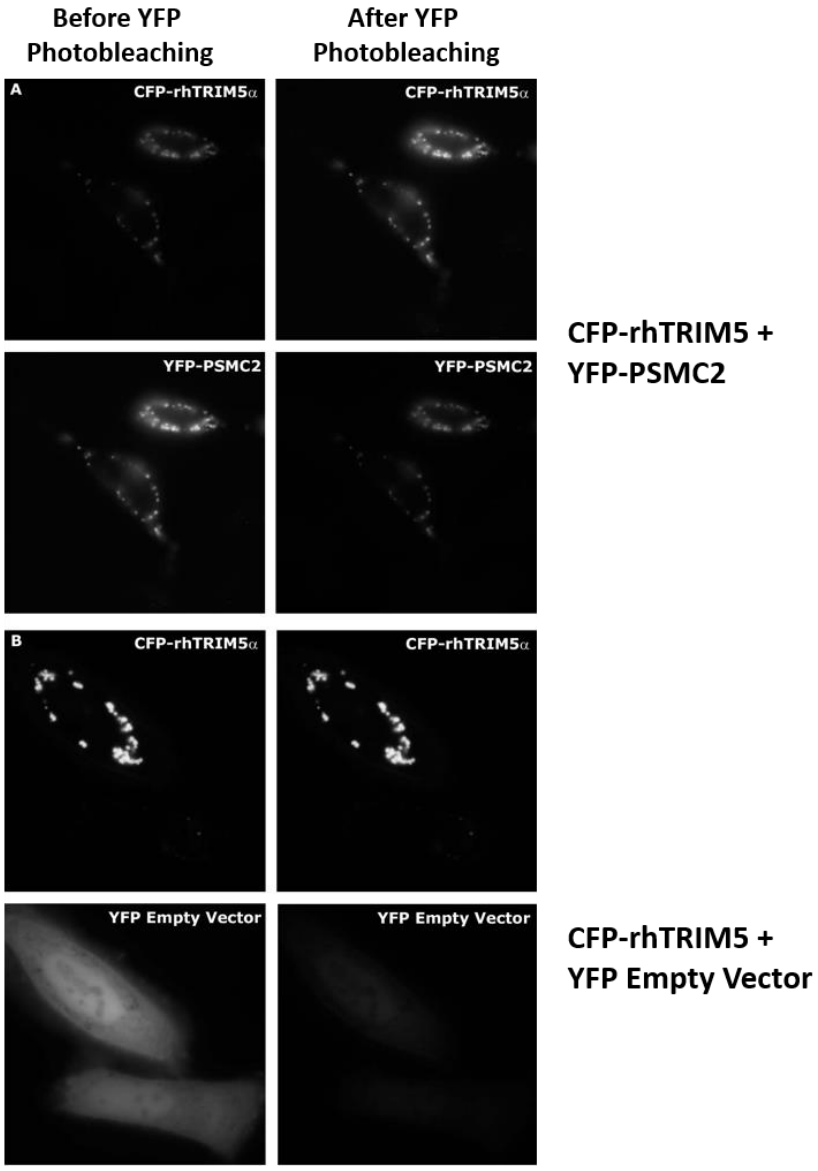

Figure 26. HeLa cells expressing CFP-rhTRIM5α and YFP-PSMC2 used for FRET analysis co-localize with each other. HeLa cells were transfected with CFP-rhTRIM5α and YFP-PSMC2 for 16 hours to allow for protein expression. Subsequently, cells underwent FRET analysis. YFP was progressively bleached. In image **A** there is significant co-localization between CFP-rhTRIM5α and YFP-PSMC2 (left side of the panel) that is not observed in image **B** where YFP empty vector was used (left side of the panel). Further, an increase in CFP-rhTRIM5α intensity is present when YFP-PSMC2 (Image A, right panel) was bleached as compared to the YFP empty vector, where the CFP-rhTRIMα remains the same (Image B, right panel). (Representative Images)

A.

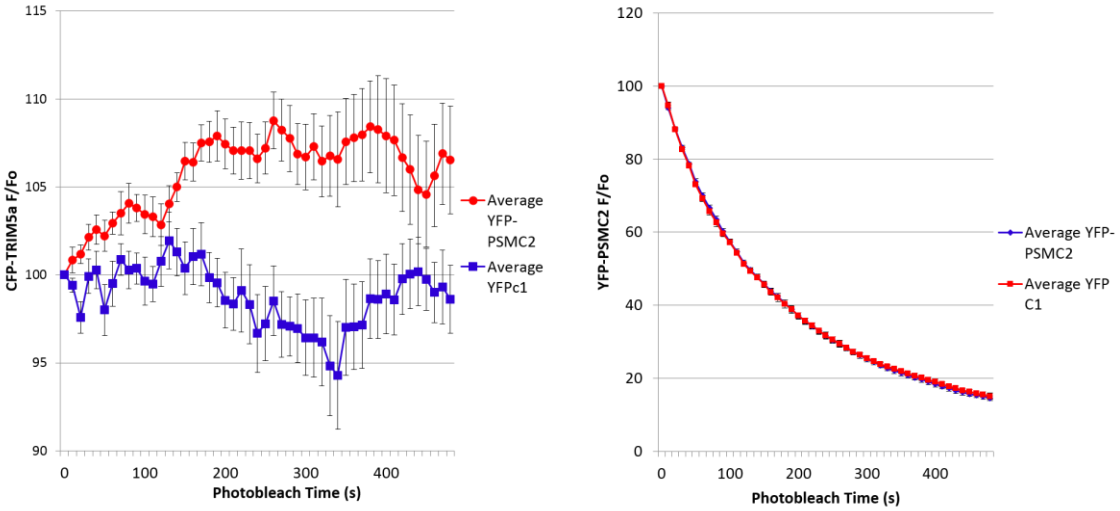
CFP-TRIM5a F/Fo
115
110
105
100
95
90
0
100
200
300
400
Photobleach Time (s)
Average YFP-PSMC2
Average YFPc1
YFP-PSMC2 F/Fo
120
100
80
60
40
20
0
0
100
200
300
400
Photobleach Time (s)
Average YFP-PSMC2
Average YFP C1

B.

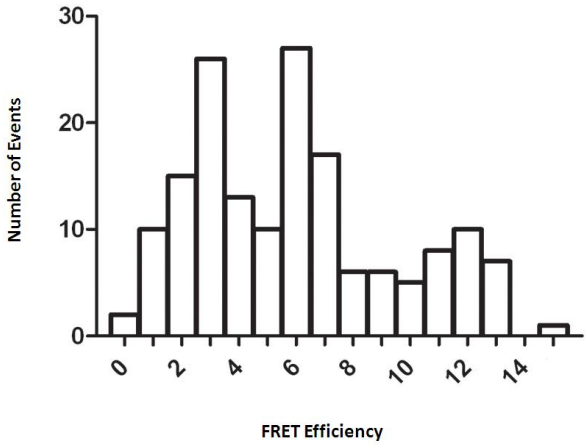
Number of Events
30
20
10
0
0
2
4
6
8
10
12
14
FRET Efficiency

Figure 27. PSMC2 directly interacts with rhTRIM5α. A. HeLa cells were transfected with YFP-PSMC2 or YFP empty vector and CFP-rhTRIM5α at a 1:1 ratio. Over the course of 10 minutes, 50 images were acquired for YFP and CFP channels. Progressive acceptor photobleaching of YFP-PSMC2 resulted in an increase in CFP-rhTRIM5α fluorescence intensity. (Error bars represent the standard error of the mean between co-localization events that were analyzed in cells. Data is representative of three independent experiments) B**.** Fluorescence intensity of YFP and CFP were recorded and E-FRET was calculated as a relative increase in YFP intensity following CFP photobleaching. (Data is representative of three independent experiments)

Subunits of the 26S proteasome are present in TRIM5α assemblies that contain HIV-1

These studies examined the localization of proteasomal subunits to rhTRIM5α assemblies that exist in cells in the absence of virus. The degree to which pre-existing rhTRIM5α cytoplasmic bodies resemble assemblies that form around individual virions (118)is unclear. One recent study found that TRIM5α forms hexagonal protein assemblies in the presence or absence of *in vitro* assembled hexameric capsid structures (122), suggesting that TRIM5α forms structurally similar assemblies in the presence or absence of restriction sensitive virus. The tendency to form such assemblies is enhanced by the presence of these hexameric capsid assemblies (122). However, there may be biologically important differences between cytoplasmic assemblies of TRIM5α that form around a restriction sensitive virus and those that form in the absence of virus. We, therefore, sought to determine if TRIM5α assemblies that form around restriction sensitive virus also contain proteasomal subunits. To this end, we infected a HeLa cell line stably expressing YFP-rhTRIM5α with low levels of pre-existing cytoplasmic bodies with VSV-g pseudotyped HIV-1 virions fluorescently labeled with a mCherry-Vpr fusion protein (30, 118). Following infection for 30 minutes, cells were fixed, stained for proteasomal subunits and quantified for any colocalization between rhTRIM5α formed cytoplasmic bodies, restriction sensitive virus, and proteasomal subunits (Figure 28). As the engagement of the viral capsid by rhTRIM5α rapidly leads to the loss of virally associated fluorescent signal (119), only a small percentage of viral

particles could be observed associating with TRIM5α in fixed cell images in the absence of proteasome inhibitor, as we have previously reported (119). However, when we did detect such complexes, both proteasomal subunit PSMC2 and the 20S core localized to cytoplasmic assemblies of TRIM5α that formed around a restriction sensitive virus (160). This demonstrates that proteasome subunits are recruited to TRIM5α assemblies that are associated with HIV-1 viral complexes.

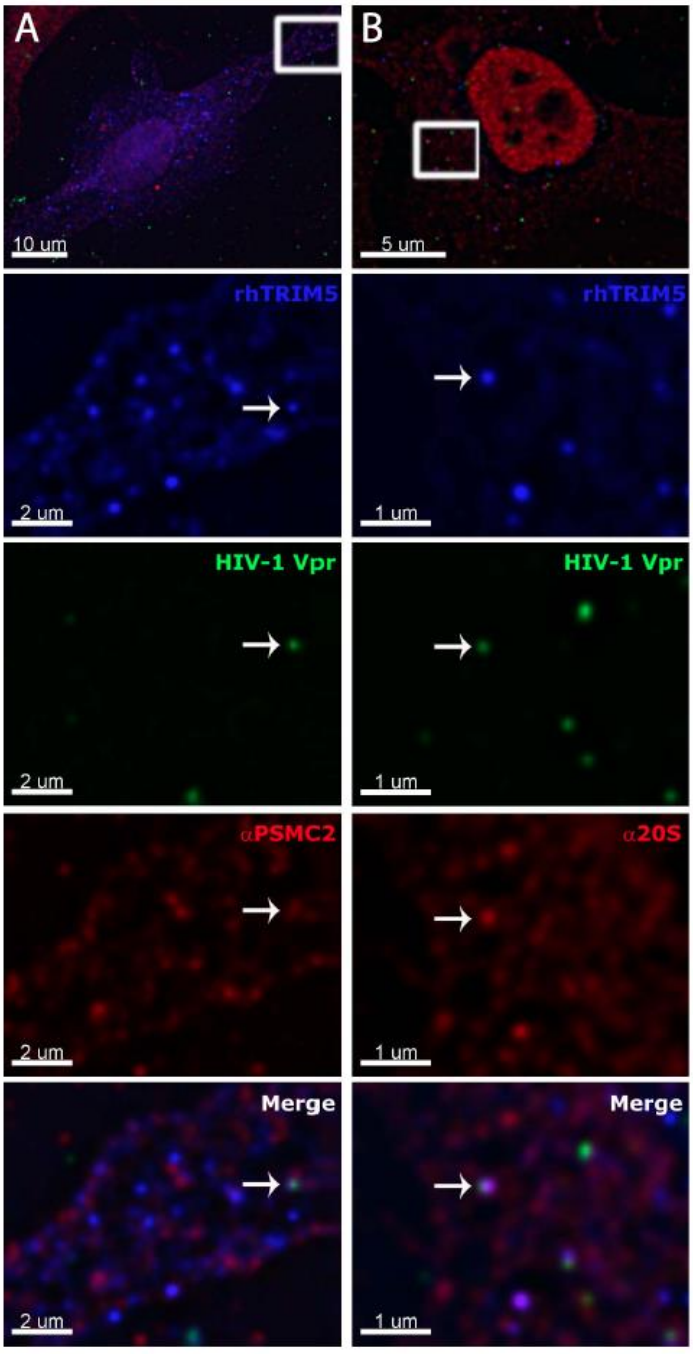

Figure 28. Proteasome subunits associate with rhTRIM5α assemblies containing HIV-1. HeLa cells stably expressing YFP-rhTRIM5α at low levels (diffuse localization of TRIM5α) were infected with VSVg-HIV-1 containing mCherry-Vpr for 30 minutes at 37°C. Cells were fixed and stained for the endogenous **A.** PSMC2 or **B.** 20S CP. (Representative Images)

Ubc13 (E2) effects on TRIM5α-mediated restriction

Since Pertel et al. demonstrated that TRIM5 utilizes Ubc13 to synthesize unanchored K63-linked polyubiquitin chains, we wanted to determine if it recapitulates the observations made with proteasome inhibition. A cell line that stably expresses YFP-rhTRIM5α was transfected with siRNA that targets Ubc13. Following the knockdown of Ubc13, individual cells were imaged and analyzed. When the proteasome is inhibited with MG132, TRIM5α cytoplasmic bodies are much larger in size, fewer in number, and are brighter in intensity. Therfore, we analyzed TRIM5α cytoplasmic bodies following Ubc13 knockdown with our analysis software. When Ubc13 was knocked down, TRIM5α cytoplasmic bodies were larger in size. The bodies increased from 0.37 um^3 to 0.78 um^3 in volume which was statistically significant ($p<0.0001$, Student T test). Furthemore, the bodies were brighter in fluorescence intensity, 4613 fluorescence units vs. 2440 fluorescence units for the control siRNA treated cells ($p<0.0001$, Student T Test). Also, as it was observed for proteasome inhibition, a decrease in number of cytoplasmic bodies. The average number of bodies decreased from 88.52 per cell to 46.31 ($p<0.0001$, Student T test) (Figure 29A). These data suggest that knockdown of Ubc13 recapitulates the phenotype observed when these cells are treated with MG132. However, the main question was whether Ubc13 knockdown relieves the inhibition of reverse transcription products in cells expressing TRIM5α, as MG132 does. Therefore, cells were knocked down for Ubc13 and infected with VSVg-HIV-1. RT-PCR data demonstrated that knockdown of Ubc13 did not relieve reverse

transcription products, as compared to MG132 treatment (Figure 29B). While Ubc13 knockdown recapitulates the observations made with TRIM5α cytoplasmic bodies, it does not alter the restriction phenotype. This suggests that Ubc13 alone is not capable of exerting the same effects that MG132 treatment has.

A.

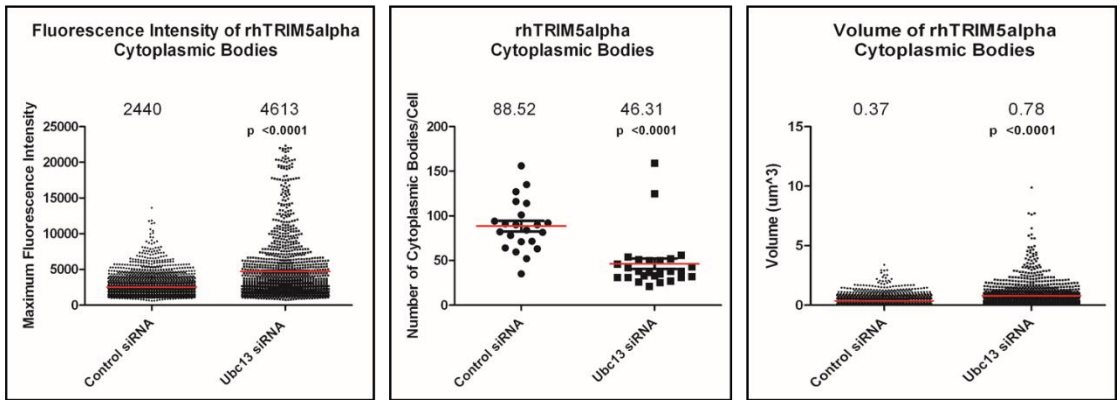

B.

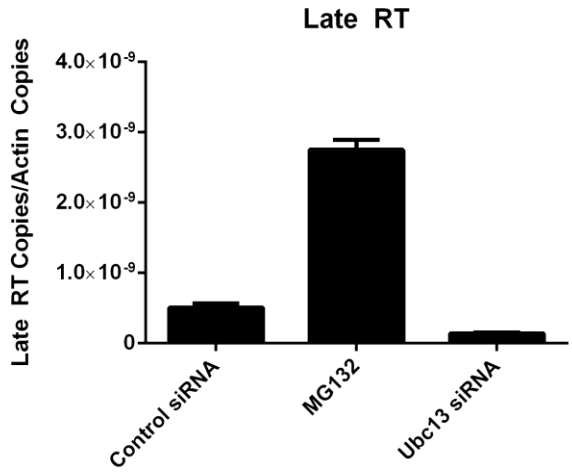

Figure 29. Ubc13 knockdown in rhTRIM5α cells A. HeLa cells stably expressing YFP-rhTRIM5α were transfected with Ubc13 siRNA. Following the treatment, cells were imaged and analyzed in the Imaris software utilizing the Surface finder feature. Surfaces were generated around YFP cytoplasmic bodies and analyzed. (Statistical significance calculated by using a student t-test, $p < 0.0001$) **B.** HeLa cells stably expressing HA-rhTRIM5α were transfected with control or UBC13 siRNA for 48 hours. Following the transfection, cells were infected with VSVg-HIV-1 for 16 hours before the cells were collected and analyzed for late reverse transcription products by RT-PCR. Cells that received MG132 treatment were treated for the entire 16 hours. B-actin was used to normalize the samples (Error bars show the standard deviation between the triplicates. Data is representative of three independent experiments).

CHAPTER V

RESULTS: SUMO-1 AND SUMO INTERACTING MOTIFS (SIMs) MEDIATE TRIM5α RESTRICTION OF RETROVIRUSES.

Mutations in rhTRIM5α SIM1 and SIM2 motifs abolish HIV-1 restriction

Previously, SIMs in huTRIM5α was demonstrated to be required for the restriction of N-MLV. To determine if the need for SIMs is conserved amongst TRIM5 proteins, we generated CRFK, HeLa, and TE671 cell lines stably expressing comparable levels of FLAG-tagged wild type rhTRIM5α or the rhTRIM5α variants with mutations in SIM1 (376–379), SIM2 (405–408) or SIM3 (430–433) (Figure 30A). These cell lines were infected with VSV-G pseudotyped HIV-1 carrying a firefly luciferase reporter gene to assess retroviral restriction. The wild type and SIM3 rhTRIM5α efficiently restricted HIV-1 infection when compared to the empty vector (EV) in CRKF (Figure 30B) and HeLa cells (Figure 29C). Conversely, mutation of SIM1 and SIM2 of rhTRIM5α completely abolished the restriction activity in these cell lines (Figure 30C). Similar results were observed in TE671 cells (Figure 30D), although the expression of the SIM1 and SIM2 mutants was noticeably reduced compared to the expression of wild type rhTRIM5α (Figure 30D). In all cell lines, mutation of rhTRIM5α lysine 10 to arginine (K10R), a predicted SUMOylation site had minimal effect on restriction (168), consistent with our previous observations

of huTRIM5α and rhTRIM5α N-MLV restriction (149). Similarly, in CRFK cells, which do not express a functional TRIM5 gene (169), the restriction of N-MLV by rhTRIM5α required a functional SIM1 and SIM2, recapitulating the restriction profile observed for HIV-1 (Figure 30E). Therefore, SIM1 and SIM2 present in rhTRIM5α are important for its antiviral activity against both N-MLV and HIV-1 and this is conserved amongst species. Consistent with this observation, another group has recently reported that the SIM1 and SIM2 mutations disrupt the binding of rhTRIM5α to the HIV-1 capsid (170), which would obviously reduce restriction.

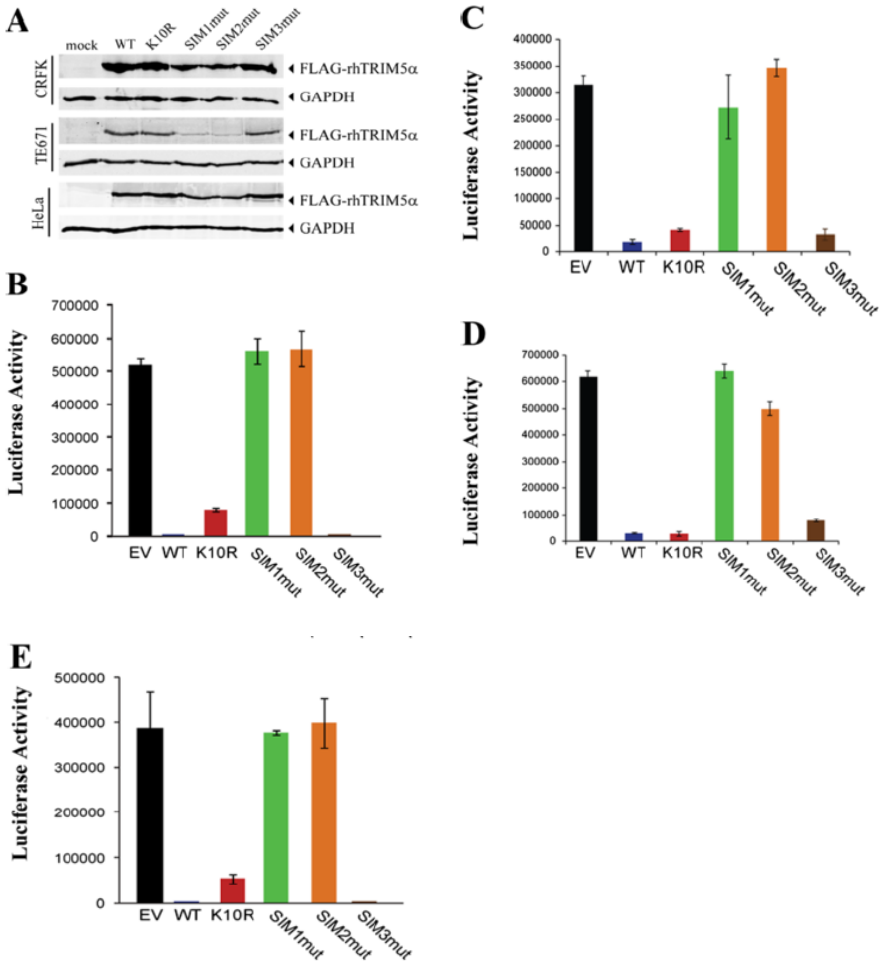

Figure 30. SIMs are important for rhTRIM5α-mediated retroviral restriction. CRFK, TE671 and HeLa cells were generated to stably express wt FLAG-rhTRIM5α, SIM1mut, SIM2mut or SIM3mut. **A.** Western blot was performed to determine the expression of these proteins in different cell lines. **B.** CRFK **C.** HeLa **D.** TE671 were infected with firefly luciferase reporter VSVg-HIV-1 for 48 hours and firefly luciferase levels were measured (Error bars show standard deviations between triplicates. Data is representative of three independent experiments). **E.** CRFK cells expressing wt FLAG-rhTRIM5α, SIM1mut, SIM2mut or SIM3mut were infected with firefly luciferase reporter VSVg-N-MLV for 48 hours and firefly luciferase levels were measured (Error bars show standard deviations between triplicates. Data is representative of three independent experiments). Experiment by: Dr. Gloria Arriagada, Ph.D.

Restriction of HIV-1 by rhTRIM5α is reduced following SUMO-1 knockdown

To determine if the ability of rhTRIM5α to restrict HIV-1 infection was dependent on interactions with SUMO-1, we stably knocked down SUMO-1 (SUMO-1 KD) using a SUMO-1 specific shRNA in TE671 cells expressing FLAG-rhTRIM5α or empty vector. A non-silencing shRNA was used as a control. To confirm SUMO-1 KD, we performed quantitative PCR (qPCR) and found that these cells had ~70% SUMO-1 KD (Figure 31B). Control cells transduced with empty vector did not show appreciable differences in HIV-1 infection following SUMO-1 KD (Figure 31A). Cells transduced to express FLAG-rhTRIM5α showed considerable restriction of HIV-1. Notably, following SUMO-1 KD the restriction activity of cells expressing FLAG-rhTRIM5α was reduced to levels similar to cells expressing empty vector (Figure 31A). This demonstrates that rhTRIM5α restriction of HIV-1 is sensitive to SUMO-1 depletion.

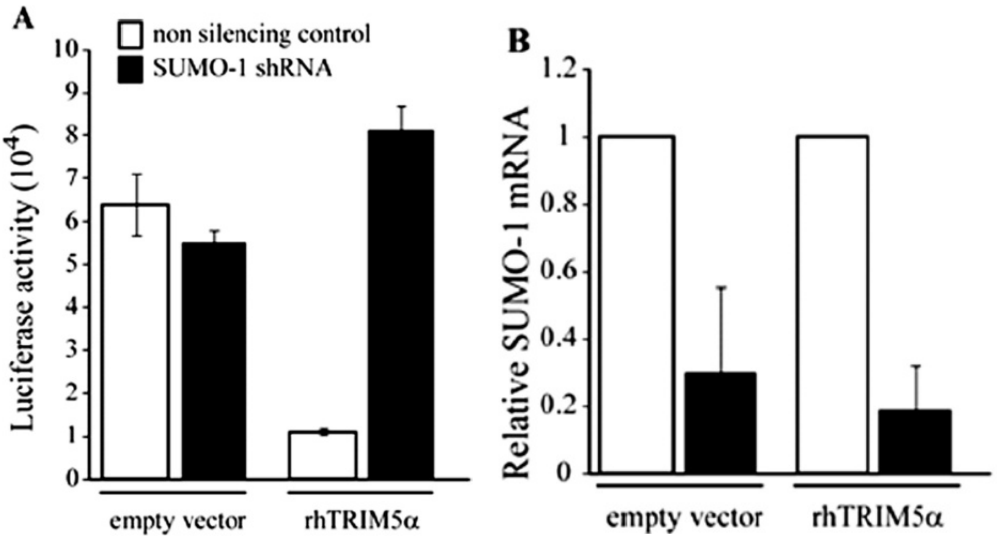

Figure 31. rhTRIM5α-mediated restriction of HIV-1 is reduced following SUMO-1 knockdown. Empty TE671 cells or cells expressing FLAG-rhTRIM5α were transduced with a vectors encoding a non-silencing (white bars) or SUMO-1 shRNA (black bars). **A.** Cell lines were infected with a firefly luciferase reporter VSVg-HIV-1. 48 hours post infection luciferase was measured. (Representative experiment of three independent experiments. Error bars show standard deviation between triplicates). **B.** mRNA levels of SUMO-1 were determined by quantitative PCR. Values were normalized by GAPDH mRNA and expressed as fold over the non-silencing controls. (Error bars show standard deviation between three different experiments). Experiment by: Dr. Gloria Arriagada, Ph.D.

SUMO-1 enhances rhTRIM5α stability in cells

As noted earlier, TE671 cells expressing rhTRIM5α SIM mutants showed reduced expression compared to TE671 cell lines expressing wild type or K10R forms of rhTRIM5α (Figure 30A). This suggests that disrupting interactions with SUMO-1 may increase the turnover of rhTRIM5α. It was previously reported that knockdown of host cellular protein p62 that interact with rhTRIM5α increased rhTRIM5α turnover (152), suggesting that p62 is required for rhTRIM5α stability. Therefore, we examined rhTRIM5α protein expression levels by Western blot following SUMO-1 siRNA treatment in a HeLa cell line stably expressing HA-rhTRIM5α (101). In these cells, SUMO-1 knockdown reduced HA-rhTRIM5α expression (Figure 32), although this reduction did not correlate with the degree of restriction observed (Figure 31A). Other studies have noted that small alterations in TRIM5α expression do not dramatically affect restriction activity at non-saturating amounts of virus (121, 171). However, these observations make it difficult to separate the contribution of reduced protein expression and the relief of restriction observed in these studies. Therefore, it remains possible that the effects of SUMO-1 knockdown on restriction are not entirely due to reduced expression of rhTRIM5α.

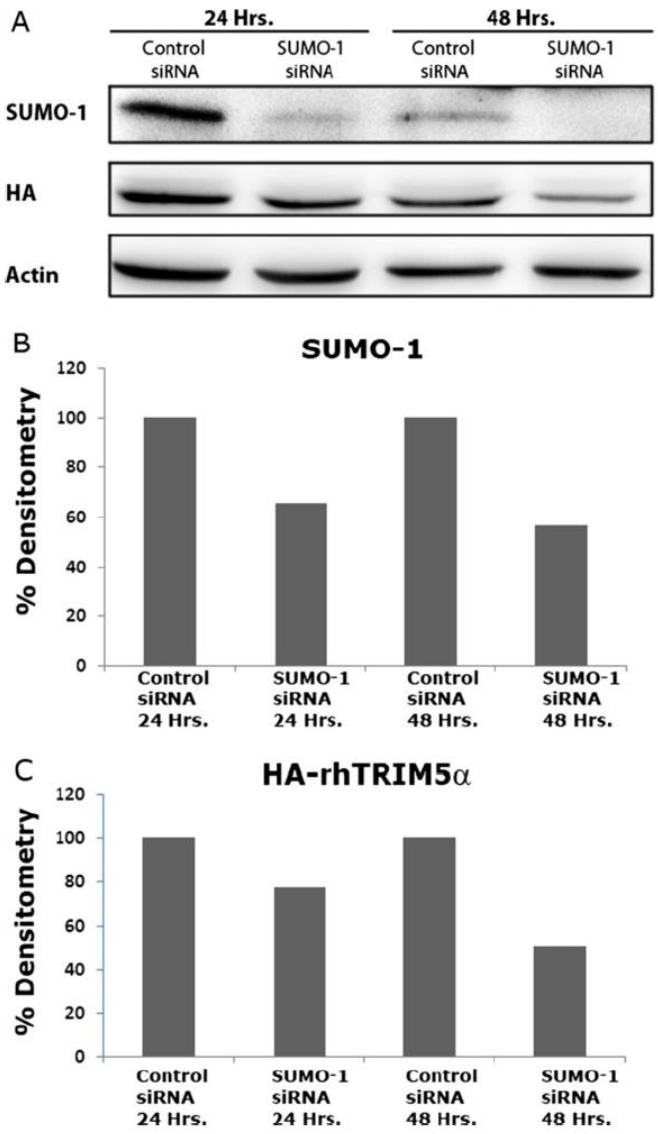

Figure 32. SUMO-1 stabilizes rhTRIM5α in cells. A. HeLa cells stably expressing HA-rhTRIM5α were transfected with SUMO-1 or non-targeting siRNA. Cells were collected 24 and 48 hours post transfection and analyzed by Western blot for HA, SUMO-1 and β-actin. **B.** Densitometry analysis using ImageJ on SUMO-1 protein levels. SUMO-1 siRNA treated cells were normalized to control siRNA cells. **C.** Densitometry analysis of HA-rhTRIM5α (Representative of three independent experiments),

NF-κB activation by rhTRIM5α is sensitive to SUMO-1 expression

Recent studies have shown that TRIM5 proteins can activate intracellular signaling pathways that culminate in AP-1 and NF-κB activation (136, 172). In order to understand the role of SUMO-1 and SIMs in rhTRIM5α-mediated signaling, we transiently expressed wild type and rhTRIM5α mutants along with an NF-κB luciferase reporter. Both the wild type and SIM3 mutant form of rhTRIM5α were able to activate NF-κB. On the other hand, the SIM1 and SIM2 mutants did not induce significant signaling above background in this context (Figure 33A, top panel). However, following transient transfection, the protein expression levels of the SIM1 and SIM2 mutants were reduced compared to wild type and SIM3 mutants, possibly explaining the loss of NF-κB activation (Figure 33A, bottom panel). To assess NF-κB signaling by rhTRIM5α SIM mutants at comparable protein levels, we generated 293A cell lines stably expressing wild type rhTRIM5α and the SIM mutants and measured NF-κB activation in these cells. Under these conditions, when the SIM mutants were expressed at comparable levels to wild type rhTRIM5α, they elicited similar levels of NF-κB activation (Figure 33B). Consistent with a previous report that showed normal oligomerization of these mutants (170), and the data here that demonstrate the ability of these mutants to activate NF-κB, we conclude that the defect in restriction by rhTRIM5α SIM mutants is not due to gross misfolding of the protein.

We next asked how SUMO-1 depletion affected the ability of wild type rhTRIM5α to induce NF-κB activation. We co-transfected 293T cells with wild type

HA-rhTRIM5α, SUMO-1 or control siRNA and an NF-κB driven luciferase reporter. We measured NF-κB activation by rhTRIM5α in SUMO-1 siRNA treated cells compared to rhTRIM5α cells treated with control siRNA. As shown in Figure 28C knocking down SUMO-1 had little effect on NF-κB activation when transfected with EV (~10%, black bar). However, depletion of SUMO-1 significantly reduced (~60%, $p<0.004$, Student's T-test) NF-κB activation by wild type rhTRIM5α (Figure 31C, grey bar). The reduction of NF-κB activation in the presence of SUMO-1 siRNA was not due to reduced rhTRIM5α protein levels (Figure 33C inset). In this case SUMO-1 knockdown did not affect TRIM5α protein levels because it was transfected (much more protein is present) as opposed to cells that stably express rhTRIM5α (less protein in cells) (Figure 32). Conversely, overexpression of SUMO-1 increased NF-κB activation following transfection with empty vector or vector expressing wild type rhTRIM5α (Figure 33D). This increase was more pronounced when rhTRIM5α was present, although this result was not statistically significant ($p=0.187$, Student T-test). These experiments demonstrate that the ability to associate with SUMO-1 or SUMOylated proteins is relevant to rhTRIM5α-mediated NF-κB signaling.

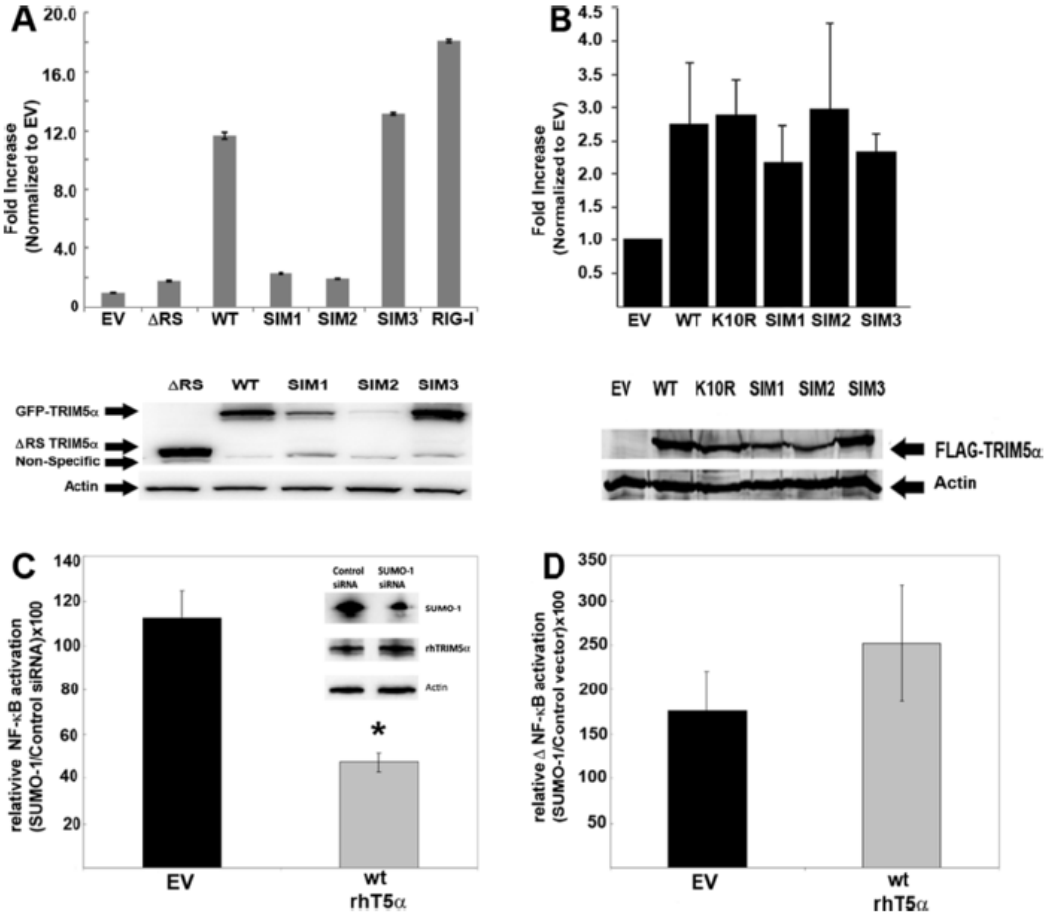
A
Fold Increase (Normalized to EV)
20.0
16.0
12.0
8.0
4.0
0
EV
ΔRS
WT
SIM1
SIM2
SIM3
RIG-I
B
Fold Increase (Normalized to EV)
4.5
4.0
3.5
3.0
2.5
2.0
1.5
1.0
0.5
EV
WT
K10R
SIM1
SIM2
SIM3
ΔRS
WT
SIM1
SIM2
SIM3
GFP-TRIM5α
ΔRS TRIM5α
Non-Specific
Actin
EV
WT
K10R
SIM1
SIM2
SIM3
FLAG-TRIM5α
Actin
C
relativive NF-κB activation (SUMO-1/Control siRNA)x100
140
120
100
80
60
40
20
Control siRNA
SUMO-1 siRNA
SUMO-1
rhTRIM5α
Actin
*
EV
wt rhT5α
D
relative Δ NF-κB activation (SUMO-1/Control vector)x100
350
300
250
200
150
100
50
EV
wt rhT5α

Figure 33. SIMs and SUMO-1 role in rhTRIM5α activation of NF-κB. A. 293T or **B.** 293A cells were transfected with empty vector (EV), ΔRING/SPRY rhTRIM5α (ΔRS), wild typer hTRIM5α, SIM mutants or RIG-I along with NF-κB-responsive firefly luciferase construct. 48-hours post transfection, luciferase activity was measured. NF-κB luciferase readings were normalized to renilla luciferase, and plotted as an average fold increase over empty vector. Upper panel-representative NF-κB activity in presence of wt rhTRIM5α and SIM mutants. (Error bars represent the standard error of the mean between the triplicates. Lower panel-Western blot of samples in the upper panel. Data is representative of 4 independent experiments.) **C.** 293T cells were transfected with Control siRNA or SUMO-1siRNA for 48 hours. Cells were then seeded in a 96-well plate in triplicate and transfected with empty vector or wild type rhTRIM5α. NF-κB activity was measured as in A. Data were plotted by dividing SUMO-1 siRNA activation by control siRNA activation x 100. Inset, representative Western blot. (Statistical significance was calculated by using a Student's t-test, $p<0.004$. Error bars represent the standard error of the mean between the triplicates). **D.** 293T cells were transfected with empty vector, and wild type rhTRIM5α constructs in presence and absence of SUMO-1. NF-κB activity was measured as in A. Data were plotted as in C. (Statistical significance was calculated by using a Student's t-test, no significant difference. Error bars represent the standard error of the mean between triplicates. Representative of 3 independent experiments.

The SIM1 and SIM2 mutations disrupt rhTRIM5α trafficking to nuclear bodies containing PML and SUMO-1

We next analyzed the association of rhTRIM5α and SUMO-1 by immunofluorescence to determine if SIM1 and SIM2 interact with SUMO-1 or SUMO-1 modified proteins. In HeLa cells stably expressing YFP-rhTRIM5α, we examined the co-localization of rhTRIM5α and endogenous SUMO-1. We used two antibodies to SUMO-1 to examine both the cytoplasmic and nuclear fractions of SUMO-1. The first antibody (GMP1, clone 21C7) recognized nuclear SUMO-1 as well as numerous cytoplasmic puncta. However, the cytoplasmic SUMO-1 did not co-localize with YFP-rhTRIM5α (Figure 34). SUMO-1 positive structures in the nucleus are well characterized and known to contain PML (173, 174), we used a second antibody (clone Y299) that recognized most of the larger nuclear structures that were PML positive (Figure 35). This antibody detected primarily punctate nuclear SUMO-1. We used this antibody in subsequent experiments to examine SIM1 and SIM2 localization with SUMO-1. A recent study demonstrated that while steady state rhTRIM5α is excluded from the nucleus, it can transiently enter and exit the nucleus, where it associates with PML bodies. This nuclear localization of rhTRIM5α to PML bodies is observed when the nuclear export of rhTRIM5α is inhibited with Leptomycin B (LMB), which is an inhibitor of CRM1 mediated nuclear export (175). Inhibiting the nuclear export of rhTRIM5α using LMB revealed that wt and all three SIM mutants localized to the nucleus (Figure 36A), contrary to a recent report by another group which found that the SIM1 and SIM2 mutants did not localize to the

nucleus under these conditions (170). However, when we quantified the localization of these mutants to nuclear SUMO-1 bodies, SIM1 and SIM2 mutants of rhTRIM5α failed to localize to SUMO-1 positive bodies when nuclear export is inhibited, while the SIM3 mutant associated with these bodies to an intermediate degree (Figure 36B). This data suggests that rhTRIM5 SIM1 and SIM2 cannot interact with a SUMOylated protein in the nucleus, presumably PML or other unidentified proteins in those bodies, while wt rhTRIM5 and SIM3 can. The ability to interact with SUMOylated proteins somehow dictates the ability to which HIV-1 is restricted by TRIM5α.

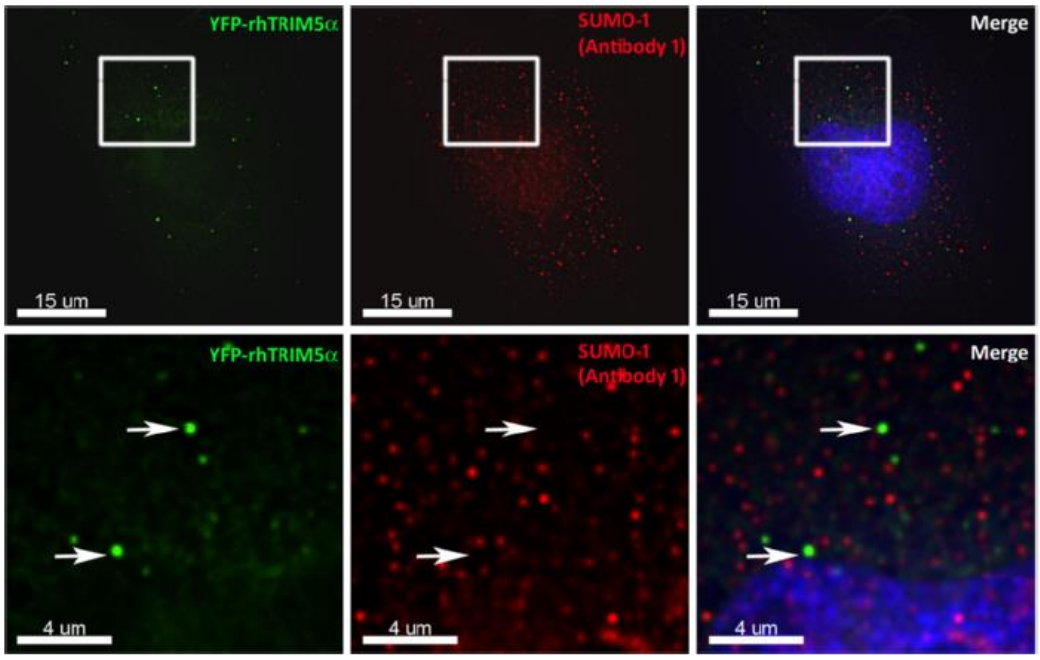

Figure 34. SUMO-1 antibody that recognizes cytoplasmic SUMO-1 does not localize to rhTRIM5α cytoplasmic bodies. HeLa cells stably expressing YFP-rhTRIM5α were immunostained with an antibody to cytoplasmic SUMO-1 (21C7 clone). The white box in the top panel represents the area that was zoomed in to create the bottom panel. White arrows point to representative rhTRIM5α cytoplasmic bodies that do not contain cytoplasmic SUMO-1. (Representative Images)

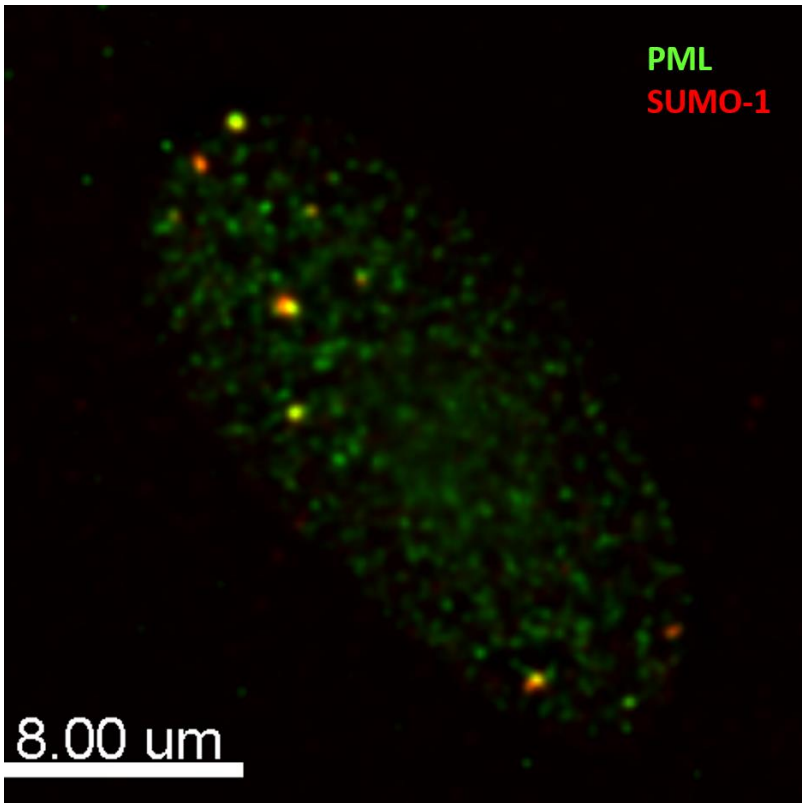

Figure 35. SUMO-1 in the nucleus localizes to PML (TRIM19). HeLa cells were fixed with 3.7% formaldehyde in PIPES buffer. Following the fixing protocol, cells were stained with an antibody to PML and an antibody to SUMO-1 (clone Y299). (Representative Image)

A.

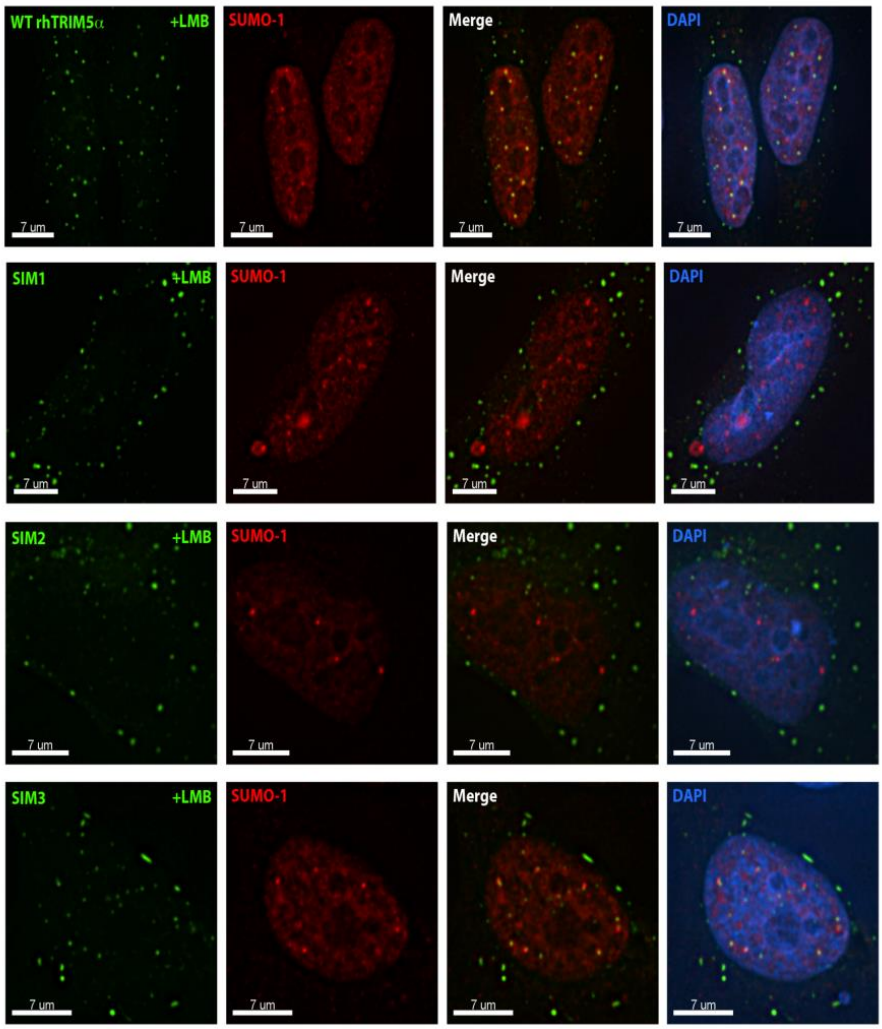
WT rhTRIM5α
+LMB
SUMO-1
Merge
DAPI
SIM1
SIM2
SIM3
7 um

B

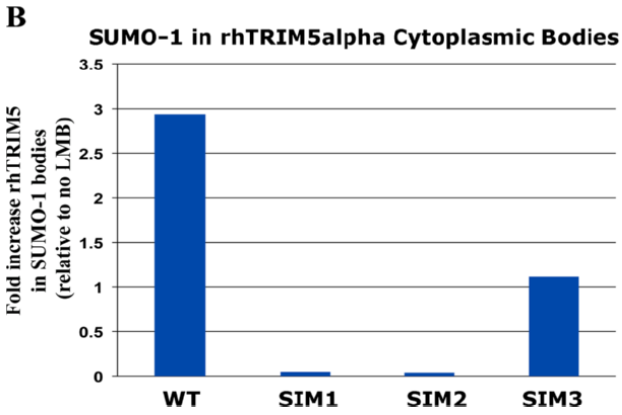
SUMO-1 in rhTRIM5alpha Cytoplasmic Bodies
Fold increase rhTRIM5 in SUMO-1 bodies (relative to no LMB)
3.5
3
2.5
2
1.5
1
0.5
0
WT
SIM1
SIM2
SIM3

Figure 36. SIM1 and SIM2 mutations disrupt rhTRIM5α localization to nuclear bodies containing PML/TRIM19 and SUMO-1. A. HeLa cells stably expressing wt YFP-rhTRIM5α or SIM mutants were treated with leptomycinB (LMB) for 4 hours. Cells were fixed, stained for SUMO-1 and DAPI (nucleus) and imaged. **B.** Images were analyzed for YFP-rhTRIM5α maximum fluorescence intensity (MFI) in SUMO-1 nuclear bodies by the use of the Surface Finder function in the Imaris software (Bitplane). (Representative Images and Quantification from three independent experiments)

CHAPTER VI

RESULTS: MICROTUBULES AND DYNEIN FACILITATE HIV-1 UNCOATING.

Effect of Microtubule Disruption on Uncoating Kinetics of HIV-1 Utilizing CsA Withdrawal Assay

Until recently, the kinetics of uncoating have been hard to determine due to the lack of assays and the instability of the HIV-1 core in experimental systems. However, utilizing TRIMCyp, a restriction factor of HIV-1, Perez-Caballero et al. designed an assay to determine the kinetics of virus sensitivity to TRIMCyp (116). Utilizing this assay, the percent of cores that have or have not uncoated can be calculated based on their sensitivity to TRIMCyp after Cyclosporin A is withdrawn (26, 116). Since TRIMCyp only recognizes HIV-1 capsid in a context of an assembled core, any cores that have shed their p24 will be insensitive to TRIMCyp following release from CsA. Therefore, this assay allows us to infer the status of the cores within living cells. Utilizing this approach, it was determined that half-life of uncoating occurs in about 40 minutes (26). This supports the model that majority uncoating occurs in the cytoplasm after entry before nuclear import. Within this same time frame, HIV-1 was shown to traffic on microtubules. Therefore, we wanted to determine whether microtubule disruption delays

uncoating. CsA withdrawal assay was employed with the addition of 2 Hours of Nocodazole treatment following a synchronized infection with VSVg and AMLV pseudotyped HIV-1 carrying a GFP reporter. With 2 hours of Nocodazole treatment, TRIMCyp restriction of incoming HIV-1 with two different pseudotypes that enter cells by different mechanisms was not inhibited. This demonstrates that TRIMCyp's ability to restrict virus is not dependent on the microtubule network allowing us to utilize it in this assay with drug treatments. Following microtubule disruption, HIV-1 uncoating was delayed with VSVg or AMLV envelope (Figure 37A and B). The delay was observed in the early time-points of the time-course, once again suggesting that uncoating occurs relatively early following infection and that this process is further delayed when microtubules are disrupted. Interestingly, when Nocodazole was washed out 2 hours following an infection and the assay was allowed to proceed, there was a significant increase in uncoating within the next hour in OMK cells. This prompted us to examine the microtubules following Nocodazole removal. Within 1 hour of Nocodazole removal, acetylated (stable) and tyrosinated (dynamic) microtubules were rebuilt (Figure 37B). In HeLa cells, Nocodazole treatment lead to the fragmentation of microtubules as opposed to the microtubules in OMK cells that were mostly depolymerized. However, within 1 hour of Nocodazole removal in both cell types the microtubule integrity was completely restored (Figure 37B). This demonstrates that HIV-1 uncoating is

delayed when microtubules are disrupted, however, when they are allowed to polymerize upon drug removal, uncoating continues.

Since microtubules are dynamic structures, it is possible that further stabilization of microtubules leads to an increase in uncoating. In OMK cells, microtubules were stabilized with a drug known as Taxol. These cells were treated with 2 Hrs. of 0.1 μM Taxol during the CsA withdrawal assay. Figure 38 shows that stabilizing microtubules slightly increased uncoating, which was not significant. These data demonstrate that the virus utilizes microtubules to facilitate uncoating of the core.

A.

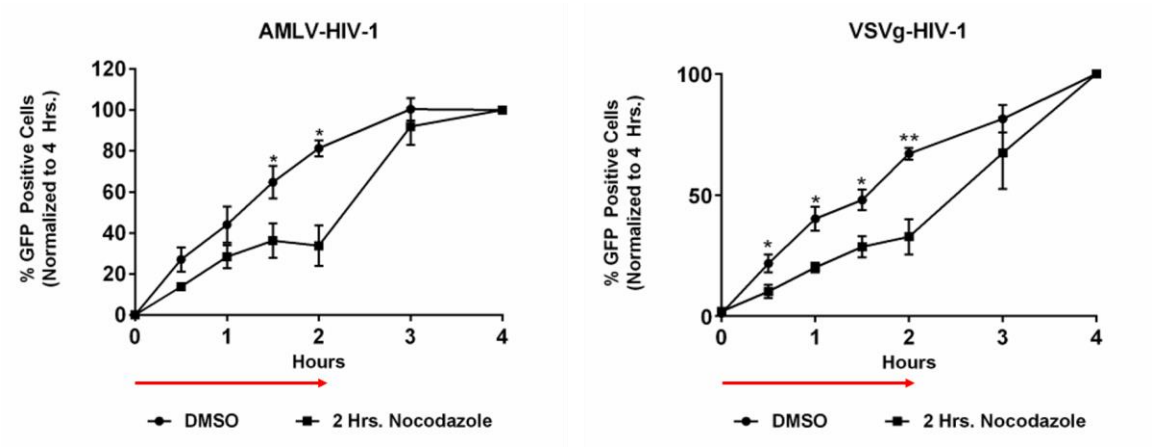
AMLV-HIV-1
% GFP Positive Cells (Normalized to 4 Hrs.)
120
100
80
60
40
20
0
0
1
2
3
4
Hours
DMSO
2 Hrs. Nocodazole
VSVg-HIV-1
% GFP Positive Cells (Normalized to 4 Hrs.)
100
50
0
0
1
2
3
4
Hours
DMSO
2 Hrs. Nocodazole

B.

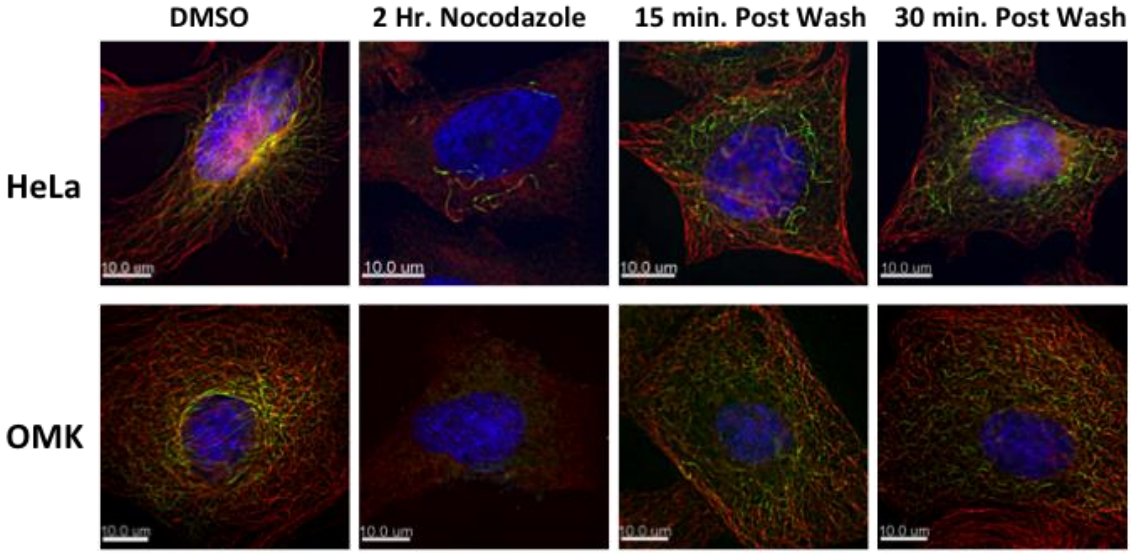
DMSO
2 Hr. Nocodazole
15 min. Post Wash
30 min. Post Wash
HeLa
OMK
10.0 um

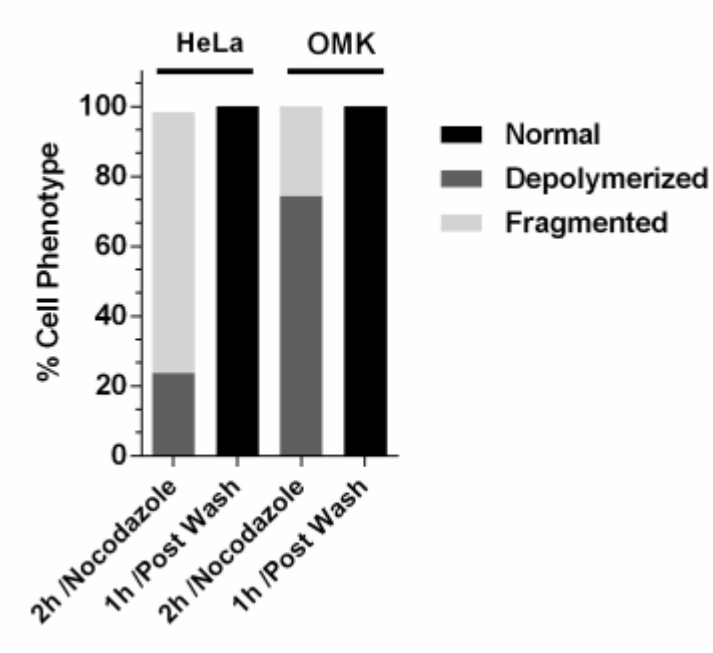

Figure 37. HIV-1 uncoating is delayed when microtubules are disrupted as measured by the CsA withdrawal assay. A. CsA withdrawal assay was performed where OMK cells were infected with VSVg or AMLV pseudotyped HIV-1 by spinoculation to synchronize the infection in presence of Nocodazole (10 μM)/CsA or DMSO/CsA. Following spinoculation the media on cells was changed to contain Nocodazole/CsA or DMSO/CsA. At each time point indicated on the axis, the CsA was removed and replaced with DMSO or Nocodazole containing media for the first two hours. Following 2 hours, Nocodazole/DMSO was removed from the cells and changed to media containing CsA for the remaining time points. Red line indicates the extent of the Nocodazole treatment. 48 hours post infection, cells were collected and analyzed by flow cytometry for GFP expression. (Significance determined by Multiple Comparisons t-test, *$p<0.05$, **$p<0.01$) **B.** Cells were treated with 2 hours of Nocodazole followed by removal of the drug for 1 hour. Cells were fixed and stained with antibodies to acetylated tubulin (red-dynamic microtubules) and tyrosinated tubulin (green-stable microtubules). Random fields on the coverslip were imaged and the phenotype was quantified as either normal (all microtubules intact), depolymerized (diffuse staining in the cells) or fragmented (shorter microtubules with diffuse staining as well).

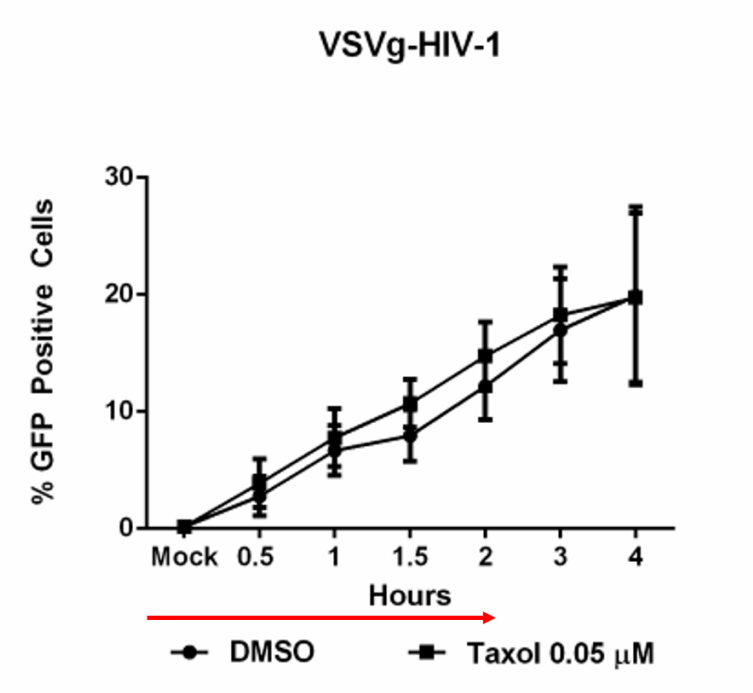

Figure 38. Taxol slightly increases HIV-1 Uncoating. CsA withdrawal assay was performed where OMK cells were infected with VSVg or AMLV pseudotyped HIV-1 by spinoculation to synchronize the infection in presence of Taxol (0.1 μM)/CsA or DMSO/CsA. Following spinoculation the media on cells was changed to contain Taxol/CsA or DMSO/CsA. At each time point indicated on the axis, the CsA was removed and replaced with DMSO or Nocodazole containing media for the first two hours. Following 2 hours, Taxol/DMSO was removed from the cells and changed to media containing CsA for the remaining time points. Red line indicates the extent of the Taxol treatment. 48 hours post infection, cells were collected and analyzed by flow cytometry for GFP expression. (No significance detected as determined by Multiple Comparisons t-test, Data is represented as the average of three independent experiments).

Effect of Microtubule Disruption on Uncoating Kinetics Utilizing In Situ Fluorescence Assay

To analyze individual viruses in cells in presence or absence of microtubules we utilized fluorescently labeled and stained HIV-1 as previously described (176). VSVg-pseudotyped HIV-1 is labeled with two fluorescent proteins to discern viruses that have productively fused from those that remain in endosomes. GFP-Vpr is incorporate within the viral core during virus production (30) and S15-mCherry is embedded in the host cell membrane and incorporated into the viral envelope during budding. Following successful fusion, the S15-mCherry labeled envelope is lost and GFPV-Vpr that is associated with the viral core is released into the cytoplasm (176-178). In the assays, infection with the double labeled HIV-1 is synchronized using spinoculation in presence or absence of drugs. Following spinoculation, the media is exchanged for warm media and the cells are shifted to a 37°C incubator to initiate fusion (BafilomycinA, an inhibitor of fusion is used as a negative control). At various time-points post spinoculation in presence or absence of nocodazole, cells were fixed and stained for p24 (CA). Cells were imaged utilizing a deconvolution wide-field microscope and analyzed for p24 fluorescence intensity. Images were analyzed by Imaris software where surfaces were generated around GFP-Vpr viruses and intensity of p24 and S15-mCherry were detected. Viruses that were S15-mCherry negative (fused) were plotted for their p24 content in presence or absence of nocodazole over the course of 4 hours. When microtubules were

disrupted, viruses contained higher levels of p24 at every time point post infection suggesting that the absence of microtubules delays the loss of p24 from viruses (Figure 39A and B). These data demonstrate that microtubules facilitate uncoating (loss of p24) of HIV-1 because in absence of microtubules GFP-Vpr viruses are not shedding p24 as fast as the DMSO treated group.

A.

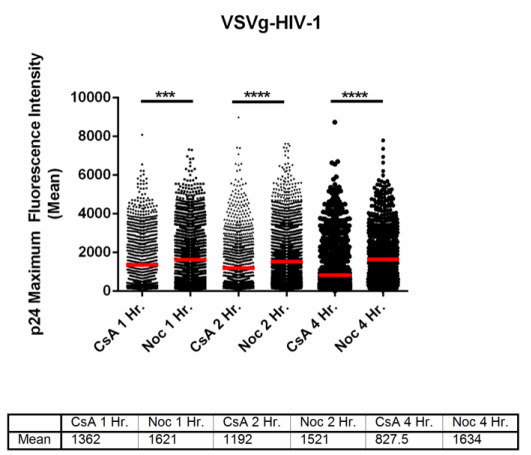

	CsA 1 Hr.	Noc 1 Hr.	CsA 2 Hr.	Noc 2 Hr.	CsA 4 Hr.	Noc 4 Hr.
Mean	1362	1621	1192	1521	827.5	1634

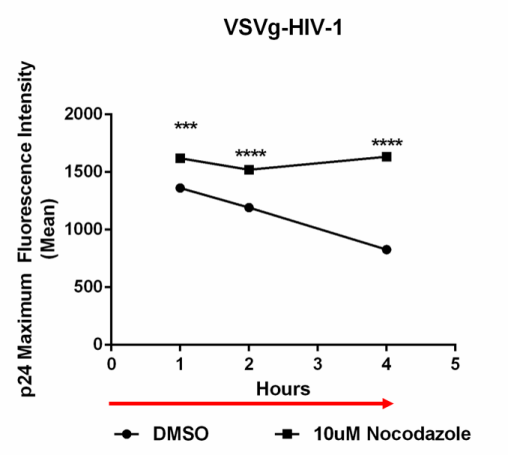

B.

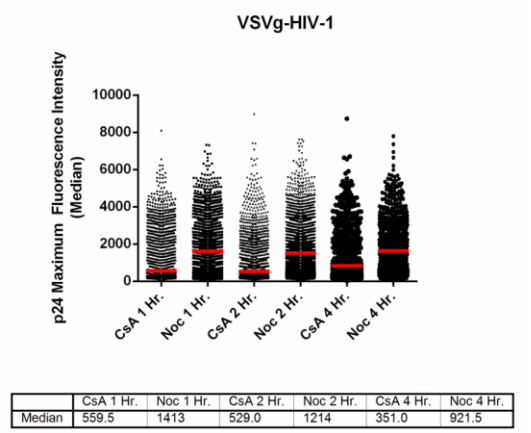

	CsA 1 Hr.	Noc 1 Hr.	CsA 2 Hr.	Noc 2 Hr.	CsA 4 Hr.	Noc 4 Hr.
Median	559.5	1413	529.0	1214	351.0	921.5

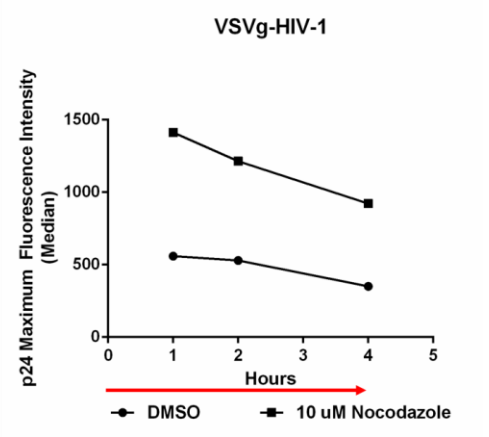

Figure 39. HIV-1 utilizes microtubules to uncoat as measured by the in situ uncoating assay. HeLa cells were infected with fluorescently labeled HIV-1 (s15-mCherry and GFP-Vpr) by spinoculating the virus on the cells with Nocodazole (10 μM)/CsA or DMSO/CsA. Following spinoculation the media on cells was changed to contain Nocodazole/CsA or DMSO/CsA. Cells were fixed at every indicated time-point. Red arrow indicates the extent of the Nocodazole/CsA or DMSO/CsA treatment. Subsequently, the cells were stained for p24 utilizing a monoclonal antibody (Ag3.0). Images were quantified by using the Imaris software. Fused viruses (S15-mCherry negative, GFP-Vpr positive) were analyzed for their p24 maximum fluorescence intensity. **A.** Graph depicting viruses that were analyzed. Each dot represents a single virus. The red bars from A. were plotted to demonstrate the average intensity (mean) of p24 at indicated time-points with or without Nocodazole treatment. (One-way ANOVA, ***$p<0.001$, ****$p<0.0001$). **B.** Data analyzed as in A. Red bars represent the median, which is graphed in the image on the right.

Dynein Facilitates HIV-1 Uncoating

Since disruption of microtubules delayed uncoating, we wanted to determine if knockdown of dynein recapitulated the phenotype that was observed. We transfected HeLa cells with dynein heavy chain siRNA (DYNC1H1) cells for 48 hours, which substantially decreased dynein levels (Figure 40A). These cells were infected with fluorescently labeled HIV-1 and fixed at various time-points post infection. The CA levels were analyzed by Imaris in viruses that successfully fused. When dynein was knocked down, viruses retained higher levels of CA as compared to control siRNA treated cells (Figure 40B). Furthermore, when an inhibitor of dynein's ATPase functinon (CiliobrevinD) was used, HIV-1 uncoating was also delayed as measured by the CsA withdrawal assay (Figure 41A). We assessed the efficacy of the dynein inhibition by staining the cells for golgi which is known to disperse throughout the cells when dynein is inhibited (Figure 41B). Alltogether, these data suggest that HIV-1 utilizes dynein that is on microtubules to mediate uncoating of the core. When dynein is knocked down, there is a delay in uncoating. Whether an opposing protein acts on the viral core to control the rate of uncoating remains to be determined. It is exciting to hypothesize that members of the kinesin family participate in the uncoating process as well. Other viruses utilize dynein and kinesin simultaneously to exert opposing forces on the capsid that eventually lead to uncoating (179) which remains to be fully explored in the case of HIV-1.

A.

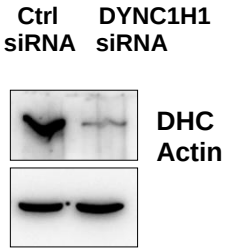
Ctrl siRNA
DYNC1H1 siRNA
DHC
Actin

B.

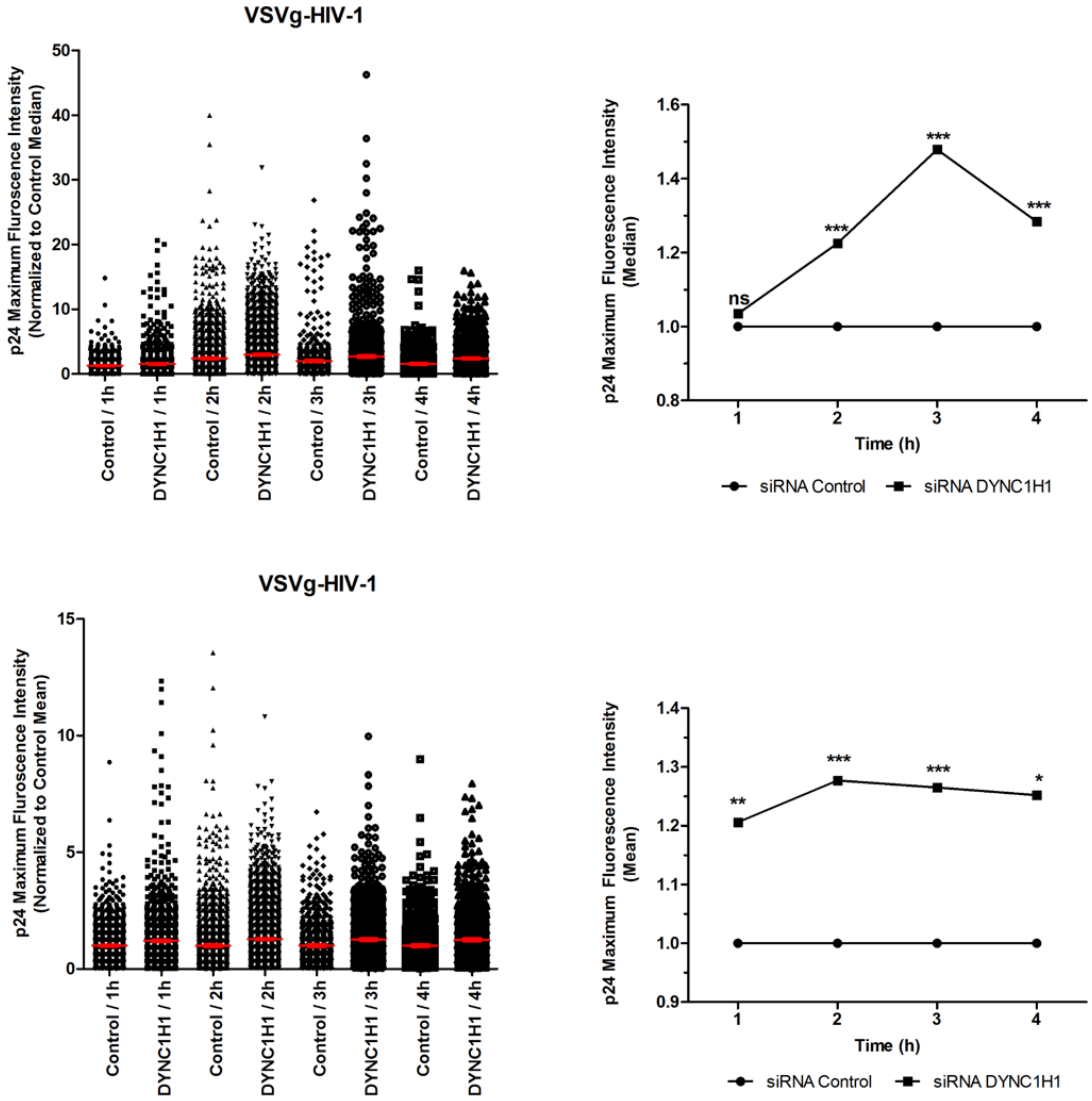
VSVg-HIV-1
p24 Maximum Fluroscence Intensity (Normalized to Control Median)
Control / 1h
DYNC1H1 / 1h
Control / 2h
DYNC1H1 / 2h
Control / 3h
DYNC1H1 / 3h
Control / 4h
DYNC1H1 / 4h
p24 Maximum Fluorescence Intensity (Median)
ns
***
Time (h)
siRNA Control
siRNA DYNC1H1
VSVg-HIV-1
p24 Maximum Fluroscence Intensity (Normalized to Control Mean)
p24 Maximum Fluorescence Intensity (Mean)
**
*

Figure 40. DYNC1H1 knockdown delays HIV-1 uncoating. HeLa cells were transfected with siRNA against DYNC1H1 for 48 hours. **A.** Western blot depicting DYNC1H1 knockdown. **B.** Following the transfection protocol, HeLa cells were infected with fluorescently labeled HIV-1 (s15-mCherry and GFP-Vpr) by spinoculating the virus on the cells. Following spinoculation, a time-course was performed where cells were fixed at every indicated time-point. Subsequently, the cells were stained for p24 utilizing a monoclonal antibody (Ag3.0). Images were quantified by using the Imaris software. Fused viruses (S15-mCherry negative, GFP-Vpr positive) were analyzed for their p24 maximum fluorescence intensity. Each dot represents a single virus. Red bars were plotted in the subsequent graph to display the median or the mean of the p24 fluorescence intensity. (DYNC1H1 data was normalized to the control data from four independent experiments. Statistical significance of the mean was calculated using a One-way ANOVA, *$p<0.05$, **$p<0.01$, ***$p<0.001$).

A.

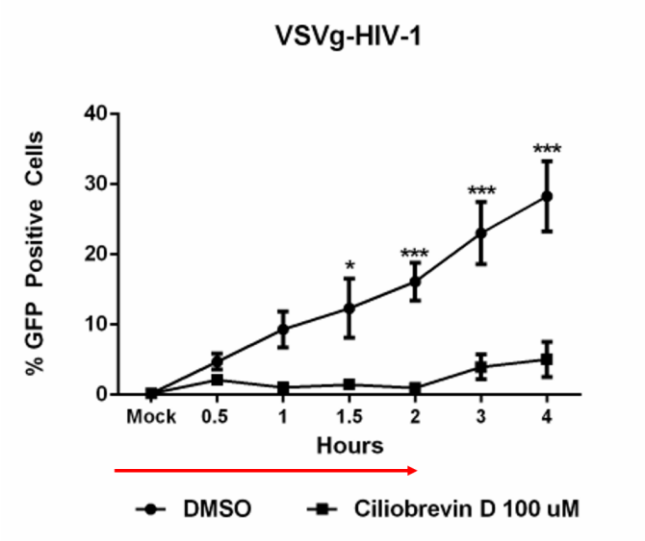
VSVg-HIV-1
% GFP Positive Cells
40
30
20
10
0
Mock
0.5
1
1.5
2
3
4
Hours
*
***
***
***
DMSO
Ciliobrevin D 100 uM

B.

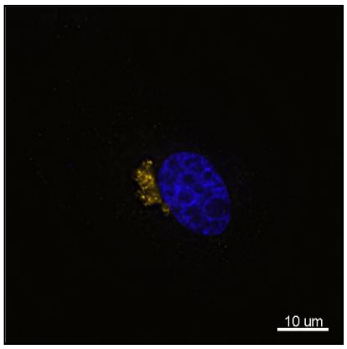
10 um

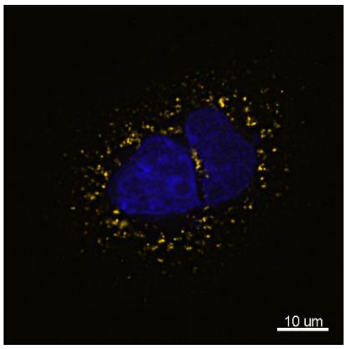
10 um

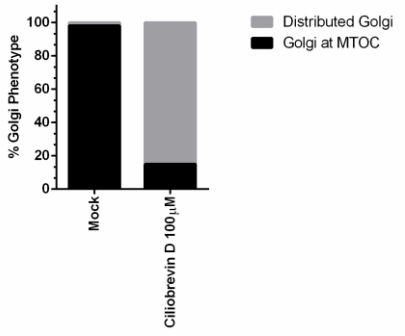
% Golgi Phenotype
100
80
60
40
20
0
Mock
Ciliobrevin D 100μM
Distributed Golgi
Golgi at MTOC

Figure 41. Inhibition of dynein function by CiliobrevinD delays HIV-1 uncoating. A. CsA withdrawal assay was performed where OMK cells were infected with VSVg or AMLV pseudotyped HIV-1 by spinoculation to synchronize the infection in presence of CiliobrevinD (100 μM)/CsA or DMSO/CsA. Following spinoculation the media on cells was changed to contain CiliobrevinD/CsA or DMSO/CsA. At each time point indicated on the axis, the CsA was removed and replaced with DMSO or CiliobrevinD containing media for the first two hours. Following 2 hours, CiliobrevinD/DMSO was removed from the cells and changed to media containing CsA for the remaining time points. Red line indicates the extent of the CiliobrebinD treatment. 48 hours post infection, cells were collected and analyzed by flow cytometry for GFP expression. (No significance detected as determined by Multiple Comparisons t-test, Data is represented as the average of three independent experiments). **B.** Cells were also stained for golgi following DMSO or 100uM CiliobrevinD treatment to quantify the extent of golgi dispersal as a measure of dynein inhibition.

Microtubule disruption and the effects on HIV-1 fusion and infectivity

To access the effect of microtubule disruption on HIV-1 infection, microtubules were disrupted and infectivity was monitored 48 hours post synchronized infection utilizing a GFP reporter virus. With 2 hour Nocodazole treatment following the infection, there was a slight decrease in infectivity. In HeLa cells the decrease in infection was more drastic than in OMK cells, but the decrease in infectivity was not significantly different. This suggests that disrupting microtubules for 2 hours does not drastically affect HIV-1 infectivity as measured 46 hours after the removal of drug (Figure 42A). We did not prolong the inhibition of microtubules further as it affects cell viability, which would impair proper analysis of the results. Additionally, since microtubule network is known to be important for vesicular trafficking, we wanted to determine whether microtubule disruption affects the virus' ability to fuse with target cells since we pseudotyped with VSVg (pH Dependent) and AMLV (pH Independent). Utilizing a β-lactamase tagged Vpr (BLaM-Vpr) containing VSVg-HIV-1 or AMLV-HIV-1, we determined that 2 Hr. Nocodazole treatment did not decrease VSVg pseudotyped HIV-1 fusion in target cells, which suggests that we are looking at downstream event of fusion such as uncoating in our CsA withdrawal assay. In fact 2 Hrs. of Nocodazole treatment slightly increased fusion, demonstrating that our phenotype is even larger than observed because more viruses are fusing in Nocodazole treated cells as compared to DMSO treatment (Figure 42B). Also, we used fluorescently labeled HIV-1 to measure fusion (S15-mCherry negative viruses) and determined that the percent of

S15-mCherry negative viruses did not change whether Nocodazole was present or not.

A.

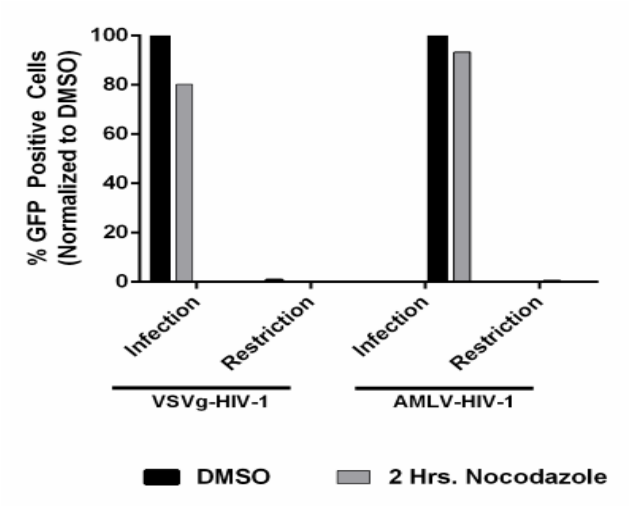
% GFP Positive Cells
(Normalized to DMSO)
100
80
60
40
20
0
Infection
Restriction
Infection
Restriction
VSVg-HIV-1
AMLV-HIV-1
DMSO
2 Hrs. Nocodazole

B.

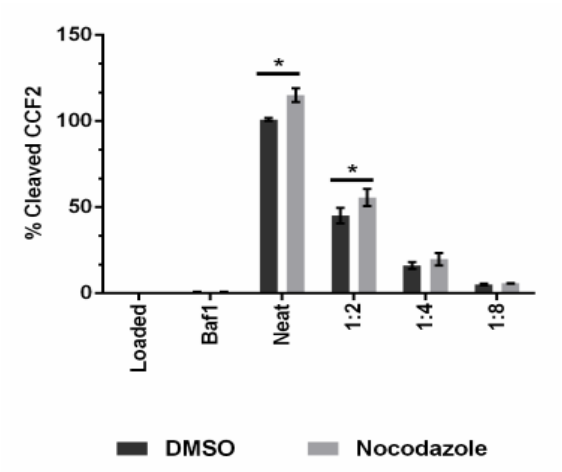
% Cleaved CCF2
150
100
50
0
*
*
Loaded
Baf1
Neat
1:2
1:4
1:8
DMSO
Nocodazole

C.

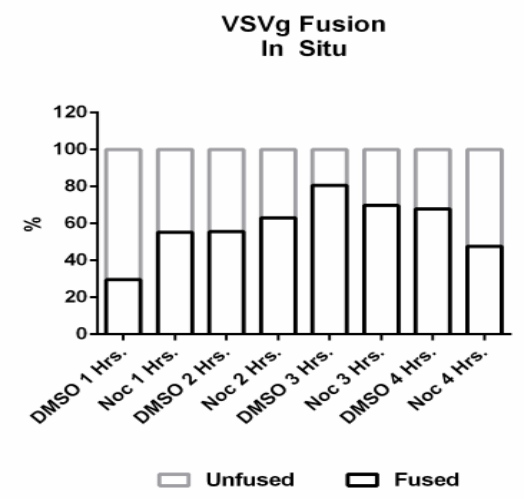
VSVg Fusion
In Situ
%
120
100
80
60
40
20
0
DMSO 1 Hrs.
Noc 1 Hrs.
DMSO 2 Hrs.
Noc 2 Hrs.
DMSO 3 Hrs.
Noc 3 Hrs.
DMSO 4 Hrs.
Noc 4 Hrs.
Unfused
Fused

Figure 42. Microtubule disruption effects on infectivity, TRIM5 restriction and virus fusion. A. Cells were infected with VSVg or AMLV pseudotyped HIV-1 with 2 Hr. Nocodazole alone or in combination with CsA. Following the treatment, media was exchanged for fresh media and infection was allowed to proceed for 46 hours. %GFP positive cells were quantified by flow cytometry. **B.** To measure fusion two assays were employed. Left image: Cells were spinoculated with VSVg- HIV-1 virus containing BLaM-Vpr in presence of DMSO or Nocodazole, and the infection was allowed to proceed for 3 hours at 37°C. Subsequently, cells were loaded with CCF2-AM for 1 hour. The reaction was allowed to proceed overnight. Cells were collected and analyzed by flow cytometry for the percent of CCF2 cleavage as a measure of HIV-1 fusion. **C.** Fluorescently labeled HIV-1 (S15-mCherry and GFP-Vpr) was spinoculated on cells and a time-course was performed in presence of DMSO or nocodazole. Images were analyzed for the percent of fused (S15-mCherry negative, GFP-Vpr positive) and unfused (S15-mCherry positive, GFP-Vpr positive) viruses. (All data is representative of three independent experiments)

Microtubule disruption does not delay HIV-1 replication

Previously, it was demonstrated that inhibition of reverse transcription of HIV-1 delays uncoating, suggesting a relationship between the two processes. Therefore, we wanted to determine whether reverse transcription and nuclear import of the viral genome were delayed when uncoating was delayed with microtubule inhibition. Since uncoating is delayed when microtubules are disrupted, the expectation is that late reverse transcription and nuclear import are delayed as well. Following a 4 Hr. Nocodazole treatment, late reverse transcription (Late RT) (Figure 43A) and nuclear import (as measured by 2-LTR circles) (Figure 43B) were not significantly decreased at any of the time points. Within 1 to 2 hours following infection, we observe no difference in the generation of Late RT products in the presence of Nocodazole in OMK cells (Figure 43A), and a slight reduction in the number of 2-circles generated in these cells (Figure 43B), consistent with the infectivity observed in these cells following Nocodazole treatment. This demonstrates that Noc treatment is not directly influencing RT in these infections, and that initiation of RT does not require intact microtubules.

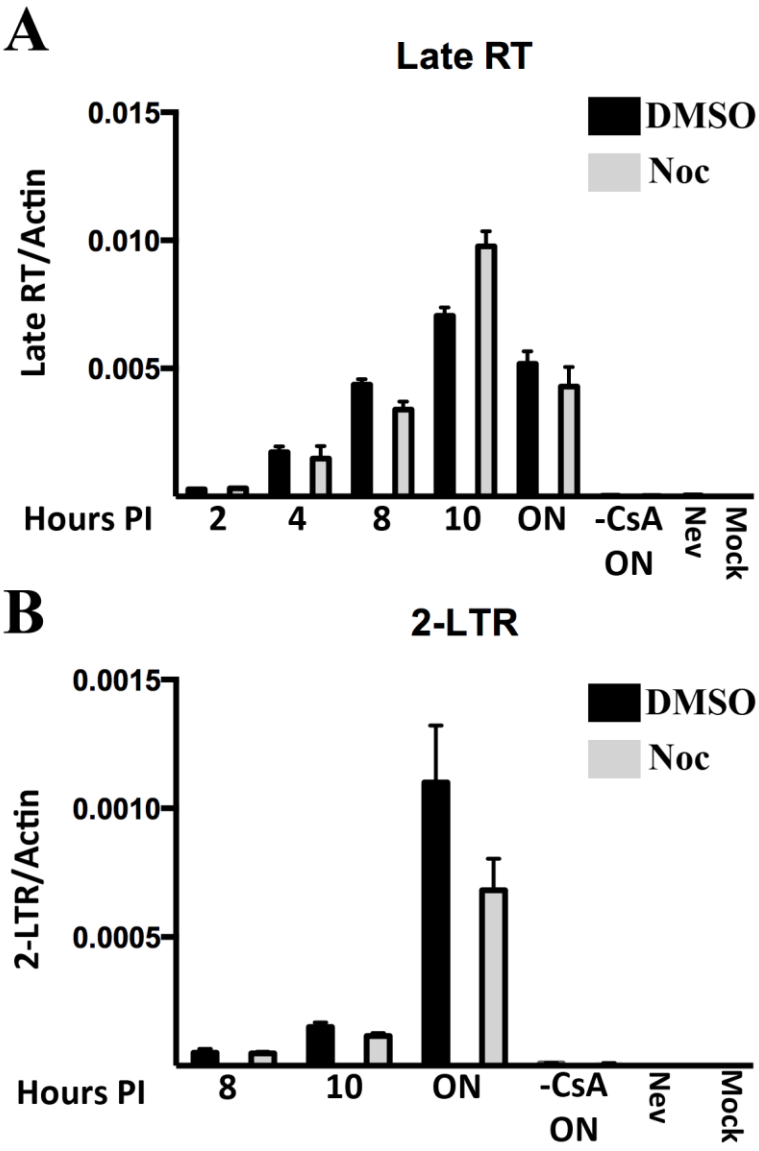
A
Late RT
DMSO
Noc
Late RT/Actin
0.015
0.010
0.005
Hours PI
2
4
8
10
ON
-CsA ON
Nev
Mock
B
2-LTR
DMSO
Noc
2-LTR/Actin
0.0015
0.0010
0.0005
Hours PI
8
10
ON
-CsA ON
Nev
Mock

Figure 43. Microtubule disruptions does not delay late reverse transcription and nuclear import of the HIV-1 genome. OMK cells were spinoculated with VSVg pseudotyped HIV-1 and a CsA withdrawal assay was performed in presence or absence of 2 or 4 hours of Nocodazole treatment. At various time-points cells were collected and analyzed by RT-PCR for **A.** Late reverse transcription products that were normalized to actin in the samples and **B.** Nuclear import, as measured by the production of 2-LTR circles that were normalized to actin in the samples. (Representative of three independent experiments. Error bars represent the standard deviation between the triplicates)

Summary

This study examined the interaction of host proteins with HIV-1 capsid that lead to facilitation or restriction of infection. We show that rhTRIM5α interacts with components of the ubiquitin-proteasome system. Moreover, the proteasome complex localizes to TRIM5 cytoplasmic bodies that contain restriction sensitive HIV-1, further confirming that the proteasome is involved in rhTRIM5-mediated restriction of retroviruses. This study also provides evidence that SIMs in TRIM5 are conserved and important for restriction because mutation of these SIMs decreases restriction. Also, SUMO-1 is required for TRIM5 protein stability because depletion of SUMO-1 reduced TRIM5 levels and consequently reduced TRIM5 restriction.

Finally, we demonstrate that HIV-1 uncoating is mediated by microtubules. When microtubules are disrupted more CA remains associated with viruses and they are sensitive to TRIMCyp restriction for a longer period of time. Depleting dynein recapitulated the phenotype that was observed when microtubules were disrupted, suggesting that motor proteins play a role in the uncoating process (Figure 44).

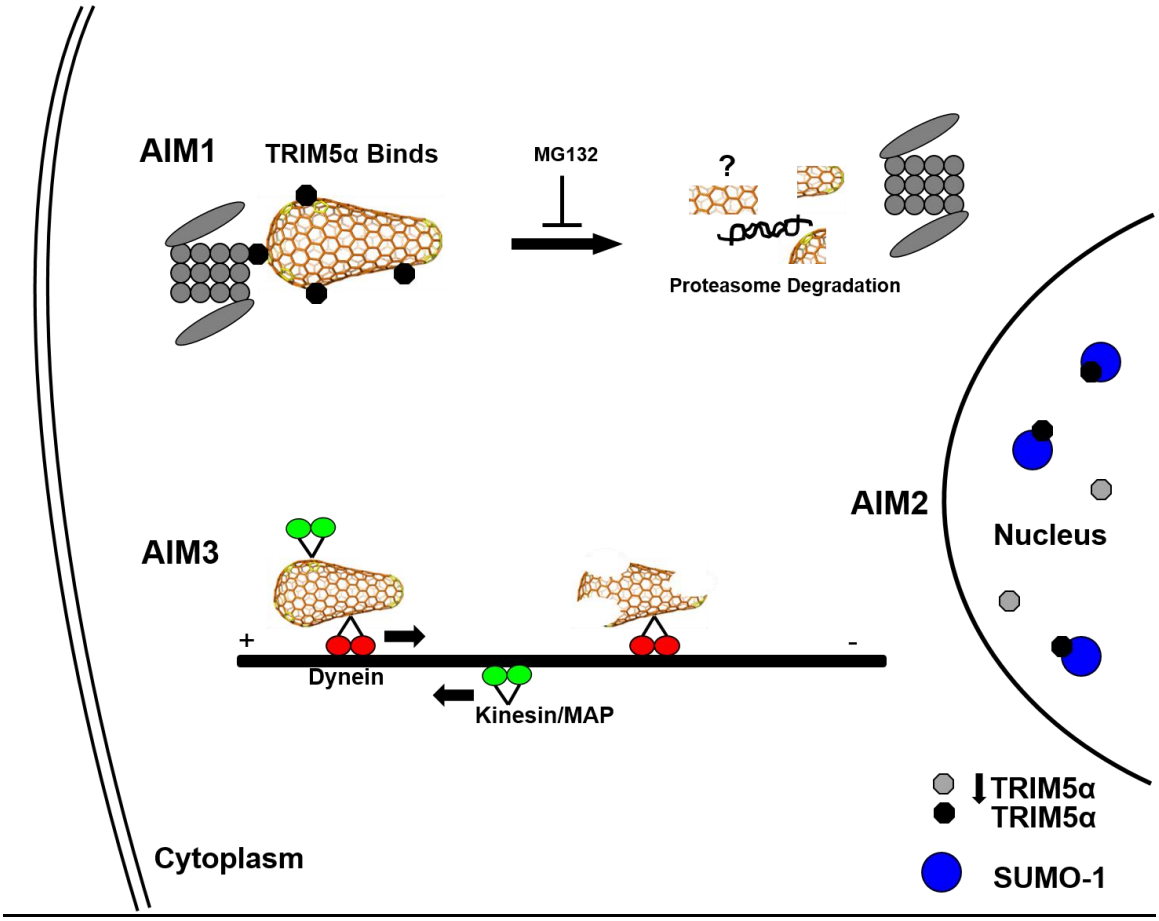

Figure 44. Summary of the aims. Aim 1. TRIM5 directly interacts with components of the proteasome during HIV-1 restriction. We observed that TRIM5 cytoplasmic bodies that form around incoming HIV-1 core are positive for proteasome subunits. TRIM5 recognition of the incoming core causes TRIM5 to be degraded in a proteasome-dependent manner as demonstrated by the Aiken lab. However, whether the capsid is degraded by the proteasome during this restriction process is currently unknown (?). **Aim 2.** TRIM5 traffics in and out of the nucleus. When it is in the nucleus, it localizes to SUMO-1 positive nuclear bodies (blue and black circles). However, if certain SIMs in TRIM5 are mutated or SUMO-1 is depleted from the cell, TRIM5 protein levels are decreased (gray circles) and so is the restriction. **Aim 3.** Following entry into the target cell, HIV-1 utilizes microtubules to traffic throughout the cell. It also utilizes microtubules to mediate uncoating of the viral core. Specifically, it utilizes dynein and probably other MAPs to mediate uncoating.

CHAPTER VII

DISCUSSION

Proteasome involvement in TRIM5α restriction of retroviruses

Since TRIM5α was identified as a restriction factor of retroviruses a decade ago, researches have been trying to identify the mechanism by which this restriction factor works. One host process that was identified to play a role is the ubiquitin-proteasome system (UPS). Proteasome inhibition alleviates TRIM5α restriction of HIV-1 reverse transcription even though infection and nuclear import remain impaired. This suggests a role for the ubiquitin-proteasome system (UPS) in TRIM5α-mediated restriction (123, 125). To this, additional data suggests that TRIM5α not only ubiquitinates itself but also generates unanchored K63-linked polyubiquitin chains. These polyubiquitin chains play a role in innate immune signaling during TRIM5α restriction of retroviruses. Therefore, these data prompted us to determine if there is an interaction between the proteasome complex and TRIM5α. Our studies demonstrate a direct interaction between the proteasome complex and TRIM5α (Figure 22, 25, 27). This complex of proteasome and TRIM5α forms around incoming virions, which further demonstrates the role of the UPS in restriction (Figure 28). In a study by Rold et al. they demonstrate that upon engagement of

restriction sensitive virus, TRIM5α itself is degraded in a proteasome-dependent manner (124).

Whether the UPS degrades viral components during restriction remains an unanswered question. Engagement of the viral capsid by TRIM5α may lead to proteasome-mediated degradation of the TRIM5α/CA complex, resulting in premature uncoating. Currently, data does not exist that demonstrates that lysines in CA are ubiquitinated. Therefore, it is possible that TRIM5α that is in complex with CA is ubiquitinated and degraded by the proteasome, which leads to the release of CA into the cytoplasm that isn't functional for further infection. In turn CA is not degraded by the proteasome but rather TRIM5α alone is. However, which particular ubiquitin linked chains and E1/E2s are involved remains to be determined. While we do know that Ubc13 aids TRIM5 in the synthesis of unanchored K63-linked polyubiquitin chains for innate immune signaling (136), it is not known whether they are important for degradation of TRIM5α. Ubc13 knockdown recapitulates the earlier observations made about TRIM5α cytoplasmic bodies with MG132 treatment (Figure 29) but specific interactions between this particular E2 and TRIM5 remain to be determined. It is possible that many E2s interact with TRIM5 to carryout diverse functions and conjugations.

To further address the importance of proteasome in TRIM5α-mediated restriction, Kutluay et al. utilized a different approach that relies on sucrose gradients to examine viral components during rhTRIM5α restriction of HIV-1 in

presence of a proteasome inhibitor (127). When rhTRIM5α expressing cells were infected in the absence of MG132, large complexes containing CA and viral RNA were lost and there was a concomitant increase in the levels of CA and viral RNA in soluble fractions. However, HIV-1 CA did not increase in soluble fractions concurrent with the loss from large complexes like N-MLV CA did following huTRIM5α restriction. Subsequently, MG132 treatment restored large subviral complexes containing CA and viral RNA and reverse transcription was restored (127). Once again these data leave us to wonder what happens to CA during rhTRIM5 restriction. This is an important question to pursue because understanding the fate of CA will allow us to target CA more efficiently.

In live cell imaging movies, TRIM5α forms de novo bodies around HIV-1 and within minutes both signals are gone (119). This suggests that both TRIM5α and the virus are degraded following the interaction. Nevertheless, it is possible that the limit of detection of the microscope prevented them from observing components of TRIM5α and/or CA that are present in the cell that were not degraded.

While the precise mechanism of TRIM5 restriction and UPS involvement has yet to be completely determined, our data on the interaction of the proteasome complex with TRIM5 adds to the knowledge that the proteasome is an important component of retroviral restriction. Other members of the TRIM family are known to utilize the proteasome complex for immune evasion and viral restriction. For example TRIM21 is known to target adenovirus for degradation via the proteasome

complex. Therefore, understanding the proteasome function in TRIM5 restriction may be utilized to study other members of the TRIM family of proteins that function in a proteasome-dependent pathway (180). Additionally, demonstrating that the proteasome complex directly interacts with TRIM5 could aid in the development of a drug that can more specifically and efficiently target TRIM5 bound to the virus to the proteasome complex for degradation/disassembly. Furthermore, a drug may be designed where the interaction between TRIM5 (bound to the capsid) and the proteasome complex is further strengthened to facilitate degradation and restriction.

SUMO-1 and SIMs role in TRIM5α restriction and cross talk with UPS

Our studies identified that SUMO-1 and SIM requirements for protein stability and restriction are conserved amongst TRIM5α species (168). Two SIMs in the B30.2 domain of rhTRIM5α are required for retroviral restriction, which is also conserved in huTRIM5-mediated restriction (Figure 30). This suggests that TRIM5α interacts with a SUMOylated protein via SIMs for stability in cells and restriction. For N-MLV restriction, it was demonstrated that SIMs in huTRIM5α interact with SUMOylated MLV CA. However, due to the difficulties associated with the fragile HIV-1 CA, it remains to be determined whether HIV-1 CA is SUMOylated. Additionally, knockdown of SUMO-1 decreased rhTRIM5α protein levels (Figure 32), which also lead to reduced restriction of HIV-1 (Figure 31). These data suggest

that SUMO-1 or a SUMOylated protein are important for the stability of rhTRIM5α (168). A similar phenotype was described for p62 interaction with rhTRIM5α (152). Therefore, it is possible to imagine that TRIM5α exists in a complex with a wide variety of proteins that are important for its stability. Understanding how TRIM5α stability is controlled will be crucial. Even though huTRIM5 is as stable as rhTRIM5, it is not enough to restrict HIV-1 (118). Therefore, identifying proteins that control the stability of TRIM5α can be exploited to further stabilize it and increase restriction of HIV-1 in human cells. HuTRIM5α does have the ability to restrict HIV-1 but it is just not enough; therefore, designing drugs that can stabilize huTRIM5α would be ideal since gene therapy is not a feasible option just yet.

Usually, several processes work together to carefully regulate proteins in cells. Few studies suggest that there is cross talk between ubiquitinated and SUMOylated proteins in coordination with the proteasome (181-183). It is possible that TRIM5α engages both processes during restriction. Another tripartite motif family member, TRIM19/PML (promyelocytic leukemia gene) is degraded in a proteasome-dependent mechanism following SUMOylation during an Encepahlomyocarditis virus (EMCV) infection (184). PML associates with TRIM5 in the nucleus and these structures are also positive for SUMO-1. Furthermore, HSV-1 ubiquitin ligase ICP0 acts as a SUMO-Targeted Ubiquitin ligase (STUbl) that induces the loss of SUMO-modified PML. ICP0 also leads to global proteasome-dependent degradation of SUMO-conjugates during infection in a RING finger-dependent

mechanism (185). If TRIM5 is ubiquitinated, and it interacts with a SUMOylated protein via SIMs in the B30.2 domain, these simultaneous processes may lead to proteasome degradation. Additionally, in absence of ubiquitination, TRIM5 interaction with a SUMOylated protein may lead to ubiquitin independent but proteasome-dependent degradation of TRIM5 and/or SUMOylated protein. However, in certain cells rhTRIM5α with mutations in SIM1 and SIM2 have an increased protein turnover rate compared to wild type. If SUMOylation played a role in TRIM5 degradation, mutating SIMs would increase protein levels and not increase protein turnover rate. Moreover, knocking down SUMO-1 would lead to an increase in TRIM5 protein levels and not decrease them as we observed (168) (Figure 32).

It is known that MLV capsid is SUMOylated, which may help huTRIM5α recognize it via its' SIMs during restriction (149) however, SUMOylated HIV-1 CA has not been detected. When SUMO-1 is knocked down TRIM5α restriction is reduced but since protein levels of TRIM5α are decreased, the requirement for SUMO-1 in restriction is difficult to interpret (168). If SUMO-1 is important in restriction, it is possible that a SUMOylated protein interacts with CA that makes it more susceptible to TRIM5α restriction. In recent years, a few proteins were shown to interact with HIV-1 CA such as CPSF6, TNPO3 and Nup358 to mediate nuclear entry of the PIC (44). While there isn't any data to support that CPSF6, or TNPO3 are SUMOylated, it remains a possibility that in complex with CA they could be

modified. Nup358, a nuclear complex protein has a domain that contains SUMO E3 ligase activity, however, a study demonstrated that the SUMO E3 ligase activity is not important in engaging CA (186). However, most of these proteins act slightly downstream from TRIM5 restriction, which occurs quickly following virus entry into cells; therefore, it is unlikely that these identified CA interacting proteins are engaging CA during TRIM5 restriction.

Uncoating and evasion of the host immune system

HIV-1 uncoating is one of the remaining steps in the viral life cycle that is not well understood. We hypothesized that microtubules may play a role in uncoating of the core since the virus was demonstrated to traffic on microtubules soon after entry into the target cell (30). Utilizing the CsA withdrawal assay, when microtubules were disrupted with Nocodazole HIV-1 CA was sensitive to TRIMCyp longer suggesting slower uncoating (Figure 37). Also, higher levels of p24 were detected in GFP-Vpr labeled viruses when microtubule integrity was disrupted (Figure 39). This suggests that HIV-1 utilizes microtubules to facilitate uncoating. Additionally, depleting dynein heavy chain delayed HIV-1 uncoating, which suggests that motor proteins engage the core to mediate uncoating (Figure 40 and 41). How this interaction happens is not known. We hypothesize that the assembled capsid lattice is the platform that is recognized by motor proteins rather than smaller units of CA since the viral core is released into the cytoplasm as an intact cone. Whether multiple motor proteins simultaneously engage the core is not known either. HSV-1

utilizes dynein and kinesin motors at the same time to engage in a tug-of-war to disassemble the core (179). It is possible that a similar scenario occurs with the HIV-1 core to control the uncoating process. Therefore, when kinesin/MAP is depleted then uncoating should be increased as compared to dynein depletion.

While in our assays we did not utilize primary cells or cells of the immune system, these assays provide a great framework for future studies that are more difficult to perform in primary cells. Microtubules are a necessary component of cell viability; therefore, it is easy to imagine that viruses in most cell types would utilize these molecular highways for transport.

Furthermore, some labs suggest that HIV-1 uncoating does not occur in the cytoplasm but rather at the nuclear pore. Data demonstrating that CA interacts with members of the nuclear pore complex to translocate the PIC into the nucleus may support this model. Additionally, recent data suggests that the viral core and its' interaction with CypA cloak the viral DNA in the cytoplasm from innate immune sensors. While this model is possible, we do not observe a substantial number of viruses that are positive for CA accumulating at the nuclear rim, even 6 hours post infection. Rather, we observe a gradual loss of CA within the first few hours. A substantial amount of CA remains associated with the PIC even after a couple hours post infection (Figure 39), which correlates well with the understanding that some CA is associated with the PIC to mediate downstream events such as nuclear import. While our data would disagree with the model that the intact core docks at the nuclear pore, it suggests that enough CA remains associated with the PIC to interact

at the nuclear pore and mediate subsequent events. An alternative model is that the CA is remodeled following entry and that our antibody loses the ability to detect the epitope during the infection, which gives a decrease in intensity of CA over time.

Since microtubule-mediated transport is relatively fast, it is a good method for viruses to traffic to the nucleus before the cytoplasmic innate immune sensors are alerted. Since it was recently reported that HIV-2 cDNA is sensed in the cytoplasm in dendritic cells by cGAS. However, HIV-1 CA prevents cDNA sensing in the cytoplasm (187). Therefore, it is possible that HIV-1 utilizes microtubules for capsid uncoating/remodeling to escape sensing in the cytoplasm by the innate immune system.

Further, motor proteins and adaptor proteins are located on microtubules; therefore viruses can utilize them to disassemble their cores to successfully deliver their genomes to the nucleus. Understanding this interaction between the viral CA and microtubules/motor proteins could lead to new therapeutics that target the core. Specifically, inhibitors that disrupt the interaction between the viral core and microtubules/dynein would be beneficial because this would possibly prevent the virus from trafficking and uncoating efficiently to escape cellular detection and successfully infect the host. Despite having a wide variety of antiretrovirals that target multiple steps of the viral life, a therapeutic that targets the viral core does not exist. However, CA is a good target because it participates in multiple steps of the life cycle and CA cannot afford too many mutations without sacrificing viral fitness (19).

This body of work has contributed to various aspects of the HIV-1 life cycle. Particularly, this dissertation addresses how HIV-1 interacts with a range of host proteins to mediate successful infection. TRIM5 interactions with the proteasome complex and SUMO-1 contribute to the understanding of the molecular mechanisms that TRIM5 utilizes to restrict HIV-1. Furthermore, our studies on HIV-1 core uncoating and how microtubules/dynein facilitate the process was previously unknown. Understanding the molecular mechanisms behind HIV-1 infection will be crucial in developing novel therapies and eradicating the virus.

REFERENCES

1. **McMichael AJ, Borrow P, Tomaras GD, Goonetilleke N, Haynes BF.** 2010. The immune response during acute HIV-1 infection: clues for vaccine development. Nat Rev Immunol **10:**11-23.

2. **Douek DC, Roederer M, Koup RA.** 2009. Emerging concepts in the immunopathogenesis of AIDS. Annu Rev Med **60:**471-484.

3. **Weiss RA.** 1993. How does HIV cause AIDS? Science **260:**1273-1279.

4. **Suzuki Y, Suzuki Y.** 2011. Gene Regulatable Lentiviral Vector System.

5. **Doms RW, Trono D.** 2000. The plasma membrane as a combat zone in the HIV battlefield. Genes Dev **14:**2677-2688.

6. **Allen SJ, Crown SE, Handel TM.** 2007. Chemokine: receptor structure, interactions, and antagonism. Annu Rev Immunol **25:**787-820.

7. **Schlyer S, Horuk R.** 2006. I want a new drug: G-protein-coupled receptors in drug development. Drug Discov Today **11:**481-493.

8. **Yeagle PL, Albert AD.** 2007. G-protein coupled receptor structure. Biochim Biophys Acta **1768:**808-824.

9. **Feng Y, Broder CC, Kennedy PE, Berger EA.** 1996. HIV-1 entry cofactor: functional cDNA cloning of a seven-transmembrane, G protein-coupled receptor. Science **272:**872-877.

10. **Choe H, Farzan M, Sun Y, Sullivan N, Rollins B, Ponath PD, Wu L, Mackay CR, LaRosa G, Newman W, Gerard N, Gerard C, Sodroski J.** 1996. The beta-chemokine receptors CCR3 and CCR5 facilitate infection by primary HIV-1 isolates. Cell **85:**1135-1148.

11. **Doranz BJ, Rucker J, Yi Y, Smyth RJ, Samson M, Peiper SC, Parmentier M, Collman RG, Doms RW.** 1996. A dual-tropic primary HIV-1 isolate that uses fusin and the beta-chemokine receptors CKR-5, CKR-3, and CKR-2b as fusion cofactors. Cell **85:**1149-1158.

12. **Dragic T, Litwin V, Allaway GP, Martin SR, Huang Y, Nagashima KA, Cayanan C, Maddon PJ, Koup RA, Moore JP, Paxton WA.** 1996. HIV-1 entry into CD4+ cells is mediated by the chemokine receptor CC-CKR-5. Nature **381:**667-673.

13. **Alkhatib G, Combadiere C, Broder CC, Feng Y, Kennedy PE, Murphy PM, Berger EA.** 1996. CC CKR5: a RANTES, MIP-1alpha, MIP-1beta receptor as a fusion cofactor for macrophage-tropic HIV-1. Science **272:**1955-1958.

14. **Schuitemaker H, Koot M, Kootstra NA, Dercksen MW, de Goede RE, van Steenwijk RP, Lange JM, Schattenkerk JK, Miedema F, Tersmette M.** 1992. Biological phenotype of human immunodeficiency virus type 1 clones at different stages of infection: progression of disease is associated with a shift from monocytotropic to T-cell-tropic virus population. J Virol **66:**1354-1360.

15. **Berger EA, Doms RW, Fenyo EM, Korber BT, Littman DR, Moore JP, Sattentau QJ, Schuitemaker H, Sodroski J, Weiss RA.** 1998. A new classification for HIV-1. Nature **391:**240.

16. **Engelman A, Cherepanov P.** 2012. The structural biology of HIV-1: mechanistic and therapeutic insights. Nat Rev Microbiol **10:**279-290.

17. **Briggs JA, Simon MN, Gross I, Krausslich HG, Fuller SD, Vogt VM, Johnson MC.** 2004. The stoichiometry of Gag protein in HIV-1. Nat Struct Mol Biol **11:**672-675.

18. **Pornillos O, Ganser-Pornillos BK, Kelly BN, Hua Y, Whitby FG, Stout CD, Sundquist WI, Hill CP, Yeager M.** 2009. X-ray structures of the hexameric building block of the HIV capsid. Cell **137:**1282-1292.

19. **Forshey BM, von Schwedler U, Sundquist WI, Aiken C.** 2002. Formation of a human immunodeficiency virus type 1 core of optimal stability is crucial for viral replication. J Virol **76:**5667-5677.

20. **Fassati A, Goff SP.** 2001. Characterization of intracellular reverse transcription complexes of human immunodeficiency virus type 1. J Virol **75:**3626-3635.

21. **Fassati A, Goff SP.** 1999. Characterization of intracellular reverse transcription complexes of Moloney murine leukemia virus. J Virol **73:**8919-8925.

22. **Yamashita M, Emerman M.** 2004. Capsid is a dominant determinant of retrovirus infectivity in nondividing cells. J Virol **78:**5670-5678.

23. **Arhel NJ, Souquere-Besse S, Munier S, Souque P, Guadagnini S, Rutherford S, Prevost MC, Allen TD, Charneau P.** 2007. HIV-1 DNA Flap

formation promotes uncoating of the pre-integration complex at the nuclear pore. EMBO J **26:**3025-3037.

24. **Schaller T, Ocwieja KE, Rasaiyaah J, Price AJ, Brady TL, Roth SL, Hue S, Fletcher AJ, Lee K, KewalRamani VN, Noursadeghi M, Jenner RG, James LC, Bushman FD, Towers GJ.** 2011. HIV-1 capsid-cyclophilin interactions determine nuclear import pathway, integration targeting and replication efficiency. PLoS Pathog **7:**e1002439.

25. **Rasaiyaah J, Tan CP, Fletcher AJ, Price AJ, Blondeau C, Hilditch L, Jacques DA, Selwood DL, James LC, Noursadeghi M, Towers GJ.** 2013. HIV-1 evades innate immune recognition through specific cofactor recruitment. Nature **503:**402-405.

26. **Hulme AE, Perez O, Hope TJ.** 2011. Complementary assays reveal a relationship between HIV-1 uncoating and reverse transcription. Proc Natl Acad Sci U S A **108:**9975-9980.

27. **Strunze S, Engelke MF, Wang IH, Puntener D, Boucke K, Schleich S, Way M, Schoenenberger P, Burckhardt CJ, Greber UF.** 2011. Kinesin-1-mediated capsid disassembly and disruption of the nuclear pore complex promote virus infection. Cell Host Microbe **10:**210-223.

28. **Rode K, Dohner K, Binz A, Glass M, Strive T, Bauerfeind R, Sodeik B.** 2011. Uncoupling uncoating of herpes simplex virus genomes from their nuclear import and gene expression. J Virol **85:**4271-4283.

29. **Zhao G, Perilla JR, Yufenyuy EL, Meng X, Chen B, Ning J, Ahn J, Gronenborn AM, Schulten K, Aiken C, Zhang P.** 2013. Mature HIV-1 capsid structure by cryo-electron microscopy and all-atom molecular dynamics. Nature **497:**643-646.

30. **McDonald D, Vodicka MA, Lucero G, Svitkina TM, Borisy GG, Emerman M, Hope TJ.** 2002. Visualization of the intracellular behavior of HIV in living cells. J Cell Biol **159:**441-452.

31. **Luby-Phelps K.** 2000. Cytoarchitecture and physical properties of cytoplasm: volume, viscosity, diffusion, intracellular surface area. Int Rev Cytol **192:**189-221.

32. **Leopold PL, Pfister KK.** 2006. Viral strategies for intracellular trafficking: motors and microtubules. Traffic **7:**516-523.

33. **Miller MD, Farnet CM, Bushman FD.** 1997. Human immunodeficiency virus type 1 preintegration complexes: studies of organization and composition. J Virol **71:**5382-5390.

34. **Dohner K, Nagel CH, Sodeik B.** 2005. Viral stop-and-go along microtubules: taking a ride with dynein and kinesins. Trends Microbiol **13:**320-327.

35. **Dohner K, Sodeik B.** 2005. The role of the cytoskeleton during viral infection. Curr Top Microbiol Immunol **285:**67-108.

36. **Hook P, Vallee RB.** 2006. The dynein family at a glance. J Cell Sci **119:**4369-4371.

37. **Hirokawa N, Nitta R, Okada Y.** 2009. The mechanisms of kinesin motor motility: lessons from the monomeric motor KIF1A. Nat Rev Mol Cell Biol **10:**877-884.

38. **Hammond JW, Griffin K, Jih GT, Stuckey J, Verhey KJ.** 2008. Co-operative versus independent transport of different cargoes by Kinesin-1. Traffic **9:**725-741.

39. **Conde C, Caceres A.** 2009. Microtubule assembly, organization and dynamics in axons and dendrites. Nature reviews. Neuroscience **10:**319-332.

40. **Vale RD.** 2003. The molecular motor toolbox for intracellular transport. Cell **112:**467-480.

41. **Coffin JM, Hughes SH, Varmus HE.** 1997. The Interactions of Retroviruses and their Hosts. *In* Coffin JM, Hughes SH, Varmus HE (ed.), Retroviruses, Cold Spring Harbor (NY).

42. **Dismuke DJ, Aiken C.** 2006. Evidence for a functional link between uncoating of the human immunodeficiency virus type 1 core and nuclear import of the viral preintegration complex. J Virol **80:**3712-3720.

43. **Zhang R, Mehla R, Chauhan A.** 2010. Perturbation of host nuclear membrane component RanBP2 impairs the nuclear import of human immunodeficiency virus -1 preintegration complex (DNA). PLoS One **5:**e15620.

44. **Lee K, Ambrose Z, Martin TD, Oztop I, Mulky A, Julias JG, Vandegraaff N, Baumann JG, Wang R, Yuen W, Takemura T, Shelton K, Taniuchi I, Li Y, Sodroski J, Littman DR, Coffin JM, Hughes SH, Unutmaz D, Engelman A,**

KewalRamani VN. 2010. Flexible use of nuclear import pathways by HIV-1. Cell Host Microbe **7:**221-233.

45. **De Iaco A, Santoni F, Vannier A, Guipponi M, Antonarakis S, Luban J.** 2013. TNPO3 protects HIV-1 replication from CPSF6-mediated capsid stabilization in the host cell cytoplasm. Retrovirology **10:**20.

46. **Brass AL, Dykxhoorn DM, Benita Y, Yan N, Engelman A, Xavier RJ, Lieberman J, Elledge SJ.** 2008. Identification of host proteins required for HIV infection through a functional genomic screen. Science **319:**921-926.

47. **Suzuki Y, Craigie R.** 2007. The road to chromatin - nuclear entry of retroviruses. Nature reviews. Microbiology **5:**187-196.

48. **Wu X, Li Y, Crise B, Burgess SM.** 2003. Transcription start regions in the human genome are favored targets for MLV integration. Science **300:**1749-1751.

49. **Wang GP, Ciuffi A, Leipzig J, Berry CC, Bushman FD.** 2007. HIV integration site selection: analysis by massively parallel pyrosequencing reveals association with epigenetic modifications. Genome Res **17:**1186-1194.

50. **Lewinski MK, Yamashita M, Emerman M, Ciuffi A, Marshall H, Crawford G, Collins F, Shinn P, Leipzig J, Hannenhalli S, Berry CC, Ecker JR, Bushman FD.** 2006. Retroviral DNA integration: viral and cellular determinants of target-site selection. PLoS Pathog **2:**e60.

51. **Jacks T, Power MD, Masiarz FR, Luciw PA, Barr PJ, Varmus HE.** 1988. Characterization of ribosomal frameshifting in HIV-1 gag-pol expression. Nature **331:**280-283.

52. **Ono A, Freed EO.** 2004. Cell-type-dependent targeting of human immunodeficiency virus type 1 assembly to the plasma membrane and the multivesicular body. J Virol **78:**1552-1563.

53. **Saad JS, Loeliger E, Luncsford P, Liriano M, Tai J, Kim A, Miller J, Joshi A, Freed EO, Summers MF.** 2007. Point mutations in the HIV-1 matrix protein turn off the myristyl switch. J Mol Biol **366:**574-585.

54. **Saad JS, Miller J, Tai J, Kim A, Ghanam RH, Summers MF.** 2006. Structural basis for targeting HIV-1 Gag proteins to the plasma membrane for virus assembly. Proc Natl Acad Sci U S A **103:**11364-11369.

55. **Yu X, Yuan X, McLane MF, Lee TH, Essex M.** 1993. Mutations in the cytoplasmic domain of human immunodeficiency virus type 1 transmembrane protein impair the incorporation of Env proteins into mature virions. J Virol **67:**213-221.

56. **Johnson SF, Telesnitsky A.** 2010. Retroviral RNA dimerization and packaging: the what, how, when, where, and why. PLoS Pathog **6:**e1001007.

57. **Lever AM.** 2007. HIV-1 RNA packaging. Adv Pharmacol **55:**1-32.

58. **Moore MD, Hu WS.** 2009. HIV-1 RNA dimerization: It takes two to tango. AIDS Rev **11:**91-102.

59. **Rulli SJ, Jr., Hibbert CS, Mirro J, Pederson T, Biswal S, Rein A.** 2007. Selective and nonselective packaging of cellular RNAs in retrovirus particles. J Virol **81:**6623-6631.

60. **Chen J, Nikolaitchik O, Singh J, Wright A, Bencsics CE, Coffin JM, Ni N, Lockett S, Pathak VK, Hu WS.** 2009. High efficiency of HIV-1 genomic RNA packaging and heterozygote formation revealed by single virion analysis. Proc Natl Acad Sci U S A **106:**13535-13540.

61. **Carlson LA, de Marco A, Oberwinkler H, Habermann A, Briggs JA, Krausslich HG, Grunewald K.** 2010. Cryo electron tomography of native HIV-1 budding sites. PLoS Pathog **6:**e1001173.

62. **Fuller SD, Wilk T, Gowen BE, Krausslich HG, Vogt VM.** 1997. Cryo-electron microscopy reveals ordered domains in the immature HIV-1 particle. Curr Biol **7:**729-738.

63. **Morita E, Sundquist WI.** 2004. Retrovirus budding. Annu Rev Cell Dev Biol **20:**395-425.

64. **Bieniasz PD.** 2009. The cell biology of HIV-1 virion genesis. Cell Host Microbe **5:**550-558.

65. **Carlton JG, Martin-Serrano J.** 2009. The ESCRT machinery: new functions in viral and cellular biology. Biochem Soc Trans **37:**195-199.

66. **Usami Y, Popov S, Popova E, Inoue M, Weissenhorn W, H GG.** 2009. The ESCRT pathway and HIV-1 budding. Biochem Soc Trans **37:**181-184.

67. **Navia MA, McKeever BM.** 1990. A role for the aspartyl protease from the human immunodeficiency virus type 1 (HIV-1) in the orchestration of virus assembly. Ann N Y Acad Sci **616:**73-85.

68. **Swanstrom R, Wills JW.** 1997. Synthesis, Assembly, and Processing of Viral Proteins. *In* Coffin JM, Hughes SH, Varmus HE (ed.), Retroviruses, Cold Spring Harbor (NY).

69. **Hill M, Tachedjian G, Mak J.** 2005. The packaging and maturation of the HIV-1 Pol proteins. Curr HIV Res **3:**73-85.

70. **Briggs JA, Wilk T, Welker R, Krausslich HG, Fuller SD.** 2003. Structural organization of authentic, mature HIV-1 virions and cores. EMBO J **22:**1707-1715.

71. **Benjamin J, Ganser-Pornillos BK, Tivol WF, Sundquist WI, Jensen GJ.** 2005. Three-dimensional structure of HIV-1 virus-like particles by electron cryotomography. J Mol Biol **346:**577-588.

72. **Martin-Serrano J, Neil SJ.** 2011. Host factors involved in retroviral budding and release. Nature reviews. Microbiology **9:**519-531.

73. **Arts EJ, Hazuda DJ.** 2012. HIV-1 antiretroviral drug therapy. Cold Spring Harb Perspect Med **2:**a007161.

74. **Harrigan PR, Whaley M, Montaner JS.** 1999. Rate of HIV-1 RNA rebound upon stopping antiretroviral therapy. AIDS **13:**F59-62.

75. **Lisziewicz J, Rosenberg E, Lieberman J, Jessen H, Lopalco L, Siliciano R, Walker B, Lori F.** 1999. Control of HIV despite the discontinuation of antiretroviral therapy. N Engl J Med **340:**1683-1684.

76. **Jessen H, Allen TM, Streeck H.** 2014. How a single patient influenced HIV research--15-year follow-up. N Engl J Med **370:**682-683.

77. **Hatziioannou T, Cowan S, Goff SP, Bieniasz PD, Towers GJ.** 2003. Restriction of multiple divergent retroviruses by Lv1 and Ref1. Embo J **22:**385-394.

78. **Hatziioannou T, Perez-Caballero D, Yang A, Cowan S, Bieniasz PD.** 2004. Retrovirus resistance factors Ref1 and Lv1 are species-specific variants of TRIM5alpha. Proc Natl Acad Sci U S A **101:**10774-10779.

79. **Blanco-Melo D, Venkatesh S, Bieniasz PD.** 2012. Intrinsic cellular defenses against human immunodeficiency viruses. Immunity **37:**399-411.

80. **Santa-Marta M, de Brito PM, Godinho-Santos A, Goncalves J.** 2013. Host Factors and HIV-1 Replication: Clinical Evidence and Potential Therapeutic Approaches. Frontiers in immunology **4:**343.

81. **Meroni G, Diez-Roux G.** 2005. TRIM/RBCC, a novel class of 'single protein RING finger' E3 ubiquitin ligases. Bioessays **27:**1147-1157.

82. **Ozato K, Shin DM, Chang TH, Morse HC, 3rd.** 2008. TRIM family proteins and their emerging roles in innate immunity. Nat Rev Immunol **8:**849-860.

83. **Nisole S, Stoye JP, Saib A.** 2005. TRIM family proteins: retroviral restriction and antiviral defence. Nat Rev Microbiol **3:**799-808.

84. **Reymond A, Meroni G, Fantozzi A, Merla G, Cairo S, Luzi L, Riganelli D, Zanaria E, Messali S, Cainarca S, Guffanti A, Minucci S, Pelicci PG, Ballabio A.** 2001. The tripartite motif family identifies cell compartments. Embo J **20:**2140-2151.

85. **Barlow PN, Luisi B, Milner A, Elliott M, Everett R.** 1994. Structure of the C3HC4 domain by 1H-nuclear magnetic resonance spectroscopy. A new structural class of zinc-finger. J Mol Biol **237:**201-211.

86. **Deshaies RJ, Joazeiro CA.** 2009. RING domain E3 ubiquitin ligases. Annu Rev Biochem **78:**399-434.

87. **Freemont PS.** 2000. RING for destruction? Curr Biol **10:**R84-87.

88. **Hashizume R, Fukuda M, Maeda I, Nishikawa H, Oyake D, Yabuki Y, Ogata H, Ohta T.** 2001. The RING heterodimer BRCA1-BARD1 is a ubiquitin ligase inactivated by a breast cancer-derived mutation. J Biol Chem **276:**14537-14540.

89. **Linares LK, Scheffner M.** 2003. The ubiquitin-protein ligase activity of Hdm2 is inhibited by nucleic acids. FEBS Lett **554:**73-76.

90. **Massiah MA, Matts JA, Short KM, Simmons BN, Singireddy S, Yi Z, Cox TC.** 2007. Solution structure of the MID1 B-box2 CHC(D/C)C(2)H(2) zinc-binding domain: insights into an evolutionarily conserved RING fold. J Mol Biol **369:**1-10.

91. **Torok M, Etkin LD.** 2001. Two B or not two B? Overview of the rapidly expanding B-box family of proteins. Differentiation **67:**63-71.

92. **Diaz-Griffero F, Kar A, Perron M, Xiang SH, Javanbakht H, Li X, Sodroski J.** 2007. Modulation of Retroviral Restriction and Proteasome Inhibitor-resistant Turnover by Changes in the TRIM5{alpha} B-box 2 Domain. J Virol.

93. **Diaz-Griffero F, Qin XR, Hayashi F, Kigawa T, Finzi A, Sarnak Z, Lienlaf M, Yokoyama S, Sodroski J.** 2009. A B-box 2 surface patch important for TRIM5alpha self-association, capsid binding avidity, and retrovirus restriction. J Virol **83:**10737-10751.

94. **Javanbakht H, Diaz-Griffero F, Stremlau M, Si Z, Sodroski J.** 2005. The contribution of RING and B-box 2 domains to retroviral restriction mediated by monkey TRIM5alpha. J Biol Chem **280:**26933-26940.

95. **Li X, Sodroski J.** 2008. The TRIM5alpha B-box 2 domain promotes cooperative binding to the retroviral capsid by mediating higher-order self-association. J Virol **82:**11495-11502.

96. **Peng H, Feldman I, Rauscher FJ, 3rd.** 2002. Hetero-oligomerization among the TIF family of RBCC/TRIM domain-containing nuclear cofactors: a potential mechanism for regulating the switch between coactivation and corepression. J Mol Biol **320:**629-644.

97. **Grignani F, Gelmetti V, Fanelli M, Rogaia D, De Matteis S, Ferrara FF, Bonci D, Grignani F, Nervi C, Pelicci PG.** 1999. Formation of PML/RAR alpha high molecular weight nuclear complexes through the PML coiled-coil region is essential for the PML/RAR alpha-mediated retinoic acid response. Oncogene **18:**6313-6321.

98. **Ohkura S, Yap MW, Sheldon T, Stoye JP.** 2006. All three variable regions of the TRIM5alpha B30.2 domain can contribute to the specificity of retrovirus restriction. J Virol **80:**8554-8565.

99. **Stremlau M, Perron M, Welikala S, Sodroski J.** 2005. Species-specific variation in the B30.2(SPRY) domain of TRIM5alpha determines the potency of human immunodeficiency virus restriction. J Virol **79:**3139-3145.

100. **Perron MJ, Stremlau M, Sodroski J.** 2006. Two surface-exposed elements of the B30.2/SPRY domain as potency determinants of N-tropic murine leukemia virus restriction by human TRIM5alpha. J Virol **80:**5631-5636.

101. **Stremlau M, Owens CM, Perron MJ, Kiessling M, Autissier P, Sodroski J.** 2004. The cytoplasmic body component TRIM5alpha restricts HIV-1 infection in Old World monkeys. Nature **427:**848-853.

102. **Sayah DM, Sokolskaja E, Berthoux L, Luban J.** 2004. Cyclophilin A retrotransposition into TRIM5 explains owl monkey resistance to HIV-1. Nature **430:**569-573.

103. **Stoye JP, Yap MW.** 2008. Chance favors a prepared genome. Proc Natl Acad Sci U S A **105:**3177-3178.

104. **Carthagena L, Parise MC, Ringeard M, Chelbi-Alix MK, Hazan U, Nisole S.** 2008. Implication of TRIM alpha and TRIMCyp in interferon-induced anti-retroviral restriction activities. Retrovirology **5:**59.

105. **Sawyer SL, Wu LI, Emerman M, Malik HS.** 2005. Positive selection of primate TRIM5alpha identifies a critical species-specific retroviral restriction domain. Proc Natl Acad Sci U S A **102:**2832-2837.

106. **Yamauchi K, Wada K, Tanji K, Tanaka M, Kamitani T.** 2008. Ubiquitination of E3 ubiquitin ligase TRIM5 alpha and its potential role. FEBS J **275:**1540-1555.

107. **Mische CC, Javanbakht H, Song B, Diaz-Griffero F, Stremlau M, Strack B, Si Z, Sodroski J.** 2005. Retroviral restriction factor TRIM5alpha is a trimer. J Virol **79:**14446-14450.

108. **Nepveu-Traversy ME, Berube J, Berthoux L.** 2009. TRIM5alpha and TRIMCyp form apparent hexamers and their multimeric state is not affected by exposure to restriction-sensitive viruses or by treatment with pharmacological inhibitors. Retrovirology **6:**100.

109. **Diaz-Griffero F, Vandegraaff N, Li Y, McGee-Estrada K, Stremlau M, Welikala S, Si Z, Engelman A, Sodroski J.** 2006. Requirements for capsid-binding and an effector function in TRIMCyp-mediated restriction of HIV-1. Virology **351:**404-419.

110. **Javanbakht H, Diaz-Griffero F, Yuan W, Yeung DF, Li X, Song B, Sodroski J.** 2007. The ability of multimerized cyclophilin A to restrict retrovirus infection. Virology **367:**19-29.

111. **Yap MW, Nisole S, Lynch C, Stoye JP.** 2004. Trim5alpha protein restricts both HIV-1 and murine leukemia virus. Proc Natl Acad Sci U S A **101:**10786-10791.

112. **Luban J.** 2007. Cyclophilin A, TRIM5, and resistance to human immunodeficiency virus type 1 infection. Journal of virology **81:**1054-1061.

113. **Burkhard P, Stetefeld J, Strelkov SV.** 2001. Coiled coils: a highly versatile protein folding motif. Trends Cell Biol **11:**82-88.

114. **Li X, Song B, Xiang SH, Sodroski J.** 2007. Functional interplay between the B-box 2 and the B30.2(SPRY) domains of TRIM5alpha. Virology **366:**234-244.

115. **Sastri J, O'Connor C, C. D, M. M, P. P, Diaz-Griffero F, Campbell EM.** 2010. Identification of residues within the L2 region of TRIM5α that are required for retroviral restriction and cytoplasmic body localization. Virology **405:**259-266.

116. **Perez-Caballero D, Hatziioannou T, Zhang F, Cowan S, Bieniasz PD.** 2005. Restriction of Human Immunodeficiency Virus Type 1 by TRIM-CypA Occurs with Rapid Kinetics and Independently of Cytoplasmic Bodies, Ubiquitin, and Proteasome Activity. J Virol **79:**15567-15572.

117. **Song B, Diaz-Griffero F, Park DH, Rogers T, Stremlau M, Sodroski J.** 2005. TRIM5alpha association with cytoplasmic bodies is not required for antiretroviral activity. Virology.

118. **Campbell EM, Dodding MP, Yap MW, Wu X, Gallois-Montbrun S, Malim MH, Stoye JP, Hope TJ.** 2007. TRIM5 alpha cytoplasmic bodies are highly dynamic structures. Mol Biol Cell **18:**2102-2111.

119. **Campbell EM, Perez O, Anderson JL, Hope TJ.** 2008. Visualization of a proteasome-independent intermediate during restriction of HIV-1 by rhesus TRIM5alpha. J Cell Biol **180:**549-561.

120. **Song B, Gold B, O'Huigin C, Javanbakht H, Li X, Stremlau M, Winkler C, Dean M, Sodroski J.** 2005. The B30.2(SPRY) domain of the retroviral restriction factor TRIM5alpha exhibits lineage-specific length and sequence variation in primates. J Virol **79:**6111-6121.

121. **Sebastian S, Luban J.** 2005. TRIM5alpha selectively binds a restriction-sensitive retroviral capsid. Retrovirology **2:**40.

122. **Ganser-Pornillos B, Chandrasekaran V, Pornillos O, Sodroski J, Sundquist WI, Yeager M.** 2010. Hexagonal assembly of a restricting TRIM5alpha protein. Proc Natl Acad Sci U S A **Manuscript in press**.

123. **Anderson JL, Campbell EM, Wu X, Vandegraaff N, Engelman A, Hope TJ.** 2006. Proteasome inhibition reveals that a functional preintegration complex intermediate can be generated during restriction by diverse TRIM5 proteins. J Virol **80:**9754-9760.

124. **Rold CJ, Aiken C.** 2008. Proteasomal degradation of TRIM5alpha during retrovirus restriction. PLoS Pathog **4:**e1000074

.

125. **Wu X, Anderson JL, Campbell EM, Joseph AM, Hope TJ.** 2006. Proteasome inhibitors uncouple rhesus TRIM5alpha restriction of HIV-1 reverse transcription and infection. Proc Natl Acad Sci U S A **103:**7465-7470.

126. **Stremlau M, Perron M, Lee M, Li Y, Song B, Javanbakht H, Diaz-Griffero F, Anderson DJ, Sundquist WI, Sodroski J.** 2006. Specific recognition and accelerated uncoating of retroviral capsids by the TRIM5{alpha} restriction factor. Proc Natl Acad Sci U S A.

127. **Kutluay SB, Perez-Caballero D, Bieniasz PD.** 2013. Fates of retroviral core components during unrestricted and TRIM5-restricted infection. PLoS Pathog **9:**e1003214.

128. **Chatterji U, Bobardt MD, Gaskill P, Sheeter D, Fox H, Gallay PA.** 2006. Trim5alpha accelerates degradation of cytosolic capsid associated with productive HIV-1 entry. J Biol Chem **281:**37025-37033.

129. **Rajsbaum R, Garcia-Sastre A.** 2013. Viral evasion mechanisms of early antiviral responses involving regulation of ubiquitin pathways. Trends Microbiol **21:**421-429.

130. **Uchil PD, Quinlan BD, Chan WT, Luna JM, Mothes W.** 2008. TRIM E3 ligases interfere with early and late stages of the retroviral life cycle. PLoS Pathog **4:**e16.

131. **Versteeg GA, Rajsbaum R, Sanchez-Aparicio MT, Maestre AM, Valdiviezo J, Shi M, Inn KS, Fernandez-Sesma A, Jung J, Garcia-Sastre A.** 2013. The E3-ligase TRIM family of proteins regulates signaling pathways triggered by innate immune pattern-recognition receptors. Immunity **38:**384-398.

132. **Towers GJ, Goff SP.** 2003. Post-entry restriction of retroviral infections. AIDS Rev **5:**156-164.

133. **Bieniasz PD.** 2004. Intrinsic immunity: a front-line defense against viral attack. Nat Immunol **5:**1109-1115.

134. **Goff SP.** 2007. Host factors exploited by retroviruses. Nat Rev Microbiol **5:**253-263.

135. **Gack MU, Shin YC, Joo CH, Urano T, Liang C, Sun L, Takeuchi O, Akira S, Chen Z, Inoue S, Jung JU.** 2007. TRIM25 RING-finger E3 ubiquitin ligase is essential for RIG-I-mediated antiviral activity. Nature **446:**916-920.

136. **Pertel T, Hausmann S, Morger D, Zuger S, Guerra J, Lascano J, Reinhard C, Santoni FA, Uchil PD, Chatel L, Bisiaux A, Albert ML, Strambio-De-Castillia C, Mothes W, Pizzato M, Grutter MG, Luban J.** 2011. TRIM5 is an innate immune sensor for the retrovirus capsid lattice. Nature **472:**361-365.

137. **Murata S, Yashiroda H, Tanaka K.** 2009. Molecular mechanisms of proteasome assembly. Nat Rev Mol Cell Biol **10:**104-115.

138. **Xie Y.** 2010. Structure, assembly and homeostatic regulation of the 26S proteasome. Journal of molecular cell biology **2:**308-317.

139. **Ciechanover A, Stanhill A.** 2014. The complexity of recognition of ubiquitinated substrates by the 26S proteasome. Biochim Biophys Acta **1843:**86-96.

140. **Lienlaf M, Hayashi F, Di Nunzio F, Tochio N, Kigawa T, Yokoyama S, Diaz-Griffero F.** 2011. Contribution of E3-Ubiquitin Ligase Activity to HIV-1 Restriction by TRIM5{alpha}rh: Structure of the RING Domain of TRIM5{alpha}. J Virol **85:**8725-8737.

141. **Li X, Kim J, Song B, Finzi A, Pacheco B, Sodroski J.** 2013. Virus-specific effects of TRIM5alpha(rh) RING domain functions on restriction of retroviruses. J Virol **87:**7234-7245.

142. **Woelk T, Sigismund S, Penengo L, Polo S.** 2007. The ubiquitination code: a signalling problem. Cell division **2:**11.

143. **Watts FZ.** 2013. Starting and stopping SUMOylation. What regulates the regulator? Chromosoma **122:**451-463.

144. **Boggio R, Chiocca S.** 2006. Viruses and sumoylation: recent highlights. Curr Opin Microbiol **9:**430-436.

145. **Boggio R, Colombo R, Hay RT, Draetta GF, Chiocca S.** 2004. A mechanism for inhibiting the SUMO pathway. Mol Cell **16:**549-561.

146. **Gurer C, Berthoux L, Luban J.** 2005. Covalent modification of human immunodeficiency virus type 1 p6 by SUMO-1. J Virol **79:**910-917.

147. **Weldon RA, Jr., Sarkar P, Brown SM, Weldon SK.** 2003. Mason-Pfizer monkey virus Gag proteins interact with the human sumo conjugating enzyme, hUbc9. Virology **314:**62-73.

148. **Yueh A, Leung J, Bhattacharyya S, Perrone LA, de los Santos K, Pu SY, Goff SP.** 2006. Interaction of moloney murine leukemia virus capsid with Ubc9 and PIASy mediates SUMO-1 addition required early in infection. J Virol **80:**342-352.

149. **Arriagada G, Muntean LN, Goff SP.** 2011. SUMO-interacting motifs of human TRIM5alpha are important for antiviral activity. PLoS Pathog **7:**e1002019.

150. **Bergink S, Jentsch S.** 2009. Principles of ubiquitin and SUMO modifications in DNA repair. Nature **458:**461-467.

151. **Bieniasz PD, Cullen BR.** 2000. Multiple blocks to human immunodeficiency virus type 1 replication in rodent cells. Journal of virology **74:**9868-9877.

152. **O'Connor C, Pertel T, Gray S, Robia SL, Bakowska JC, Luban J, Campbell EM.** 2010. p62/Sequestosome1 associates with and sustains the expression of the retroviral restriction factor TRIM5{alpha}. J Virol.

153. **Kelly EM, Hou Z, Bossuyt J, Bers DM, Robia SL.** 2008. Phospholamban oligomerization, quaternary structure, and sarco(endo)plasmic reticulum calcium ATPase binding measured by fluorescence resonance energy transfer in living cells. J Biol Chem **283:**12202-12211.

154. **Zal T, Gascoigne NR.** 2004. Photobleaching-corrected FRET efficiency imaging of live cells. Biophys J **86:**3923-3939.

155. **Butler SL, Hansen MS, Bushman FD.** 2001. A quantitative assay for HIV DNA integration in vivo. Nature medicine **7:**631-634.

156. **Nisole S, Lynch C, Stoye JP, Yap MW.** 2004. A Trim5-cyclophilin A fusion protein found in owl monkey kidney cells can restrict HIV-1. Proc Natl Acad Sci U S A **101:**13324-13328.

157. **Aiken C.** 2006. Viral and cellular factors that regulate HIV-1 uncoating. Curr Opin HIV AIDS **1:**194-199.

158. **Auewarakul P, Wacharapornin P, Srichatrapimuk S, Chutipongtanate S, Puthavathana P.** 2005. Uncoating of HIV-1 requires cellular activation. Virology **337:**93-101.

159. **Thylur RP, Senthivinayagam S, Campbell EM, Rangasamy V, Thorenoor N, Sondarva G, Mehrotra S, Mishra P, Zook E, Le PT, Rana A, Rana B.** 2011. Mixed lineage kinase 3 modulates beta-catenin signaling in cancer cells. J Biol Chem **286:**37470-37482.

160. **Lukic Z, Hausmann S, Sebastian S, Rucci J, Sastri J, Robia SL, Luban J, Campbell EM.** 2011. TRIM5alpha associates with proteasomal subunits in cells while in complex with HIV-1 virions. Retrovirology **8:**93.

161. **Wojcik C, DeMartino GN.** 2003. Intracellular localization of proteasomes. Int J Biochem Cell Biol **35:**579-589.

162. **Klare N, Seeger M, Janek K, Jungblut PR, Dahlmann B.** 2007. Intermediate-type 20 S proteasomes in HeLa cells: "asymmetric" subunit composition, diversity and adaptation. J Mol Biol **373:**1-10.

163. **Dahlmann B, Ruppert T, Kuehn L, Merforth S, Kloetzel PM.** 2000. Different proteasome subtypes in a single tissue exhibit different enzymatic properties. J Mol Biol **303:**643-653.

164. **Luciani A, Villella VR, Esposito S, Brunetti-Pierri N, Medina D, Settembre C, Gavina M, Pulze L, Giardino I, Pettoello-Mantovani M, D'Apolito M, Guido S, Masliah E, Spencer B, Quaratino S, Raia V, Ballabio A, Maiuri L.** 2010. Defective CFTR induces aggresome formation and lung inflammation in cystic fibrosis through ROS-mediated autophagy inhibition. Nat Cell Biol **12:**863-875.

165. **Hou Z, Kelly EM, Robia SL.** 2008. Phosphomimetic mutations increase phospholamban oligomerization and alter the structure of its regulatory complex. J Biol Chem **283:**28996-29003.

166. **Takalkar AM, Klibanov AL, Rychak JJ, Lindner JR, Ley K.** 2004. Binding and detachment dynamics of microbubbles targeted to P-selectin under controlled shear flow. J Control Release **96:**473-482.

167. **Kenworthy AK.** 2001. Imaging protein-protein interactions using fluorescence resonance energy transfer microscopy. Methods **24:**289-296.

168. **Lukic Z, Goff SP, Campbell EM, Arriagada G.** 2013. Role of SUMO-1 and SUMO interacting motifs in rhesus TRIM5alpha-mediated restriction. Retrovirology **10:**10.

169. **McEwan WA, Schaller T, Ylinen LM, Hosie MJ, Towers GJ, Willett BJ.** 2009. Truncation of TRIM5 in the Feliformia explains the absence of retroviral restriction in cells of the domestic cat. J Virol **83:**8270-8275.

170. **Brandariz-Nunez A, Roa A, Valle-Casuso JC, Biris N, Ivanov D, Diaz-Griffero F.** 2013. Contribution of SUMO-interacting motifs and SUMOylation to the antiretroviral properties of TRIM5alpha. Virology **435:**463-471.

171. **Sebastian S, Grutter C, de Castillia CS, Pertel T, Olivari S, Grutter MG, Luban J.** 2009. An invariant surface patch on the TRIM5alpha PRYSPRY domain is required for retroviral restriction but dispensable for capsid binding. J Virol **83:**3365-3373.

172. **Tareen SU, Malik HS, Emerman M.** 2009. Cold Spring Harbor Retroviruses, Cold Spring Harbor, NY.

173. **Everett RD, Chelbi-Alix MK.** 2007. PML and PML nuclear bodies: implications in antiviral defence. Biochimie **89:**819-830.

174. **Lallemand-Breitenbach V, de The H.** 2010. PML nuclear bodies. Cold Spring Harb Perspect Biol **2:**a000661.

175. **Diaz-Griffero F, Gallo DE, Hope TJ, Sodroski J.** 2011. Trafficking of some old world primate TRIM5alpha proteins through the nucleus. Retrovirology **8:**38.

176. **Campbell EM, Perez O, Melar M, Hope TJ.** 2007. Labeling HIV-1 virions with two fluorescent proteins allows identification of virions that have productively entered the target cell. Virology **360:**286-293.

177. **Rodgers W.** 2002. Automated method for quantifying fluorophore colocalization in fluorescence double-labeling experiments. Biotechniques **32:**28, 30, 32, 34.

178. **Rodgers W.** 2002. Making membranes green: construction and characterization of GFP-fusion proteins targeted to discrete plasma membrane domains. Biotechniques **32:**1044-1046, 1048, 1050-1041.

179. **Radtke K, Kieneke D, Wolfstein A, Michael K, Steffen W, Scholz T, Karger A, Sodeik B.** 2010. Plus- and minus-end directed microtubule motors bind simultaneously to herpes simplex virus capsids using different inner tegument structures. PLoS Pathog **6:**e1000991.

180. **Mallery DL, McEwan WA, Bidgood SR, Towers GJ, Johnson CM, James LC.** 2010. Antibodies mediate intracellular immunity through tripartite motif-containing 21 (TRIM21). Proceedings of the National Academy of Sciences of the United States of America **107:**19985-19990.

181. **Bailey D, O'Hare P.** 2005. Comparison of the SUMO1 and ubiquitin conjugation pathways during the inhibition of proteasome activity with evidence of SUMO1 recycling. Biochem J **392:**271-281.

182. **Mattsson K, Pokrovskaja K, Kiss C, Klein G, Szekely L.** 2001. Proteins associated with the promyelocytic leukemia gene product (PML)-containing nuclear body move to the nucleolus upon inhibition of proteasome-dependent protein degradation. Proc Natl Acad Sci U S A **98:**1012-1017.

183. **Matafora V, D'Amato A, Mori S, Blasi F, Bachi A.** 2009. Proteomics analysis of nucleolar SUMO-1 target proteins upon proteasome inhibition. Mol Cell Proteomics **8:**2243-2255.

184. **El McHichi B, Regad T, Maroui MA, Rodriguez MS, Aminev A, Gerbaud S, Escriou N, Dianoux L, Chelbi-Alix MK.** 2010. SUMOylation promotes PML degradation during encephalomyocarditis virus infection. J Virol **84:**11634-11645.

185. **Boutell C, Cuchet-Lourenco D, Vanni E, Orr A, Glass M, McFarlane S, Everett RD.** 2011. A viral ubiquitin ligase has substrate preferential SUMO targeted ubiquitin ligase activity that counteracts intrinsic antiviral defence. PLoS Pathog **7:**e1002245.

186. **Meehan AM, Saenz DT, Guevera R, Morrison JH, Peretz M, Fadel HJ, Hamada M, van Deursen J, Poeschla EM.** 2014. A Cyclophilin Homology Domain-Independent Role for Nup358 in HIV-1 Infection. PLoS Pathog **10:**e1003969.

187. **Lahaye X, Satoh T, Gentili M, Cerboni S, Conrad C, Hurbain I, El Marjou A, Lacabaratz C, Lelievre JD, Manel N.** 2013. The capsids of HIV-1 and HIV-2 determine immune detection of the viral cDNA by the innate sensor cGAS in dendritic cells. Immunity **39:**1132-1142.

VITA

The author, Zana Lukic was born in Zenica, Bosnia and Herzegovina on July 7th, 1987 to Miodrag and Svjetlana Lukic. She received a Bachelor of Science in Biology from Elmhurst College (Elmhurst, IL) in January of 2005. As an undergraduate she spent her summers at University of Chicago (Mrksich Lab) researching substrate specificity of histone deacetylases.

In August of 2005, Zana joined the Integrative Cell Biology program at Loyola University Medical Center (Maywood, IL). Shortly thereafter, she joined the laboratory of Dr. Edward M. Campbell, Ph.D., where she studied molecular biology of HIV-1 infection, focusing specifically on understanding the interactions between host proteins and HIV-1 capsid. While at Loyola, Zana mentored many medical and undergraduate students in the STAR and the Research Mentoring Programs. She also presented this work at various conferences and symposiums for which she received scholarships. Additionally, she received a pre-doctoral training grant from the Arthur J. Schmitt Dissertation Fellowship to complete her dissertation.

Currently, Zana is a post-doctoral fellow in Dr. Kathleen Collins' laboratory at University of Michigan-Ann Arbor where she will continue to study HIV-1 pathogenesis.